NASA-CR-72160

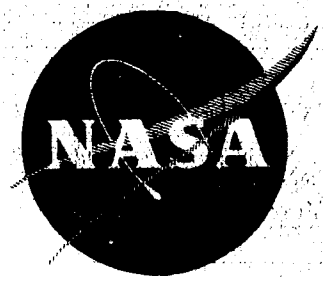

HYDRODYNAMIC JOURNAL BEARING PROGRAM

QUARTERLY PROGRESS REPORT NO. 5
For Period : April 29, 1966 Thru July 29, 1966

By

H. E. Nichols, W. D. C. Richards
R. J. Rossbach, and W. H. Bennethum,

prepared for
NATIONAL AERONAUTICS AND SPACE ADMINISTRATION
CONTRACT NAS 3-6479

SPACE POWER AND PROPULSION SECTION
MISSILE AND SPACE DIVISION
GENERAL ELECTRIC
CINCINNATI, OHIO 45215

Requests for copies of this report should be referred to:

National Aeronautics and Space Administration
Scientific and Technical Information Division
Attention: USS-A
Washington, D.C. 20546

HYDRODYNAMIC JOURNAL BEARING PROGRAM

QUARTERLY PROGRESS REPORT NO. 5

Covering the Period
April 29, 1966 Through July 29, 1966

By
H.E. Nichols, W.D.C. Richards, R.J. Rossbach, and
W.H. Bennethum

Approved by

E. Schnetzer, Manager
Development Engineering

Prepared for

NATIONAL AERONAUTICS AND SPACE ADMINISTRATION

Contract NAS 3-6479

TECHNICAL MANAGEMENT
NASA - LEWIS RESEARCH CENTER
NUCLEAR POWER TECHNOLOGY BRANCH
JOSEPH P. JOYCE, TECHNICAL MANAGER

SPACE POWER AND PROPULSION SECTION
MISSILE AND SPACE DIVISION
GENERAL ELECTRIC COMPANY
CINCINNATI, OHIO 45215

ABSTRACT

The Space Power and Propulsion Section has been under contract since April 29, 1965 to the National Aeronautics and Space Administration for the design, fabrication, and testing of journal bearings which posses characteristics required for use in space power systems. Requirements include long term unattended operation under zero "g" conditions using low viscosity lubricants such as potassium at 1200°F.

The program represents a continuation of work carried out under contract NAS 3-2111 and involves the testing and evaluation of bearings under conditions of angular and transverse linear misalignment, and non-rigid bearing supports. The four-pad pivot-pad and the three-lobed journal bearings shall be tested after the bearing test assembly including instrumentation have demonstrated the ability to obtain the required data.

The program will be a continuation of experimental investigations paralleled by analytical studies. These analytical investigations will compare the physical testing of bearing parameters with results based on theoretical assumptions. The goal of such experiments is to generalize the various bearing parameters thereby extending the usefulness of the results as design tools. The experimental tool of this program is a high speed test assembly comprised of a rotor and two test bearings which permits interchangeability of bearing and rotor. The lubricant will be distilled water,

temperature-controlled to simulate the kinematic viscosity of potassium. The stability behavior of the rotating shaft will be measured with non-contacting Bently inductance gages.

The specific requirements of the system are:

1.	Shaft speed	3600 to 30,000 rpm
2.	Inlet lubricant temperature	70 to 150°F
3.	Inlet lubricant supply pressure	0 to 150 psia
4.	Bearing linear misalignment	0 to 0.004 $\pm$ 0.0005 in.
5.	Bearing angular misalignment	0 to 400 $\pm$ 12 sec.
6.	Nominal bearing diameter	1.25 in.
7.	Bearing L/D ratio	1
8.	Diametral clearance	0.005 in.

The program will be performed in two tasks, the first of which will be the modification of the existing bearing test assembly and instrumentation and a demonstration of the ability to obtain accurate data. Task II will involve testing and analysis of the four-pad pivot-pad and three-lobed bearings.

The present report covers progress during the quarter ending July 29, 1966.

TABLE OF CONTENTS

SUMMARY

During this quarter the fabrication of both the three (3) lobe and self-aligning pivoted pad bearings were completed. Delivery of a portion of the optical tooling for utilization in bearing alignment was made. Evolution of the design and testing techniques for the piezoelectric force transducers was continued.

Calibration of test hardware and its respective read-out instrumentation was continued.

The evaluation of the displacement system was continued with preliminary calibration of the Bently probes at an elevated temperature, which is presently underway. In addition, the displacement sensor summing circuits calibration is in progress.

Efforts were initiated and are continuing to complete the external scanning network and the signal conditioning equipment.

The high frequency power supply system was completed. Portions of the test facility hardware were completed and integration of these into an operational testing system was continued.

The program schedule is shown in Figure 1.

FORECAST

During the forthcoming reporting interim, acquisition of the required remaining hardware for both the test rig and the test facility will be completed. Calibration and checkout of subassemblies, bearing alignment hardware, readout circuitry and supporting equipment will be accomplished. Once completed, the test rig will be checked-out using the two axial groove cylindrical bearings.

The next quarter should also yield an operational rotor response and a data reduction program. A test plan and the various test parameters for the initial two axial groove cylindrical bearing tests will be completed.

I. MECHANICAL DESIGN

During this quarter, the manufacture of the three (3) lobe bearings and the components required for the various configurations of the self-aligning pivoted pad bearings was completed. A detailed technique for aligning the two bearing shaft system was identified. Efforts to improve the piezoelectric force measuring system necessitated additional hardware design and fabrication. In addition, calibration of the torque shafts and torque readout was completed.

A. SELF-ALIGNING PIVOTED PAD BEARING

The design of the self-aligning pivoted pad bearing has been modified to incorporate the final-selected preload conditions and to conform to requirements of testing a pad located eccentric to the center of the bearings in two different planes, see Figure 2. Preload conditions along with their respective minimum diametral clearances are listed below.

Preload	Diametral Clearance at Min. Clearance Point
0.2	0.005 inches
0.52	0.003 inches

The eccentrically located pad condition will be accomplished using tapered pins.

All bearing components have been completed and are depicted in Figures 3,4,5 & 6. Results from the 100 percent inspection of all details and manufacturing subassemblies indicate that drawing requirements were fulfilled, Reference Figure 7.

B. THREE (3) LOBED BEARINGS

The fabrication of a pair of three (3) lobed bearings (Reference 1) has been completed. See Figure 8. Liaison inspection was performed at the vendor's facilities with both bearings meeting design requirements. A summary of the inspection points is shown in Table II, while Figure 9 & 10 depict the actual inspection contour traces of the I.D. as referenced to the O.D.

---

1. H.E. Nichols, R.J. Rossbach, W.H. Bennethum, J.C. Amos, and W.D.C. Richards: Hydrodynamic Journal Bearing Program, Quarterly Progress Report No. 4, For Period: January 29, 1966 Thru April 29, 1966, Contract NAS 3-6479

C. FORCE MEASUREMENT HARDWARE

The design of new test rig components in addition to modification of existing hardware necessary to incorporate the Kistler Model 902A piezoelectric load cells into the test rig assembly was completed, see Figure 11, (Reference 1). Spherical washer assembles were added to allow self-alignment of the load cells with the bearing housings. The fabrication of new hardware and required reworking of existing components were completed, see Figure 12 - 17.

Static calibration tests of the piezoelectric load cell instrumented bearing housing subassemblies were initiated, Reference Figure 18. The objectives of the tests were to check the assembled effective sensitivity of the load cells and the effects of preload and side loading. A discussion of the results of these preliminary investigations may be found in the instrumentation section of this report. One result indicated that any two opposed preloaded load cells located 90 degrees from the direction of loading supported a portion of the applied loads. The amount of support varried with the preload applied, thus causing changes in the sensitivity levels.

Small AlSl-01 oil hardened plates or discs were then fabricated, and these, along with tungsten carbide balls (3/8" diameter), were assembled 90 degrees apart, opposite two piezoelectric load cells in each plane, replacing two force transducers. See Figure 19. The addition of the balls and plates will reduce the side restraint to the direction of loading, thus permitting a stable effective sensitivity level. In addition, expandable arbor loading tooling was designed to

ensure that the inner bearing housings cannot distort during the calibration testing. The fabrication of the loading tooling is underway with testing to be resumed subsequent to its delivery.

D. OPTICAL TOOLING

Fabrication of the telescope mounting assembly has been completed, and it, along with the micro-alignment telescope, right angle eyepiece, and the telescope lamphouse assembly were received in a partial shipment of the total order (Reference 1) see Figures 20 & 21. Completion of the remainder of the optical equipment--two reflecting target assemblies, is expected during the latter portion of August, Reference Figure 22. Checkout of the telescope assembly atop the modified instrumentation housing was successfully completed. Results of experimentation indicate that squareness of the axis of the telescope to the plane of a reflecting mirror and/or coincidence of the centerline of the telescope to the center of a target can be readily obtained within the specified tolerances in the abstract of this report.

E. TORQUE READOUT SYSTEM CALIBRATION

The checkout device for calibrating the torque readout system was comprised of two-eighteen tooth gears mounted on the shaft of the test rig drive motor by means of a small stub shaft. Attached to the drive motor was the modified instrumentation housing containing two magnetic speed pickups that sensed the rotation of the gears. Rotation of the two gears was supplied by rotating the rotor of the drive motor using

a variable speed electric motor through a belt drive system. This driving system was utilized because the high frequency power supply necessary to excite the test rig drive motor was inoperable, see Figure 23.

Calibration of both the test monitoring dial and the digital connection were performed by setting a relative angle between the two gears and reading the output voltage of the speed pickups while varying the speed of the shaft system. The gap between the circumference of the gears and the pickups was set for a maximum output amplitude of 20 volts at the highest tested speed. This is in accordance with the input signal voltage level requirements of the phase meter. A Fluke Differential Voltmeter was used to readout the digital circuity while the readout dial supplied with the phase meter was calibrated for visual use during testing.

Five angular relationships of 2.75°, 5°, 10°, 15° and 17.25° were tested over a speed range of 0 to 16,665 rpm. The data taken during the various tests is listed in Table III, while the resulting curves are shown in Figures 24-27. Values for operation at 30,000 rpm were extrapolated from the data. While the voltage level decreases as the speed was increased for a given angular setting, the results were linear indicating that the 30,000 rpm projected data is valid. Based on these tests curves for voltage versus shaft speed were made for various angles and are shown in Figure 28.

F. CALIBRATION OF QUILL SHAFTS

The test setup for the calibration of the selected quill shafts is depicted in Figures 29 & 30. This calibration device utilizes both the hardware and the technique for locating the quill shafts that will be used during actual performance testing, Reference Figure 31. Each quill shaft is held in position by means of a locking collect assembly on both the drive motor and the test shaft. Two eighteen tooth gears from which torque will be determined are located one on the hollow shaft of the drive motor and the second on the upper end of the test shaft. The angular relationship between the two gears is sensed by two magnetic speed pickups and is read out on both a phase meter and the digital recording system.

The actual torque calibration of each beryllium copper quill shaft was accomplished by holding the gear mounted on the test shaft fixed. A length of cord or wire was then fastened to the other gear (attached to the shaft of the drive motor) at a fixed radius, from which various weights were suspended, and torque measurements were made. A pointer attached to the upper gear (drive motor) indicates the zero degree position and a corresponding angular setting for a given value of torque.

Calibration procedure for establishing the various "torque curves" (Reference Figures 29 and 30) was as follows. Zero position was found by loading and unloading the setup noting the average no-load zero position. Various loads were then applied to the end of the cord and the resulting angle noted by averaging the measured cord lengths. The zero position was rechecked between each load while both increasing and decreasing the various weights. Each point was checked several

times prior to fixing the angular setting for a given value of torque. Figures 32 to 37 are the resulting angle of twist versus applied torque curves.

Two different sizes of quill shafts were calibrated with all shafts being fabricated, heat-treated and aged from the same material lot and in an identical manner. The diameters selected for use were 0.125 inch and the 0.188 inch. Each shaft is made of beryllium copper which has been processed to a hardened condition of RC 41.

Total maximum error associated with a given torque value is $\pm$ 0.15 in-# (Square root of the sum of the squares) or $\pm$ 4.75%.

II. INSTRUMENTATION

A. DISPLACEMENT MEASURING SYSTEM

The evaluation of a recently developed displacement system (Bently Nevada 306 series probe and 4000 series detector) was conducted with the hope that it would minimize the problems caused by the presence of water associated with the existing displacement transducers (Bently Nevada D152 and D252R detector driver circuits and H 1084 probes). Initial tests were conducted using a single displacement probe mounted opposite a stationary silver plated test shaft segment in the apparatus shown in Figure 38. The sensitivity of the 4000 series detector driver and 306 series probe to water could not be reduced to an insignificant level. Subsequent tests were conducted on the premises of Bently Nevada Corporation in an attempt to improve the measuring system performance. It was possible to make the measuring system completely insensitive to the presence of water by careful tuning of the detector-driver circuit. Unfortunately the insensitivity to water was valid for only one specific point on the calibration curve (output vs. distance) - the point at which the output-distance line dry crossed the output-distance line wet. Since the purpose of the measuring system is to measure a range of displacements it is not possible to operate at one probe-to-shaft gap distance and it is not possible to make the new system insensitive to water over a range of probe-to-shaft gap settings. Additional tests were conducted to compare the overall performance of the new detector driver probe system with the existing system. It should be noted that the original H1084 probes had been modified by the installation of a teflon cap over the probe end to keep the water away from the probe.

It was found that the H1084 probes and D152 detector driver performed considerably better than did the 4000-series detector and 306-series driver evaluation unit over the range of gap settings expected during test operation. Sensitivity to water for a fixed gap setting for the H1084 probe measuring system has been reported (April 1966 Quarterly). Water sensitivity as a function of probe-to-shaft gap for a typical probe is shown in Table IV. As the gap varies from 6 to 14 mils, the error varies from 6.2 to 71.2 microinches. For a probe pair the two errors are subtractative. During testing, the nominal probe-to-shaft gap is 0.010 in.

After it had been determined that the modified (teflon capped probe H1084 - D152 and D252R detector drivers) measuring system was the best available, the static calibration of the displacement sensor was initiated. The purpose of the static calibration was to determine the relationship between probe-to-shaft gap and measuring system output.

The first step in the static calibration of the 16 Bently displacement probes was to set the sensitivity of each detector-driver assembly. From an opposed pair of probes the optimum detector-driven assembly sensitivity (based upon output voltage stability) of one probe was set by variation of the scale-factor potentiometer. The detector-driven sensitivity of the other probe was adjusted to give the same sensitivity (opposite polarity). Following these adjustments, the scale-factor potentiometers were sealed to prevent addicental movement.

The next step in the static calibration of the Bently displacement probes was carried out using a micrometer-positioning stage with a probe holder assembly mounted on it shown in Figure 29. Two Electrojet micrometer contacting probes (Spring-loaded linear- variable- differential-transformer devices manufactured by Sheffield Corp., Dayton, Ohio) were mounted on either side of the Bently probe in the probe holder assembly (although the photograph was taken with only one probe installed) and were used to measure the relative movement between the probe holder assembly and a test shaft having a silver plated ring around the periphery. The Bently probe was centered adjacent to the plated ring; the Electrojet probes contacted the shaft on either side of the plating.

Two Electrojet probes were used to cover a total movement of $\pm$ 4 mils from a nominal shaft-to-probe clearance of 10 mils in order to achieve maximum accuracy. Each Electrojet probe was adjusted to provide an output of 0.1 mil inches per scale division with a total full scale deflection of 4 mils. The Electrojet probes were repeatedly calibrated with a gage calibrator (also manufactured by Sheffield Corp.) with an absolute accuracy of $\pm$ 0.02 mils, traceable to National Bureau Standards, (see Figure 40). Bently measuring system output level was measured with a differential volt meter (Fluke Model 871A with an absolute accuracy of $\pm$ 0.03% of reading +10 microvolts and a resolution of 10 microvolts). D.C. voltage was supplied to the Bently detector-driver circuits by a Harrison Laboratory model 802B power supply at a nominal level of 17.5 volts.

The next step in the static calibration of the Bently displacement probes was carried out using a micrometer-positioning stage with a probe holder assembly mounted on it shown in Figure 39. Two Electrojet micrometer contacting probes (Spring-loaded linear- variable- differential-transformer devices manufactured by Sheffield Corp., Dayton, Ohio) were mounted on either side of the Bently probe in the probe holder assembly and were used to measure the relative movement between the probe holder assembly and a test shaft having a silver plated ring around the periphery. The Bently probe was centered adjacent to the plated ring; the Electrojet probes contacted the shaft on either side of the plating.

Two Electrojet probes were used to cover a total movement of $\pm$ 4 mils from a nominal shaft-to-probe clearance of 10 mils in order to achieve maximum accuracy. Each Electrojet probe was adjusted to provide an output of 0.1 mil inches per scale division with a total full scale deflection of 4 mils. The Electrojet probes were repeatedly calibrated with a gage calibrator (also manufactured by Sheffield Corp.) with an absolute accuracy of $\pm$ 0.02 mils traceable to National Bureau Standards, (see Figure 40). Bently measuring system output level was measured with a differential volt meter (Fluke Model 871A with an obsolute accuracy of $\pm$ 0.03% of reading +10 microvolts and a resolution of 10 microvolts). D.C. voltage was supplied to the Bently detector-driver circuits by a Harrison Laboratory model 802B power supply at a nominal level of 17.5

volts. Actual level was measured and recorded. The room temperature was controlled by air conditioning to 77 $\pm$ 2°F.

The initial zero position of the Bently probe was established by moving the positioning stage until the teflon cap on the Bently probe touched the silver plating. The "nominal gap" was obtained by backing off the positioning stage 10 mils and calibration was conducted from this point with the Electrojet probes. The absolute accuracy of the "nominal" is limited by the determination of the zero gap position (initiation of contact between the teflon cap and the shaft surface), the basic accuracy of the micrometer used with the positioning stage and the relative position of the teflon cap on the probe. The total inaccuracy of all factors could possibly add up to an error of 1 mil. However, the absolute accuracy of the "nominal gap" setting is not important because the "nominal gap" is set by measuring system output voltage during assembly of the test rig.

Table V is a condensation of the results of the static calibration discussed above. Because of the subtractative nature of the water sensitivity errors when considering an opposed pair of probes, the net errors shown in the last column are always smaller than for a probe alone, see Table IV. The net errors due to water conductivity for the eight pairs of probes varies from 4.8 to 28.4 microinches with each probe gap at 0.010 in., some plus and some minus.

An attempt at determining the sensitivity of the displacement measuring system to probe temperature was made so that the relative importance of conducting a static calibration with the probes at temperature could be determined. The preliminary test was conducted using the same static calibration apparatus described above. Elevated probe temperatures were set by wrapping the probe holder with 0.040 inch diameter sheathed thermocouple wire and passing current through them. The results showed sufficient indication of a relatively significant shift in calibration as a function of temperature to warrant the making of an environmental chamber capable of housing the complete static calibration apparatus as shown in Figure 41. The walls of the chamber were made from a relay rack and lined with insulation. The support for the bench centers was rested on top of a piece of 0.5-inch thick aluminum plate. A sheathed heating element was clamped to the lower surface of this plate. A temperature control circuit consisting of an optical meter relay with a single set point was assembled. Power to the main heating element was turned on and off by the meter relay operating through a power relay and an auto-transformer. A thermocouple located inside the chamber attached to the micrometer positioning stage was connected to the meter relay. A second thermocouple was used to monitor temperatures and showed that a temperature of 120 $\pm$ 5°F could be held over any 24 hour period. Elevated temperature calibration of the displacement sensors had not been completed at the termination of this reporting period.

B. Force Measurements

A decision had been made to switch from strain-gage force buttons to piezoelectric load cells due to the inability of the strain gage type to cover the required speed range. (The system would have a resonant frequency between 300-400 cps due to the low stiffness of the strain-gage force buttons, which is about 60,000 lb/in for each button.) The load cells purchased for this application were Kistler Model 902A which have the following significant characteristics:

Stiffness: 16.7×10^6 lb./in.

Charge Sensitivity: 18 ± 2 pcb/lb

Resonant Frequency: 50 KC

Size: O.D.: 0.87 in.

I.D.: 0.41 in.

Height: 0.39

Range: 0 - 8000 lb.

These transducers consist of a quartz element hermetically sealed in a stainless steel can sandwiched between two washers which distribute the load evenly and which are structually part of the can. The output signal is brought out through a coaxial connector located on the side of the load cell and sealed against water penetration with a combination of shrinkable tubing and RTV silicone rubber. (This method was recommended by Kistler Instrument Corporation on the basis of effectiveness in similar applications.)

When used with a suitable charge amplifier it is possible to achieve accurate load measurements over a small fraction of or the entire full scale range. For example, with a Kistler 504 charge amplifier it is possible to get sensitivities as high as 10 volts per pound and still be able to measure an 8000 lb. change in load by switching to a lower sensitivity (10 volts output is maximum). Although piezoelectric load cells are usually considered to be dynamic instruments unsuitable for static measurements, the development of the Field Effect Transistor has made it possible to use them for static measurements. The charge amplifier can maintain a given charge signal for a reasonably long time period by maintaining a high input impedance so that the charge will not leak off. For example, in the case of the 504 charge amplifier the input impedance is 10^{14} ohms and the time constaint is 5000 seconds for a typical range setting (long time constant mode).

The design of the test facility included provision for four (4) load cells per instrumentation plane spaced at 90° increments around the circumference. This design resulted in pairs of gages sensing the same load. It is possible to obtain the desired dynamic force vector by measuring only one of each pair of load cells. The other one was to serve as a matching spring and makes the calculation of dynamic force possible without the necessity of an in-place calibration. Unfortunately, the manufacturer was not able to guarantee that the stiffness of any given pair of load cells would be closer than 3%. The problem of acutally

measuring the stiffness is a formidable one and was bypassed by establishing a method of in-place calibration. This consisted of assembling the individual bearing housings and hanging dead weights from a simulated shaft supported by the inner bearing housing. The results of the in-place calibration would provide the ratio between the measured force at the active load cell and the load applied at the shaft. This number would not require a knowledge of the stiffness of the opposed load cell.

The original calibration curves supplied by Kistler consisted of a plot of charge versus applied load over a 0-6000 pound range. Typically, all points fell within a 9% (slope) tolerance band of a best straight line passing through zero. The greatest deviation did occur at loads less than 500 lbs. If these points are excluded the calibration curve tolerance (slope) is within a 5% band over the entire 0-6000 lb. range. Kistler did rerun the calibration curves over a 0-600 lb. range so that the load cells could be used at the low end of their range with a more precise knowledge of sensitivity (calibration curve slope) for any given load. A 200 lb. span from any area of a typical calibration curve (above 500 lbs.) will have all points within a 1% (slope) tolerance band.

Initial attempts to calibrate the load cells in the assembled lower bearing housing indicated the presence of several significant effects.

1. The load cells are sensitive to very small temperature changes because the case expansion or contraction causes a load change on the crystal. The crystal sensitivity to temperature is .01%/°F. This should not be a significant problem during test operation.

2. The net force transmitted to any pair of load cells was significantly affected by the restraint to movement of the inner bearing housing caused by preload on the pair located 90° to the pair being loaded. This problem appears to be important because of the uncertainty that the preloads will remain constant under test conditions and the fact that change in preload can have a significant effect on gage output. Several alternate methods are being considered as a possible solution. All consist of removing the inactive load cell of each pair and replacing it with a member which will permit tangential movement of the inner bearing housing at the point of contact.

3. When a force was applied to the inner bearing housing by the dead weights, the reading at the upper load cell was considerably below the reading at the lower load cell. This was caused by distortions in the inner and outer bearing housings and is of concern because of the importance of duplicating test conditions during in-place static calibration procedures. It is thought that an improved arbor through the bearing will alleviate this problem.

C. Torque Measurement

The torque measuring system was reworked and recalibrated. The 18-toothed gears for the torque measuring system permit only 17° of twist from zero to full scale. The quill-shaft diameter is to be selected for a given set of test runs to give the highest sensitivity

commensurate with the maximum torque to be measured. Extended range can be achieved by removing teeth from the gears which provide the output pulses to the phase measuring circuits.

The electronic system was calibrated by mechanically setting a phase angle between the two 18 teeth gears mounted on a fixture attached directly to the rig drive motor. Output readings were taken at several speeds up to 15000 rpm. Calibration results are included in Figures 24-27.

These curves permit determination of twist as a function of phase meter reading. Coupled with a calibration of the individual quill shaft obtained by applying various loads and measuring the resulting deflections it is possible to obtain torque. Quill shaft load vs. deflection curves are included in Figure 32-37.

D. External Scanning and Signal Conditioning Equipment

1. Switching Network

In Figure 42 is shown the overall scanning system which includes provision for selection of an intermediate level of signal conditioning equipment (peak to peak and average level detector and phase measuring equipment) in addition to scanning of the conventional signals from pressure transducers, thermocouples, etc., which can be fed directly into the existing digital recording system.

The proposed method for accomplishing the scanning procedure for those sensors for which the intermediate signal-conditioning equipment is required is shown in Figure 43. The corresponding instrumentation planes are shown in Figure 44. It is necessary to switch each force cell into one of two charge amplifiers which converts the charge signal to a voltage proportional to dynamic load. These signals are directed to either the peak-to-peak detector or the phase measuring system. It is necessary to switch the output of a pair of displacement sensor output signals into a summing network and thence into either the peak-to-peak or average level detector or the phase measuring system. Provision is made for including a tracking type filter in series with the peak detector to eliminate all but fundamental waves at the shaft rotational frequency.

The method of achieving synchronization with the digital recording switching system will be as follows. Two separate "decks" (100 2 pole circuits per deck) will be required. Any two sequential decks may be used but for purposes of explanation they will be called 0 & 1. The switches normally used for the low signal input to the digital recorder will be used to provide synchronization by connecting a $\neq$ 3 volt signal to the "0 deck" switch common and feeding the 3 volt signal selected by the scanning process into the appropriate selection circuitry and coil driving network required to obtain the switching sequence.

This system will provide synchronization between the digital recorder scanner and the external relays shown in Figure 43. Only one pole of the digital recorder scanner will be available for signal input on the "0 deck" since the other pole is required to provide the synchronization for the external relays. This means that all signal inputs to the "0 deck" will be single ended.

All output signals from the peak-to-peak and average level detectors and the phase measuring system will be fed into the "high" side of the "0 deck". All other signals will be fed into the high and low sides of the "1 deck". This technique will make it possible to use the range change capabilities of the existing digital recorder and will provide synchronization for up to a total of 100 separate measurements.

The digital recorder is located in Building 309 and the test rig and external switching circuits and peak to peak and average level detectors and phase measuring equipment will be located in the control room of Building 314. A 350 ft. transmission line (Belden 8773) will be required to connect the two locations.

2. Peak to Peak Detector

Figure 45 shows a typical signal from a pair of displacement sensors or a force load cell. The function of the peak-to-peak detector is to provide a d.c. voltage o-10V full scale proportional

to Vp when Vp varies from 0-10 volts. Rejection of d.c. voltage will be achieved by a coupling condenser and level will then be shifted so that output of peak-to-peak detecter will be proportional to peak signal voltage.

Frequency range of fundamental wave will be from 20 - 500 cps. The tracking filter provides a 20.5 Kc signal frequency output proportional in amplitude to the fundamental of the input (20 - 500 cps) signal.

Functionally, the peak-to-peak detector is composed of two parts a level shifter and a level converter. The level shifter converts the capacitor coupled input waveform from a symmetrical variation about 0 volts to a similar wave with the negative peak coinciding with 0 volts. The level converter changes the zero to peak volts into a proportional d.c. level. Included with the level shifter circuity is provision for intermittent short circuity (one per channel) of the input during automatic scanning to prevent channel intereference.

Due to the uncertainties concerning the distortion of input waveforms the tracking filter required for phase measurements will be used with the peak detector to provide a constant-frequency, 20.5-kc pure since waves proportional to amplitude of fundamental component of input signal. If this system increases measurement errors due to nonlinearity in the filter, the filter will be bypassed and signals will be fed directly into the peak detector.

3. Average Level Detector

Measurement of absolute position with respect to 0 volts of since wave (Vdc, Figure 44) will be accomplished with the average level detector. A d.c. output voltage from 0 to $\pm$ 10 V proportional to average of sine wave input 0 to $\pm$ 10 V will be generated by the circuit which is a filter with 80 db/octave attenuation and a time constant which will limit scanning speed to 1 channel per second.

E. Displacement Sensor Summing Circuit

Displacement sensore consisting of Bently-Nevada Corporation H1084 probes, D152 and D252R detectors are mounted in opposed pairs in the test rig to provide a continuous indication of relative shaft position within the bearing housing. The use of opposed pairs of probes is based on the fact that thermal expansion and other factors which cause symmetrical movement between the test shaft and bearing housing can be cancelled in the measuring circuit and only that part of the signal due to relative movement of the shaft within the bearing housing will appear as an output signal. In order for this technique to be successful, it is necessary that both probes in a given pair have identical sensitivities in terms of voltage change per unit distance change. Practical considerations make it necessary also to have a nearly constant d.c. output at initial conditions for the probe pair.

Figure 46 is a graphical representation of the adjustments required for a single pair of displacement sensing probes and detectors. A static calibration will be conducted to determine the volts/unit distance relationship for each probe-detector assembly individually. Adjustments to signal level and slope of calibration curve can be made by means of the detector and by mechanical positioning of the probe assembly relative to the test shaft. However, it will be necessary to include provision for changing the slope of the calibration curve as shown in Figure 46 so that the slopes may be matched precisely in the combining circuits. Once the slopes have been matched, the symmetrical effects discussed previously will be eliminated from the output signal.

Typical input signals to summing circuit from detectors will be 6 - 10V volts with a slope of 0.4 volts per mil. Input resistors will be capable of continuously varying this slope from 0.9 to 1 to 10 to 1 and will consist of multi-turn wire wound potentiometers with a turn counting dial for accurate positioning. A biasing circuit is required to permit setting an absolute output level (zero) for a given shaft position due to the fact that the mechanical zero cannot be set during initial setup and calibration. The amplifier and associated power supply has been designed for maximum long term stability and reliability since calibration of probe assemblies cannot be accomplished at frequent intervals due to complex disassembly procedures.

III. TEST FACILITY PREPARATION

The control room of Building 314 is presently being renovated to accept the high speed test rig and the majority of its associated equipment (Reference 1). All services including domestic water, drainage, instrumentation and both 208 and 110 volt electrical power have been installed. The test rig support structure has been fixed in position and a wall has been constructed surrounding the testing area. Completion of the test facility is presently scheduled during the month of August.

The high frequency power supply system has been completed. This includes overhaul operations of the Ward-Leonard M. G. set located in Building 309, and both the high frequency power cable and the control wiring for remote operation of the aforementioned M. G. set from Building 314. The power console for this system also has been completed, see Figures 47-49. G. E. Apparatus Service Shop personnel cleaned and internally re-connected the wiring of the test rig's fifteen horsepower drive motor and subsequently matched it with the M. G. set for optimum performance. Checkout of this system indicates excellent starting characteristics, ample horsepower and a speed range of 7500 to 30,000 rpm.

Both the operational control panel for the test rig and the distilled water loop package have been completed, see Figures 50-53. These components have been installed and connected to the building services. Interconnection between the test rig and the

distilled water loop system has begun. Completion of the above and calibration of the instrumentation is scheduled during August.

Completion of the digital data link between Buildings 309 and 314 was delayed because of extended delivery of suitable cable,* (Reference 1). Delivery was achieved during the latter portion of July, resulting in the overhead conduit run being completed and the cable having been pulled. Connection of the cable to the digital patch work boards in the test cell and subsequently to the digital data recorder in Building 309 still remains to be finished and checked out. The scheduled completion date for this portion of the facility preparations is August 31, 1966, reference Figure 54.

* Beldon Cable S/N 8773

TABLE I

INSTRUMENTATION AND EQUIPMENT LIST

	Name	Model No.	Manufacturer
1.	Differential Voltmeter	801	John Fluke Co.
2.	Single Channel Recorder	19301-01-01	Honeywell Corp.
3.	Proximity Probe	H-1-084-3	Bently Nevada
4.	Proximity Detector	D152 D252R	Bently Nevada
5.	Power Supply	802B	Harrison Lab. Inc.
6.	Dial-A-Volt	DAV46D	General Resistance Inc.
7.	Accutron Transistor Amplifier	51	Sheffield Corp.
8.	Electrojet Cartridges	59230108 59230119	Sheffield Corp.
9.	Linearchek Gage Calibrator		Sheffield Corp.
10.	Sundstrand Bench Centers	BC 6"x36"	Sundstrand Machine Tool
11.	Leitz Optical Stage	1"x1"	Opto-Metric Tools Inc.
12.	Oscilloscope	RM561A	Tektronix Corp.
13.	Oscilloscope	RM535	Tektronix Corp.
14.	Oscilloscope	8151R	Beckman
15.	Phase Meter	320-AB	Technology Inst. Corp.
16.	Differential Comparator	3A7	Tektronix Corp.
17.	Scope Camera		Dumont
18.	Balance Machine	MU-6	Micro Balancing Inc.
19.	Differential Voltmeter	871A	John Fluke Co.
20.	Charge Amplifier	504	Kistler Inst. Corp.

TABLE I
(Continued)

	Name	Model No.	Manufacturer
21.	Piezoelectric Force Trans.	902A	Kistler Inst. Corp.
22.	Accelerometers	2213C	ENDEVCO
23.	Cathode Follower	2608	ENDEVCO
24.	Power Supply	2621	ENDEVCO
25.	Power Supply	160A	Tektronix Inc.
26.	Wave form Generator	162	Tektronix Inc.
27.	Scope Indicator	360	Taktronix Inc.
28.	Temperature Recorder (Speedomax G)	60362	Leeds and Northrup Co.
29.	Speed Counter	5500	Berkeley Corp.
30.	Power Supply (dc)	6263A	Harrison Labs
31.	Carrier Demodulator	CD11	Pace Engineering
32.	Oscillater Pre-Amplifier	55GE2239	Fisher and Portor Co.
33.	Pressure Transducers	P76-100 psig	Pace Engineering
34.	Turbine Flowmeter	10C1510A	Fisher and Portor Co.
35.	Power Supply	C1580	Lambda
36.	Power Supply	C280M	Lambda
37.	Universal Microalignment-telescope	112/637	Rank Taylor Hobson Inc.
38.	Right Angle Eye Piece	112/568	Rank Taylor Hobson Inc.
39.	43x Eye Piece	112/383	Rank Taylor Hobson Inc.
40.	Telescope Lamphouse Assy	112/638	Rank Taylor Hobson Inc.
41.	Heat Exchanger	4810	Heliflow Corp.
42.	Filter (20 micron)	55B10D-3/4	Commercial Filters Inc.
43.	3 Way Air Operated Valves ($\frac{1}{2}$")	$\frac{1}{2}$"-3 way	Taylor Inst. Corp.

TABLE I
(Continued)

44.	Lin-E-Aire Control Valve	240VM1240-21995	Taylor Inst. Corp.
45.	80 gal. Hot Water Heater	200YRGF821525	G. E. Company
46.	Water Pump-Lube Supply	SRM 204-22	Robbins and Meyers Inc.
47.	Water Pump-Sump Scavange	EM 818	Robbins and Meyers Inc.

TABLE II

THREE (3) LOBED BEARING INSPECTION SUMMARY

P/N 4012000-796 P1 REV D

Condition	Specification (in)	Actual (in) Pt #1	Pt #2
Diameter of Lobes	1.2600	1.2600 - 1.2602	1.2600 - 1.25995
Roundness of Lobes	W/in 0.000050	0.000050	0.000050
Diameter of O. D.	2.5001 - 2.5004	2.50026	2.50037
Roundness of O. D.	W/in 0.000050	0.000020	0.000020
Taper of Lobes (Axially)	W/in 0.0002	0.00011	0.000050
Tolerance of Loc. Coordinates	W/in 0.000050	0.000050	0.000050
Surface Finish, I. D.	8 ✓	8 ✓	8 ✓

TABLE III

TORQUE SYSTEM CALIBRATION DATA

Set Point*	Speed, rpm	Speed, cps	Dial Degrees	Fluke Volts	Duo-Dial Setting	Dial Avg.	Fluke Avg.
10°	3,333	1000	20	10,008	4.254	19.95	10.016
10°	6,666	2000	19.9	9,905		19.80	9.910
10°	9,999	3000	19.7	9,755		19.60	9.753
10°	13,332	4000	19.1	9,591		19.10	9.594
10°	16,665	5000	18.9	9,458		18.90	9.458
10°	13,332	4000	19.1	9,598			
10°	9,999	3000	19.5	9,751			
10°	6,666	2000	19.7	9,915			
10°	3,333	1000	19.9	10,024			
15°	3,333	1000	31.4	15,656		31.45	15.649
15°	6,666	2000	31.2	15,554		31.25	15.556
15°	9,999	3000	31.0	15,386		31.00	15.389
15°	13,332	4000	30.7	15,200		30.60	15.229
15°	16,665	5000	30.3	15,036		30.20	15.036
15°	13,332	4000	30.5	15,238			
15°	9,999	3000	31.0	15,392			
15°	6,666	2000	31.3	15,558			
15°	3,333	1000	31.5	15,641			
17.25°	3,333	1000	36.5	18,392		36.5	18.403
17.25°	6,666	2000	36.4	18,311		36.4	18.320
17.25°	9,999	3000	36.2	18,156		36.2	18.160
17.25°	13,332	4000	35.8	17,978		35.75	17.983
17.25°	16,665	5000	35.4	17,812		35.4	17.812
17.25°	13.332	4000	35.7	17,988			
17.25°	9,999	3000	36.2	18,164			
17.25°	6,666	2000	36.4	18,329			
17.25°	3,333	1000	36.5	18,414			
5°	3,333	1000	8.9	4,704		8.9	4.691
5°	6,666	2000	8.7	4,614		8.7	4.599
5°	9,999	3000	8.4	4,544		8.4	4.483
5°	13,332	4000	8.1	4,310		8.1	4.305
5°	16,665	5000	7.9	4,180		7.9	4.180
5°	13,332	4000	8.1	4,300			
5°	9,999	3000	8.4	4,422			
5°	6,666	2000	8.7	4,584			
5°	3,333	1000	8.9	4,677			
2.75°	3,333	1000	4.3	2,422		4.3	2.419

TABLE III
(Continued)

Set Point	Speed, rpm	Speed, cps	Dial Degrees	Fluke Volts	Duo-Dial Setting	Dial Avg.	Fluke Avg.
2.75°	6,666	2000	4.2	2,343		4.15	2.338
2.75°	9,999	3000	3.9	2,197		3.9	2.196
2.75°	13,332	4000	3.6	2,068		3.65	2.067
2.75°	16,665	5000	3.4	1,950		3.4	1.950
2.75°	13,332	4000	3.7	2,065			
2.75°	9,999	3000	3.9	2,195			
2.75°	6,666	2000	4.1	2,332			
2.75°	3,333	1000	4.3	2,415			

* All angular settings established within $\pm$ 0°4'.

TABLE IV

EFFECT OF WATER ON PROBE OUTPUT AS A FUNCTION OF GAP SETTING FOR PROBE MEASURING SYSTEM NO. 5

Probe to Shaft Gap	Output Dry	Output Wet	Net Change Output	Net Change*
Mils	Volts	Volts	Millivolts	Microinches
6	-4.683	-4.678	5	12.4
8	-5.470	-5.451	19	47.6
10	-6.273	-6.243	30	75.0
12	-7.111	-7.063	48	120.0
14	-7.975	-7.918	57	142.4

Probe: Bently Nevada H1084, S/N 15292

Detector Driver: Bently Nevada D152, S/N 3451

Power Supply: Harrison Lab 802 B at 17.5V

Output Meter: Fluke 871A

Gap Measured with Sheffield Electrojet Gage Cartridge

*Based upon a nominal sensitivity of 400 mv/mil. In actual operation probes are used in pairs with a nominal sensitivity of 1.0 volts/mil. Net change due to water is in opposite directions for each probe, thereby diminishing the effect for the summed pair.

The intended probe-to-shaft probe setting during testing will be a nominal 0.010 in.

TABLE V

Summary of Displacement Sensor
Static Calibration Results at 77°F

Gage Pair Identification Number	Detector Model & S/N	Sensor Head S/N	Scale Factor Pot Turns From Full ccw Pos.	Probe to Shaft Clearance Gage Zero	Unamplified Output Gage Zero	Unamplified Gage Sensitivity mv/mil	Deflection Due to H_2O, mv	Net Error Of Pair, Microinches
1	D152 3459	15273	-	10	6.134	397.0	33.	
1R	D252 R5522	14439	7.5	10	5.7279	404.9	12.	26.2
2	D152 3447	15284	3.25	10	6.215	408.3	8.	
2R	D252R 5519	1444	6.0	10	7.300	404.0	28.	-24.6
3	D152 3462	15296	4.0	10	7.421	410.6	13.	
3R	D252R 5518	14438	9.0	10	7.1785	417.5	39.	-31.4
4	D152 3458	15287	5.5	10	7.830	405.1	19.	
4R	D252R 5521	15281	6.0	10	7.128	399.1	30.	-13.7
5	D152 3451	15292	2.5	10	6.276	411.5	35.	
5R	D252R 5515	15289	6.5	10	8.942	397.0	58.	-28.4
6	D152 3453	15288	2.75	10	7.856	414.5	21.	
6R	D252R 5550	15279	7.0	10	7.510	414.0	17.	4.8
7	D152 3454	15250	4.0	10	7.096	386.2	25.	
7R	D252R 5520	14770	6.5	9	7.192	407.5	21.	5.0
8	D152 3464	16763	3.0	9	6.574	421.5	14.	
8R	D252R 5517	16758	6.0	10	5.330	412.5	9.	6.0

*Based on sum of unamplified gage sensitivities for pair.

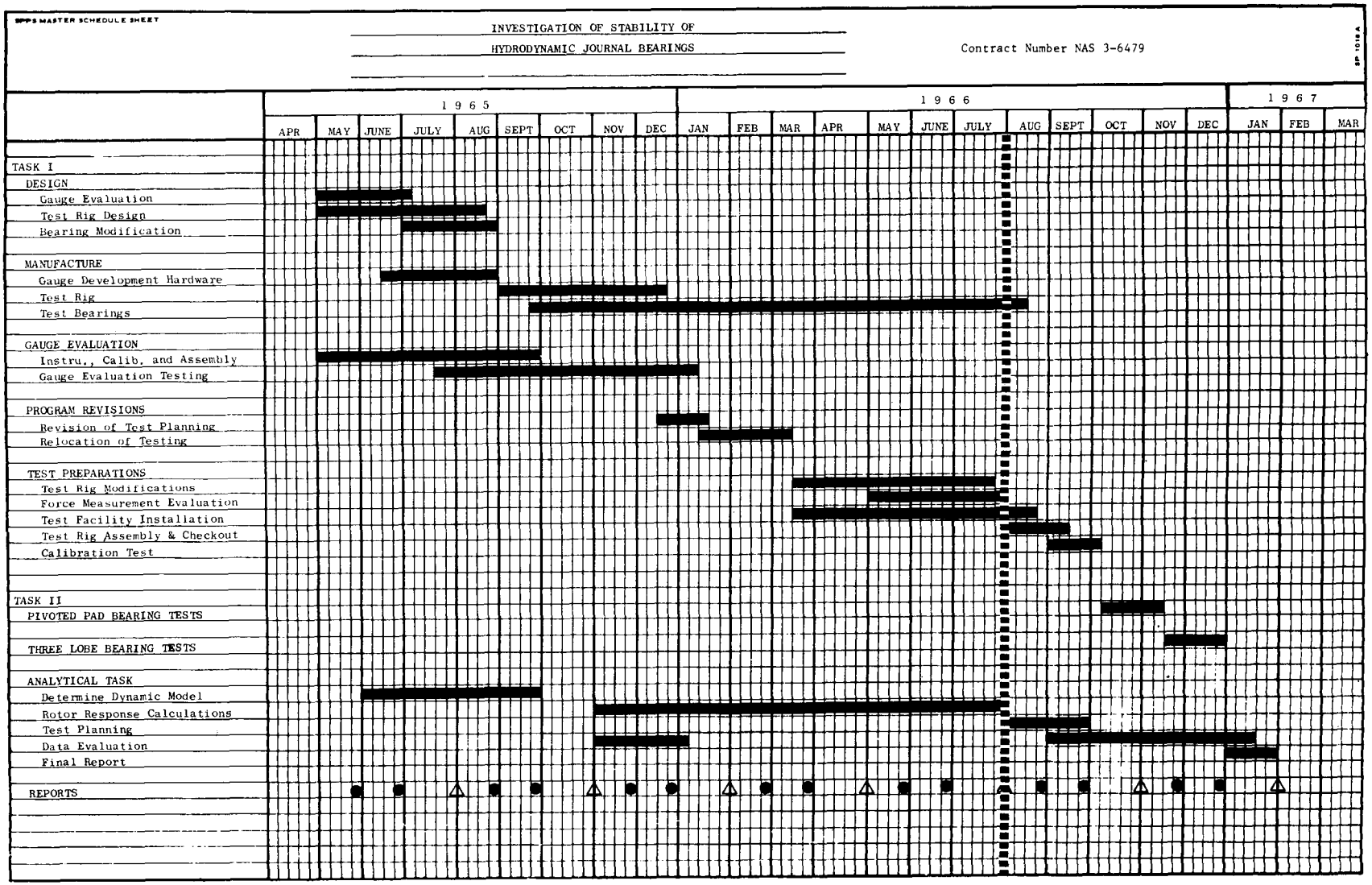

Figure 1. Program Schedule

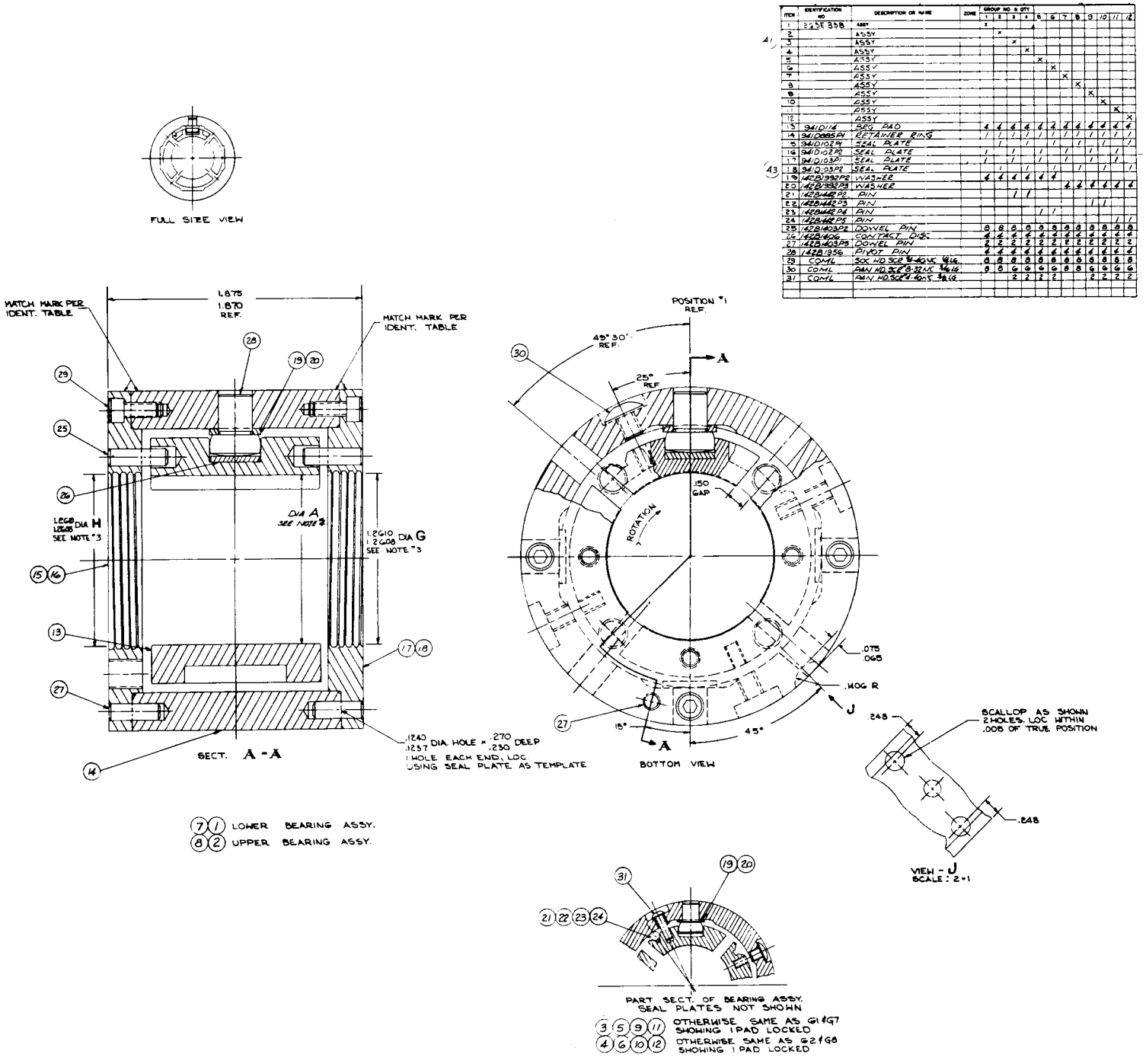

ITEM	IDENTIFICATION NO.	DESCRIPTION OR NAME	ZONE	GROUP NO. & QTY. 1	2	3	4	5	6	7	8	9	10	11	12
1	2256 338	ASSY		1											
2		ASSY			x										
3		ASSY				x									
4		ASSY					x								
5		ASSY						x							
6		ASSY							x						
7		ASSY								x					
8		ASSY									x				
9		ASSY										x			
10		ASSY											x		
11		ASSY												x	
12		ASSY													x
13	341D114	REG PAD		4	4	4	4	4	4	4	4	4	4	4	4
14	341D085P1	RETAINER RING		1	1	1	1	1	1	1	1	1	1	1	1
15	341D102P1	SEAL PLATE		1		1		1		1		1		1	
16	341D102P2	SEAL PLATE			1		1		1		1		1		1
17	341D103P1	SEAL PLATE		1		1		1		1		1		1	
18	341D103P2	SEAL PLATE			1		1		1		1		1		1
19	42B/992P2	WASHER		4	4	4	4	4	4	4					
20	42B/992P3	WASHER									4	4	4	4	4
21	42B442P2	PIN				1	1								
22	42B442P3	PIN											1	1	
23	42B442P4	PIN						1	1						
24	42B442P5	PIN													1
25	42B403P2	DOWEL PIN		8	8	8	8	8	8	8	8	8	8	8	8
26	42B406	CONTACT DISC		4	4	4	4	4	4	4	4	4	4	4	4
27	42B403P3	DOWEL PIN		2	2	2	2	2	2	2	2	2	2	2	2
28	42B356	PIVOT PIN		4	4	4	4	4	4	4	4	4	4	4	4
29	COML	SOC HD SCR 1/4-20 UNC 1/16		8	8	8	8	8	8	8	8	8	8	8	8
30	COML	PAN HD SCR 8-32 UNC 3/16		8	8	6	6	6	6	8	8	6	6	6	6
31	COML	PAN HD SCR 4-40 UNC 3/16				2	2	2	2			2	2	2	2

Figure 2. Self-Aligning Pivoted Pad Bearing.

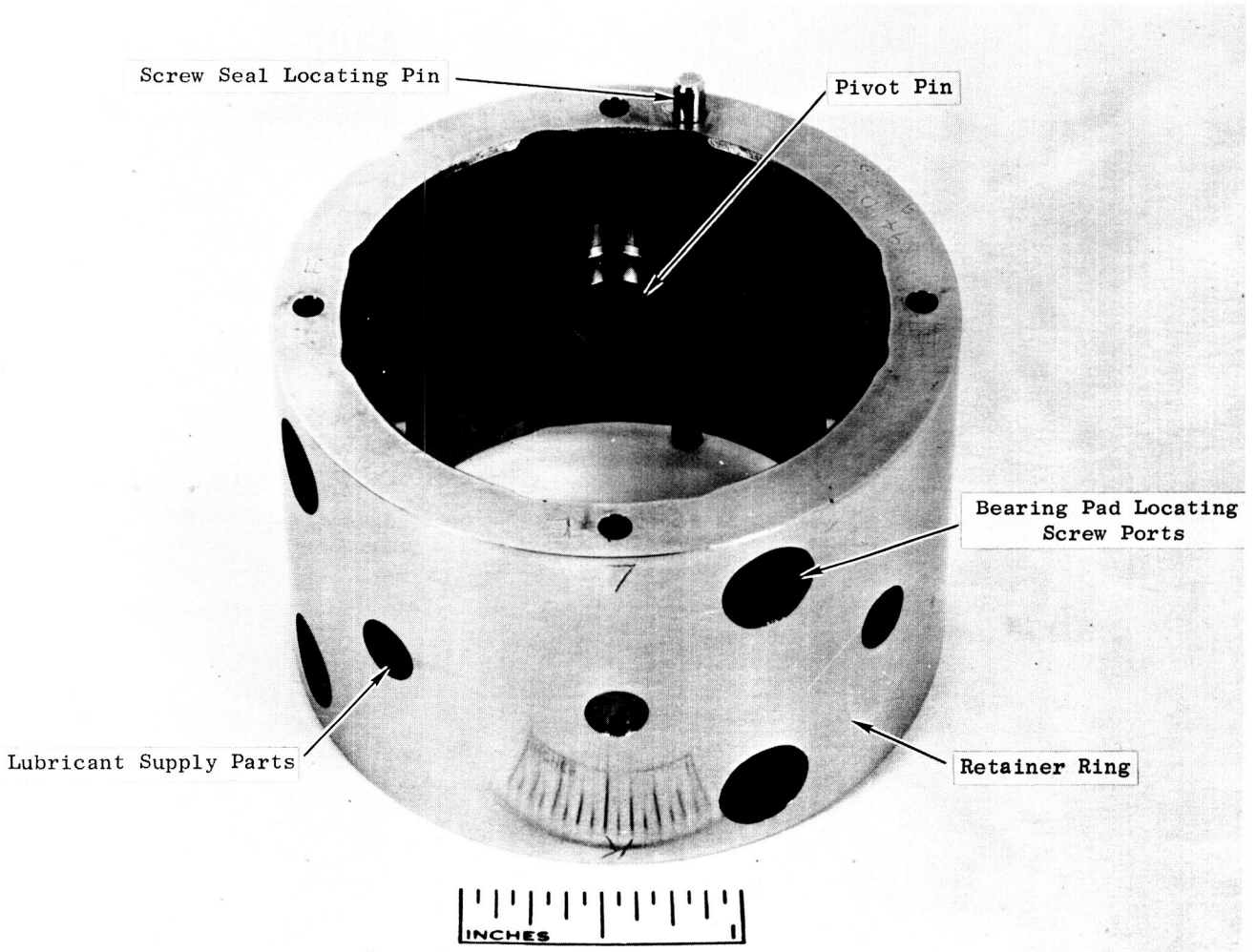

Figure 3. Self-Aligning Pivoted Pad Bearing Retainer Ring Sub-Assembly.

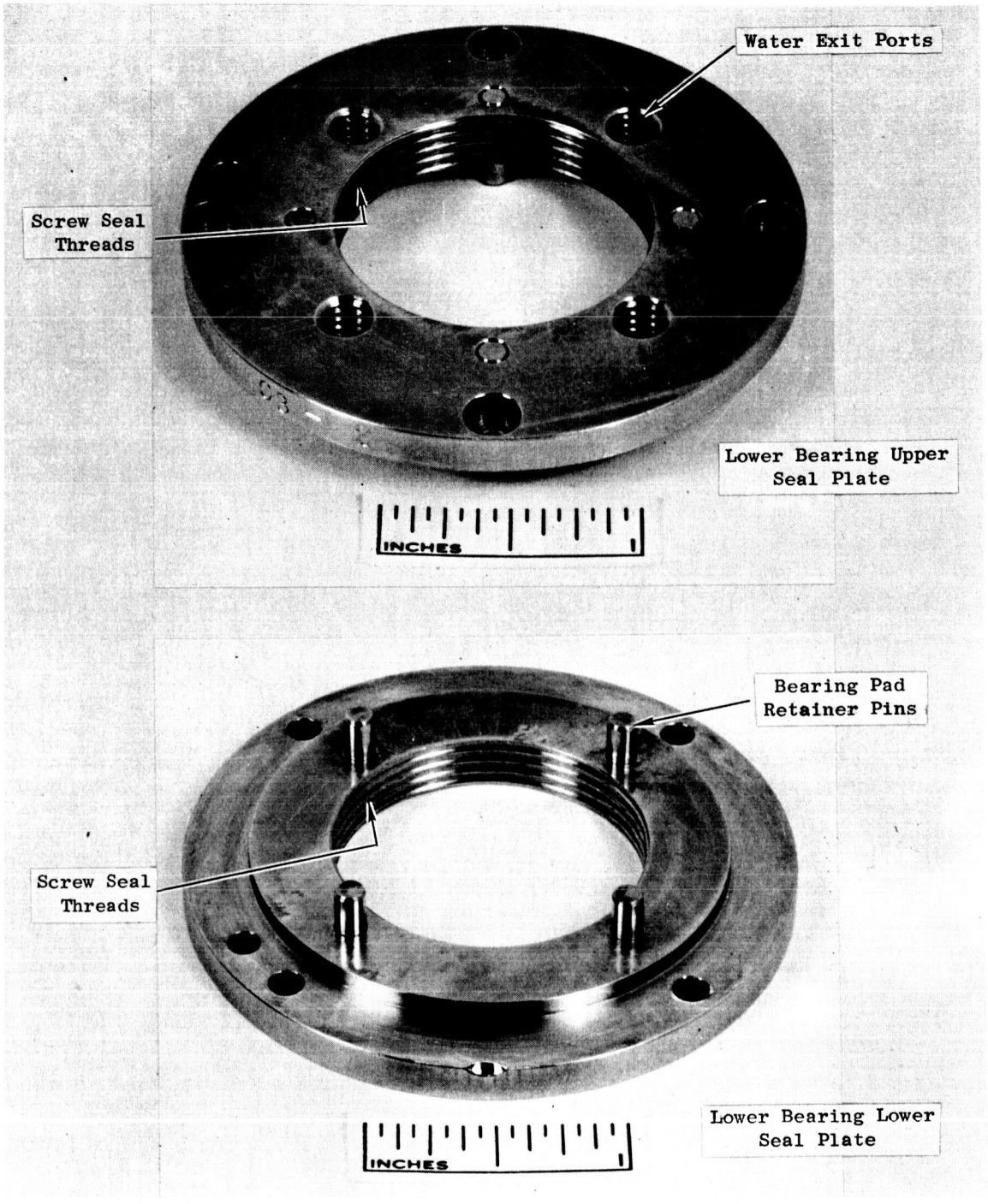

Figure 4. Self-Aligning Pivoted Pad Bearing Seal Plates.

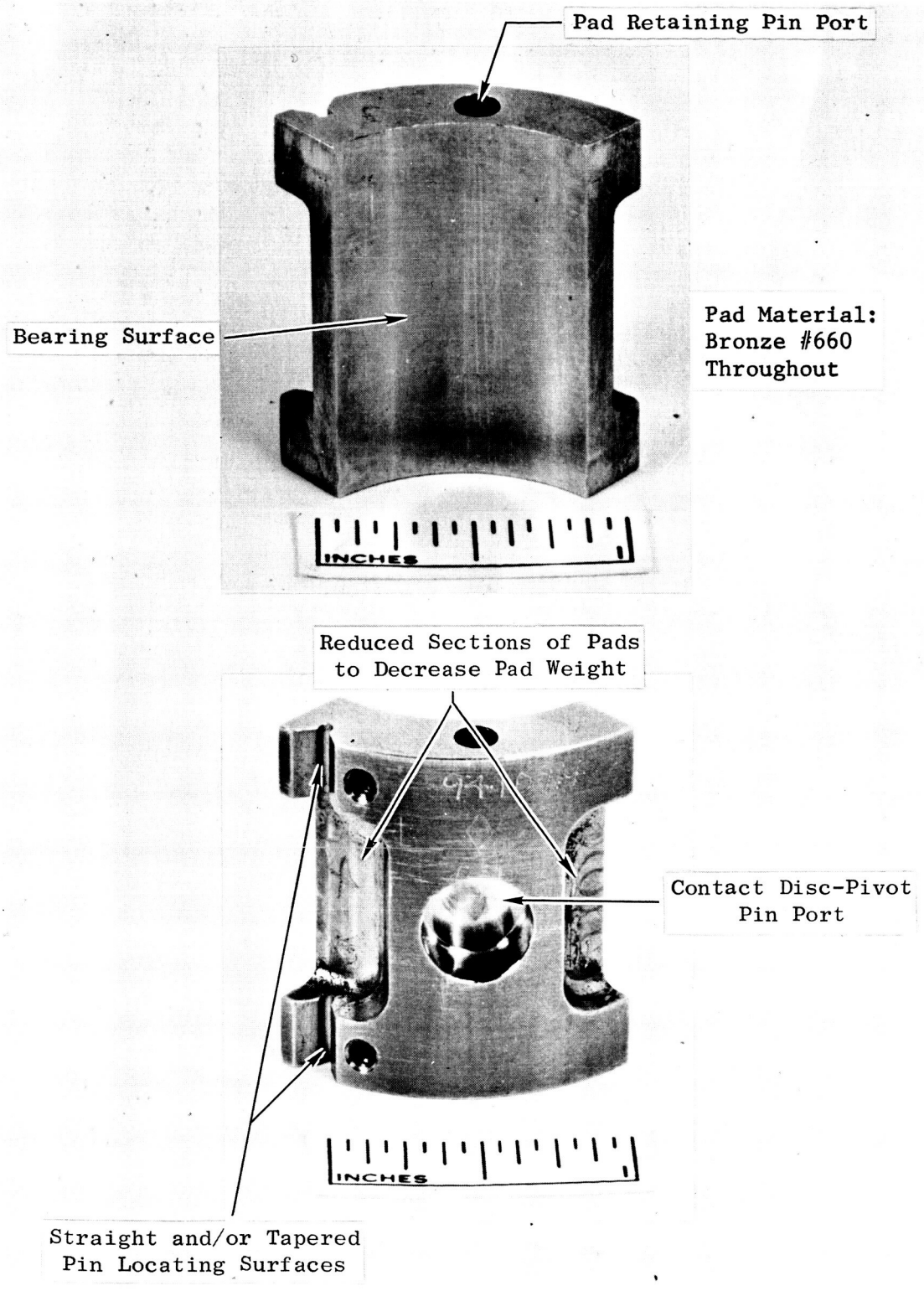

Figure 5. Self-Aligning Pivoted Pad Bearing-Pads.

Pivot Pin (Mat'l: Stellite #3)

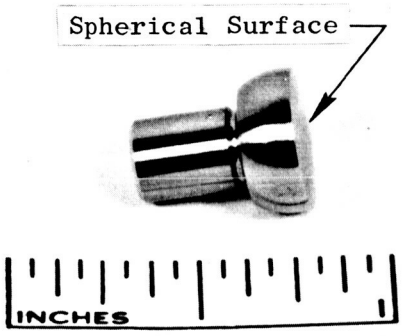

Locating Pin (Mat'l: 316SST)

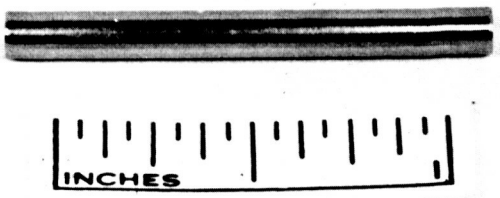

Pivot Pin Washer (Mat'l: 316SS)

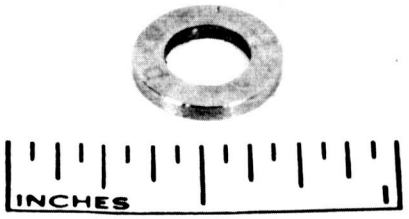

Contacting Disc (Mat'l: Stellite #3)

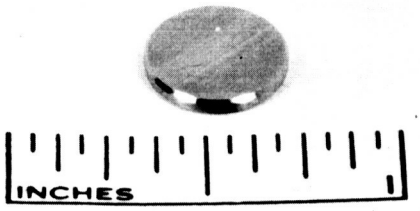

Figure 6. Self-Aligning Pivoted Pad Bearing Components.

IDENTIFICATION TABLE		
BEARING PLANE (RIG)	POSITION NUMBER	CODE
TOP	# 1	A
TOP	# 2	B
TOP	# 3	C
TOP	# 4	D
BOTTOM	# 1	E
BOTTOM	# 2	F
BOTTOM	# 3	G
BOTTOM	# 4	H

ITEM	IDENTIFICATION NO.	DESCRIPTION OR NAME	ZONE	GROUP NO. & QTY 1	2	3	4
1	941D118	ASSY		X			
2	142B1442P1	PIN	E6				
3	COML	BOLT	E6				
4	142B1356	PIN-PIVOT	E6				
5	142B1932P1	WASHER	E5				
6	142B1406	DISC - CONTACT	E5				
7	941D114	PAD - BEARING	E5				
8	941D885	RING - RETAINER	D5				

(A1) (B)

(B) ALLMETAL SCREW PRODUCTS CO. INC., CHICAGO, ILL.

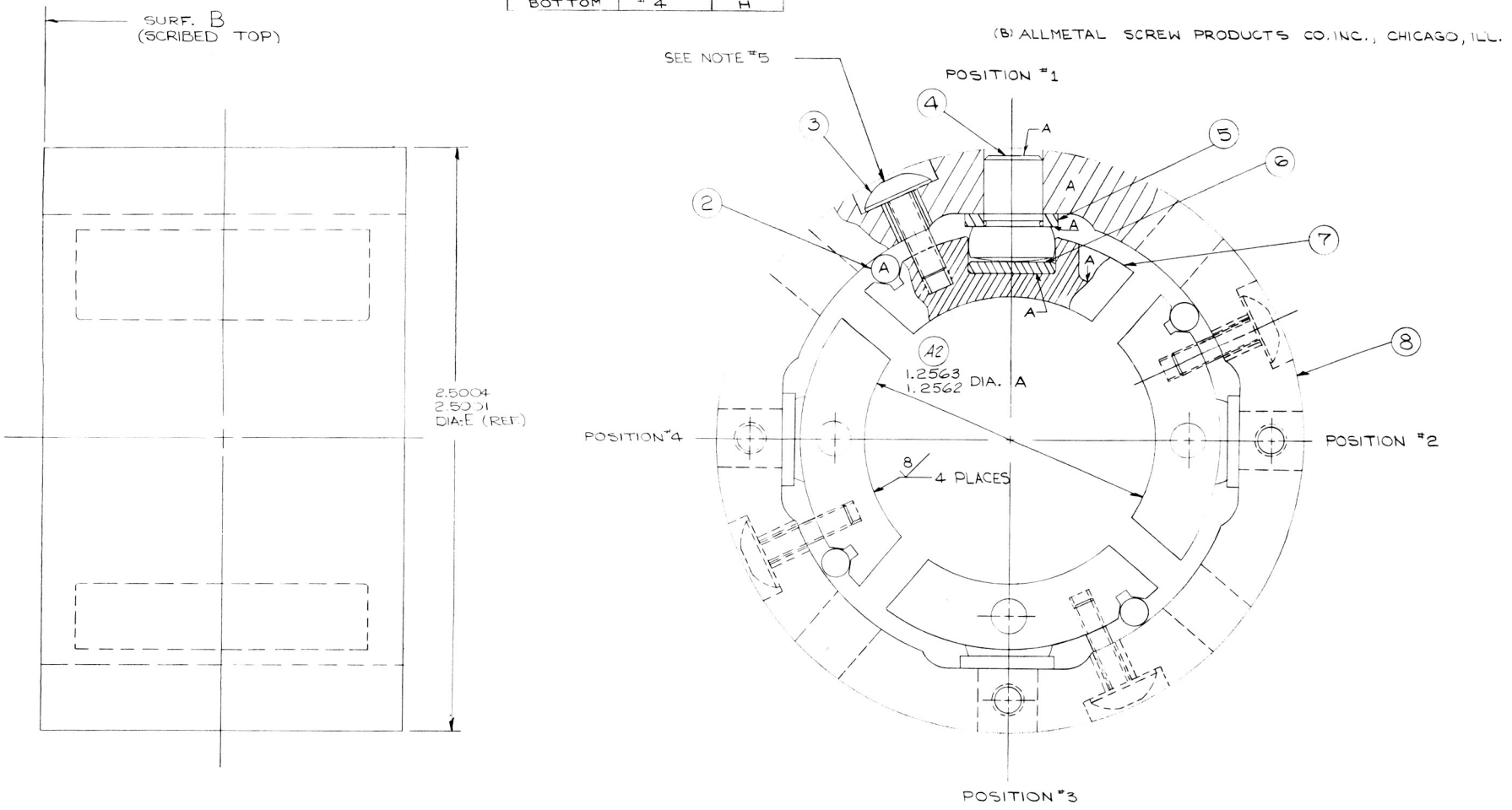

Figure 7. Bearing I.D. Machining Fixture.

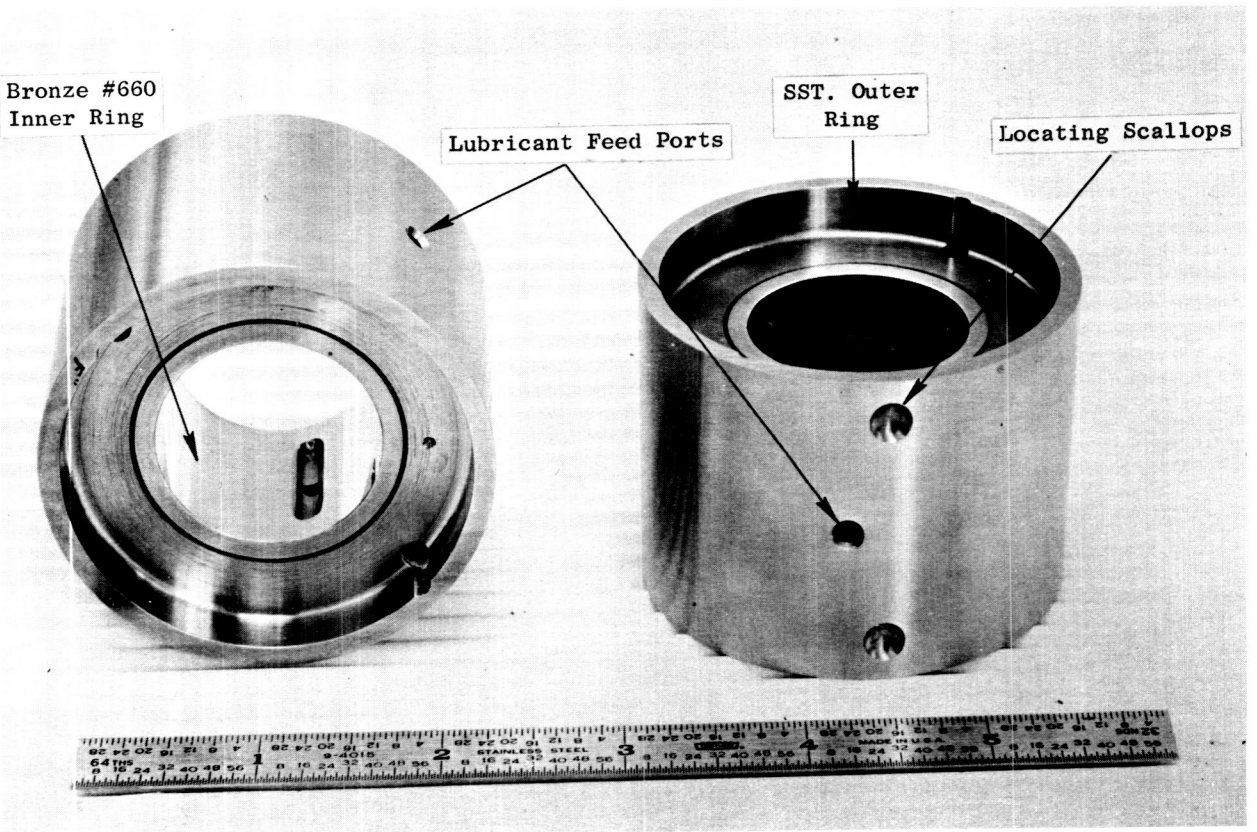

Figure 8. Three (3) Lobed Bearings.

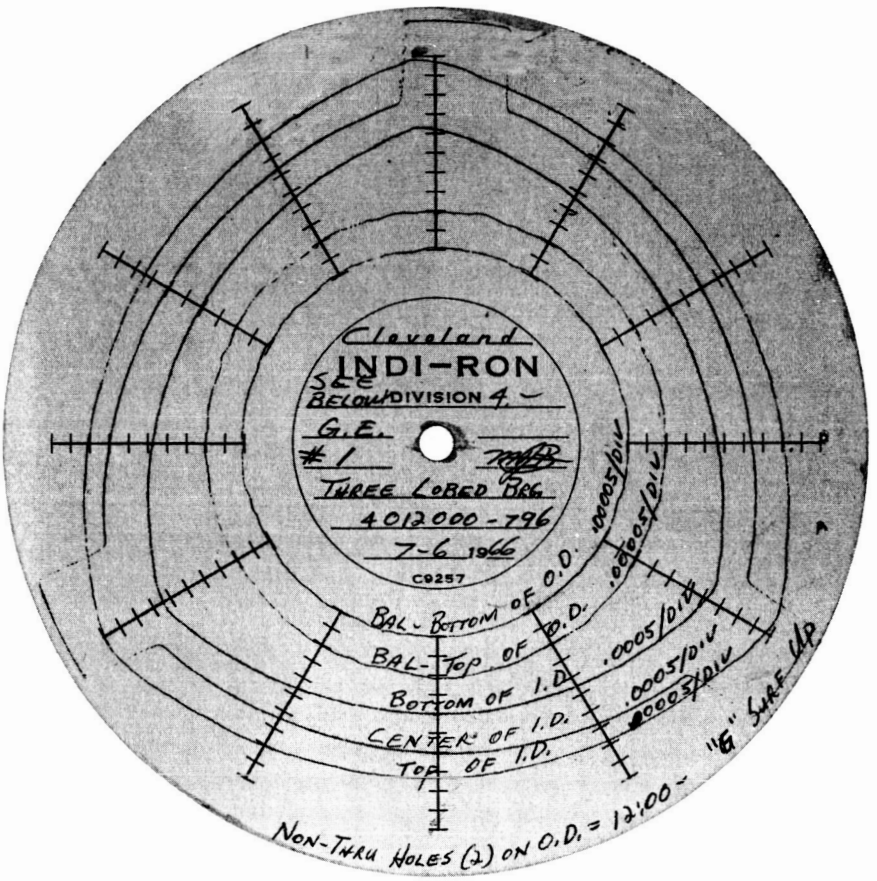

Figure 9. Indi-Ron Inspection Traces of Three Lobed Bearing - PT #1.

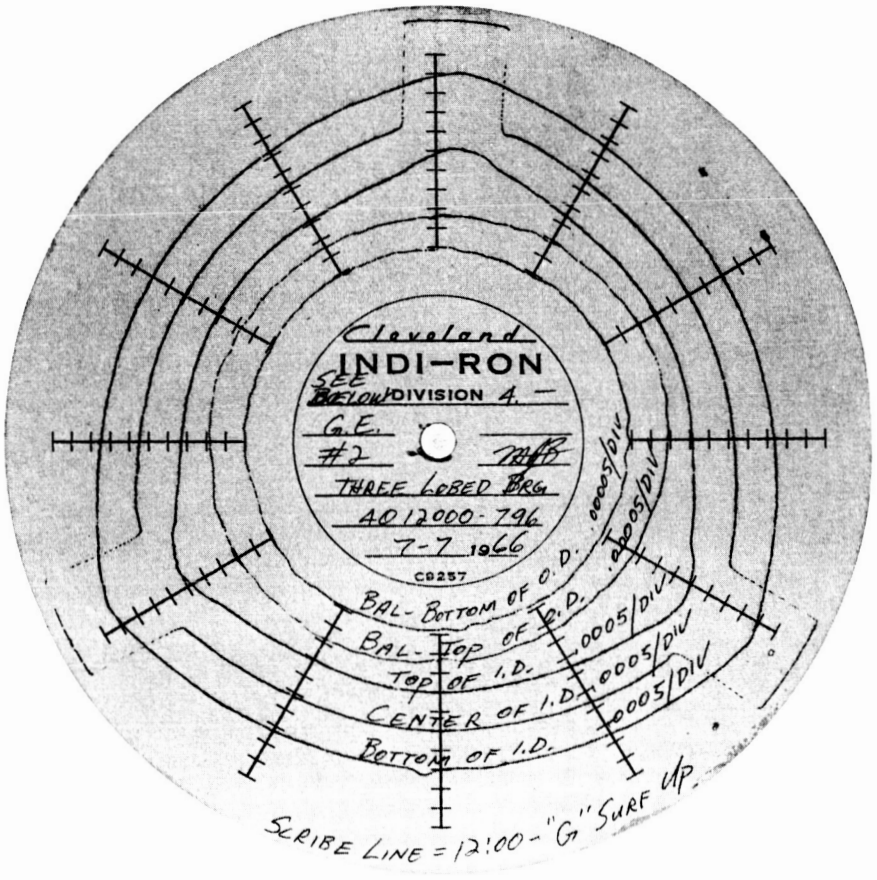

Figure 10. Indi-Ron Inspection Traces of Three Lobed Bearing - PT #2.

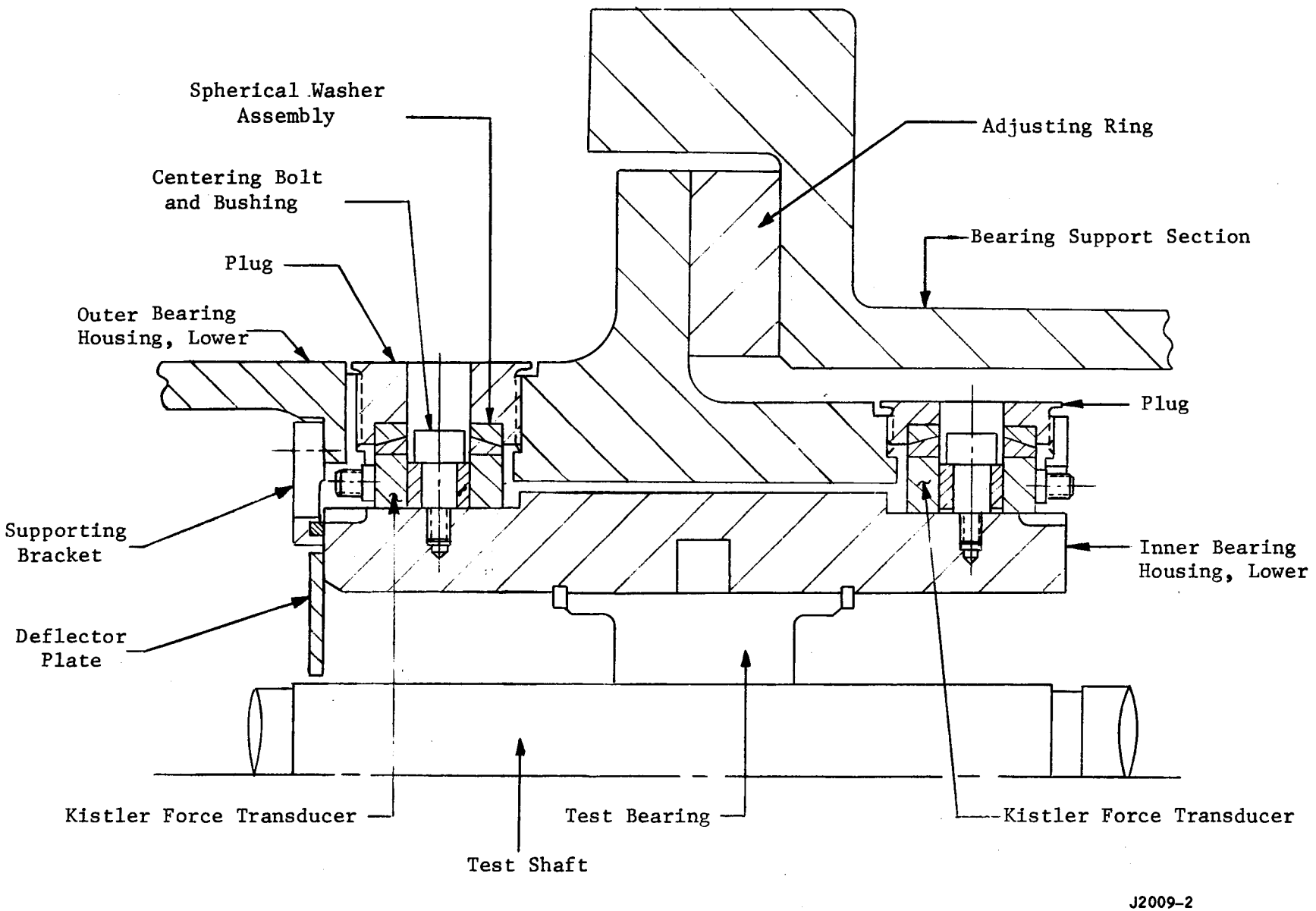

Figure 11. Force Transducer Assembly.

Figure 12. Modified Upper Outer Bearing Housing.

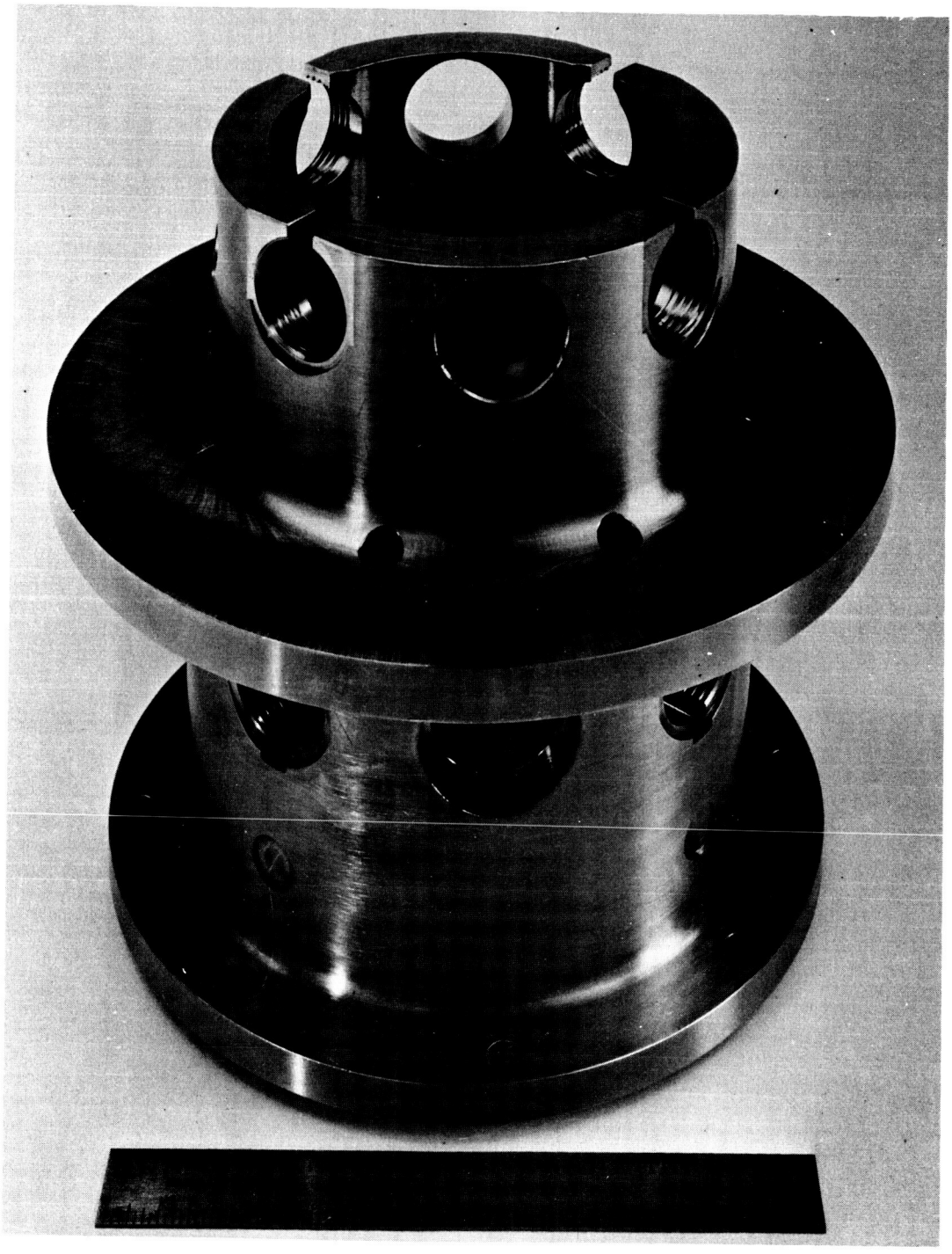

Figure 13. Modified Lower Outer Bearing Housing.

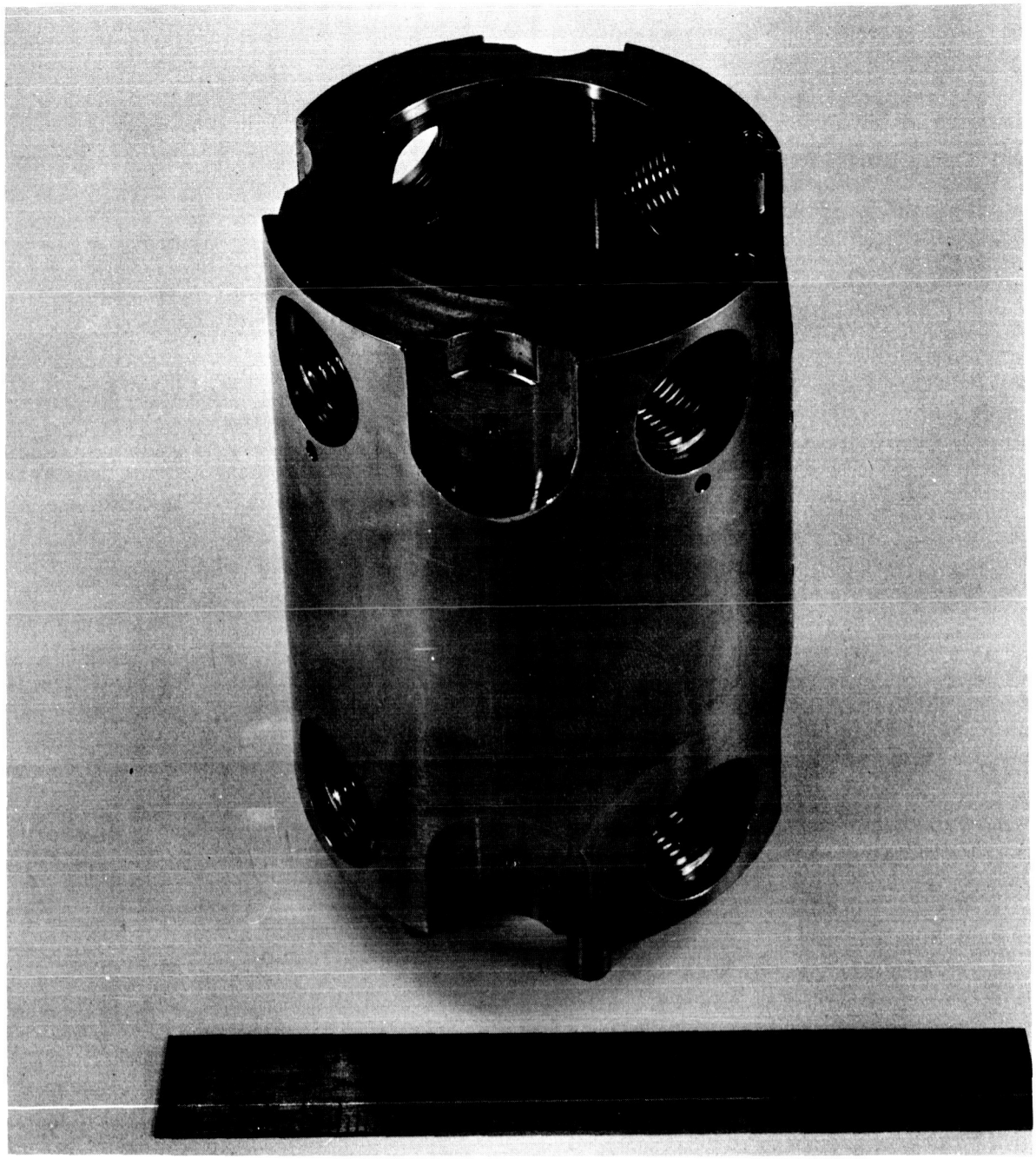

Figure 14. Modified Upper Inner Bearing Housing.

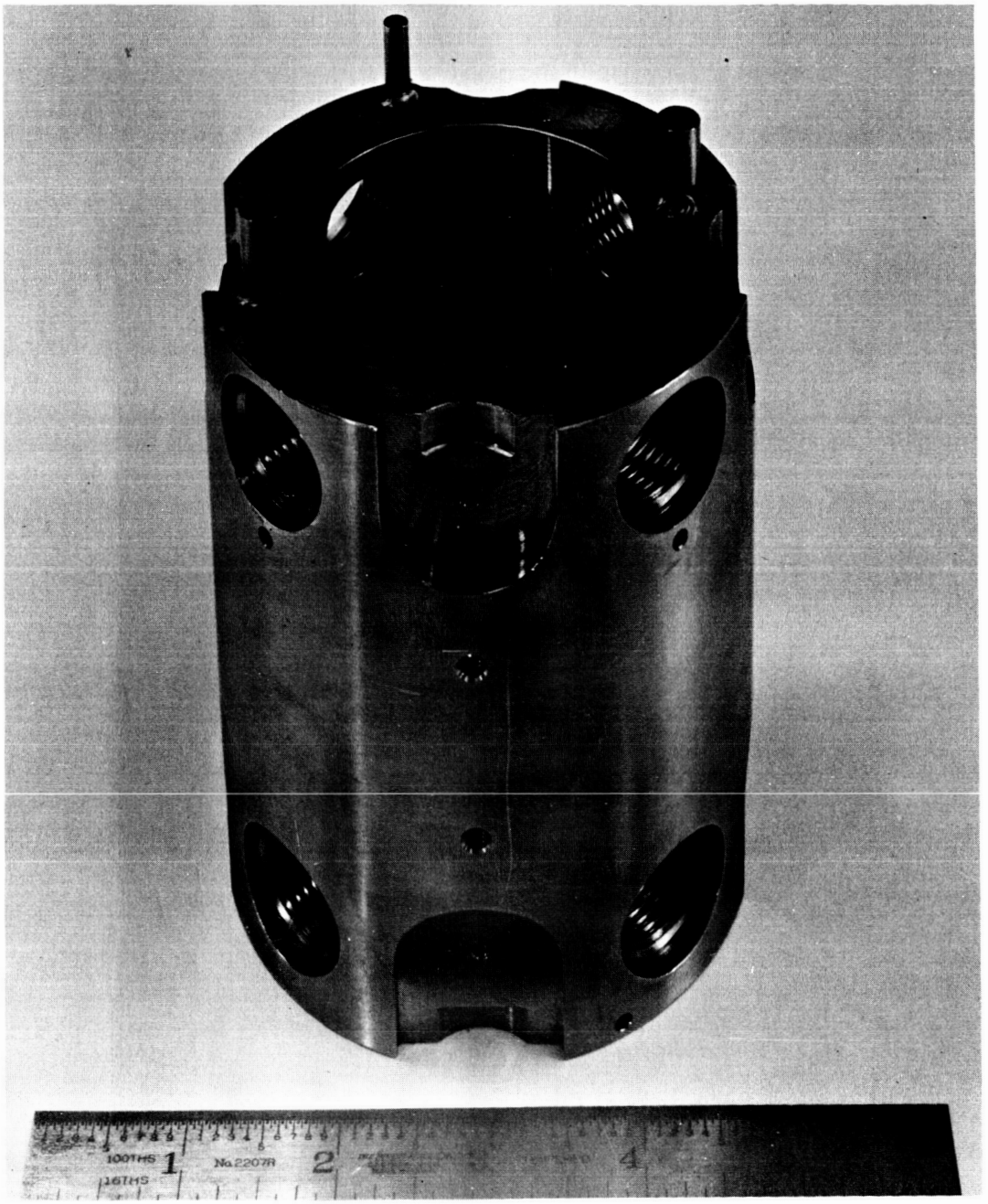

Figure 15. Modified Lower Inner Bearing Housing.

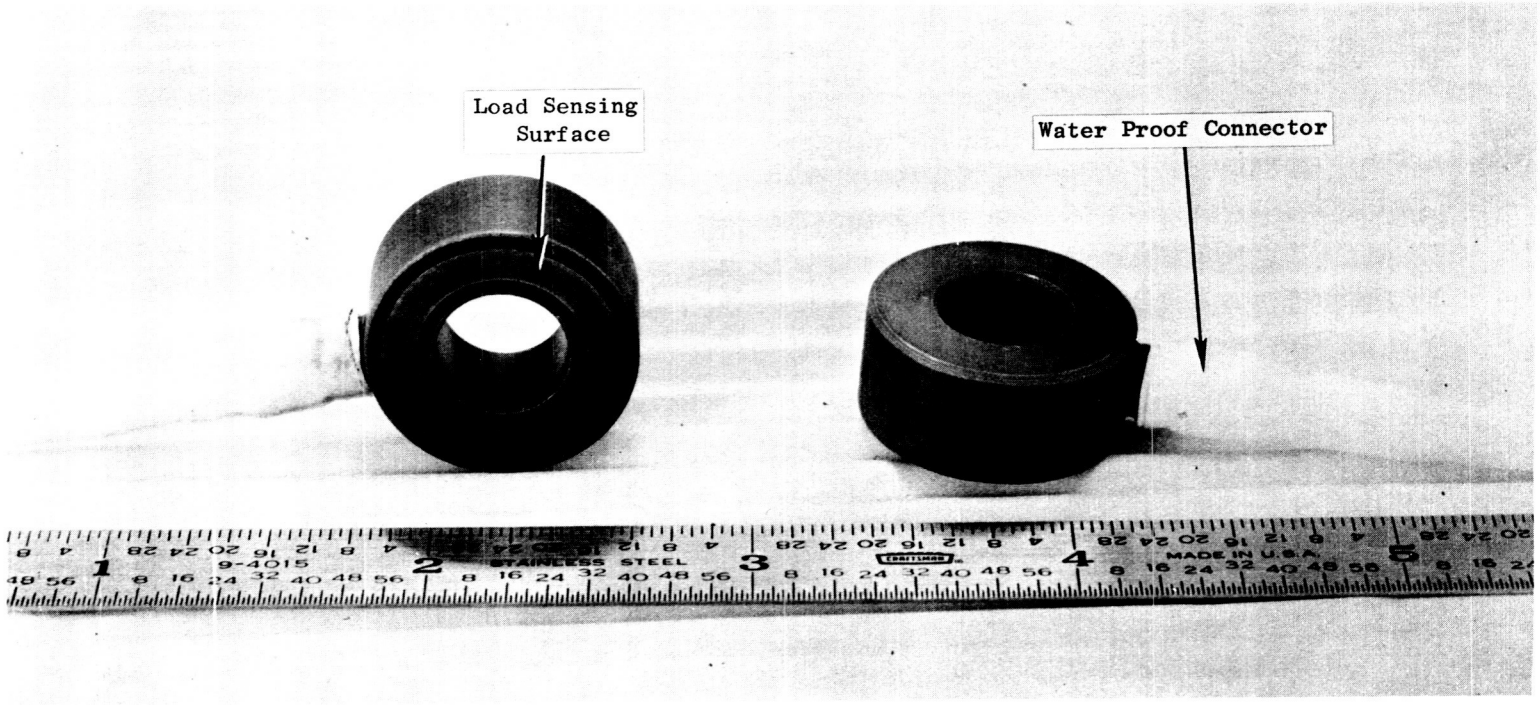

Figure 16. Kistler-Model 902A Piezoelectric Force Transducers.

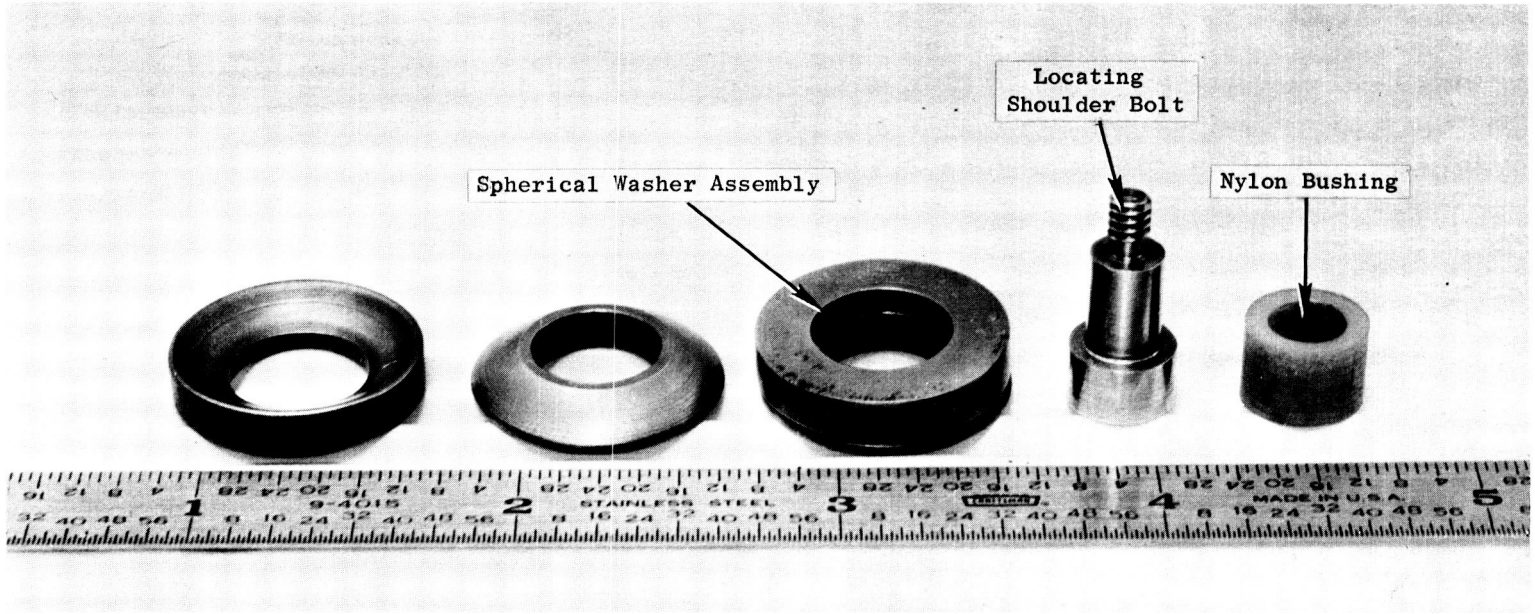

Figure 17. Kistler Force Transducer Assembly Components.

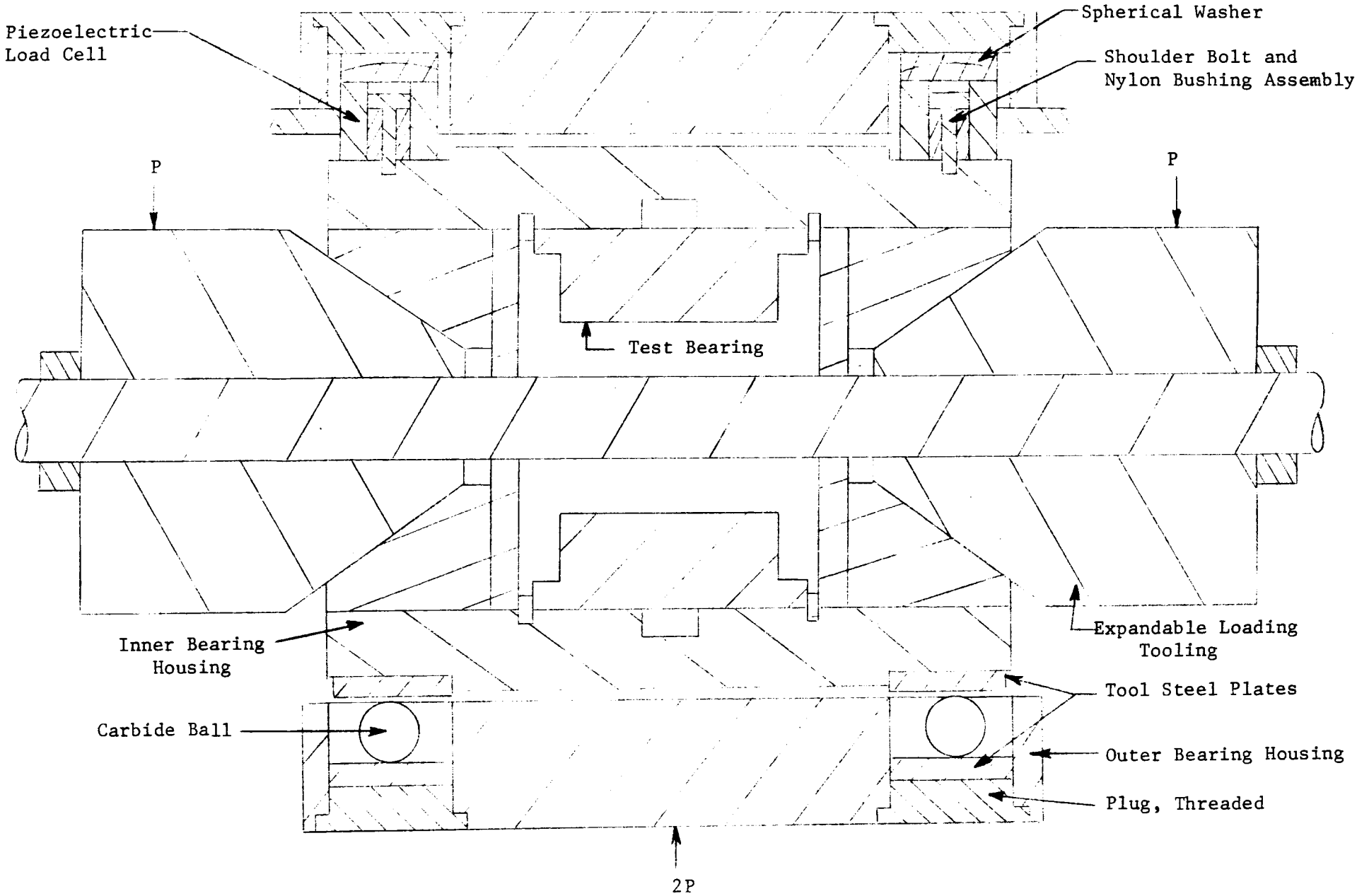

Figure 18. Assembled Force Transducer Calibration Setup.

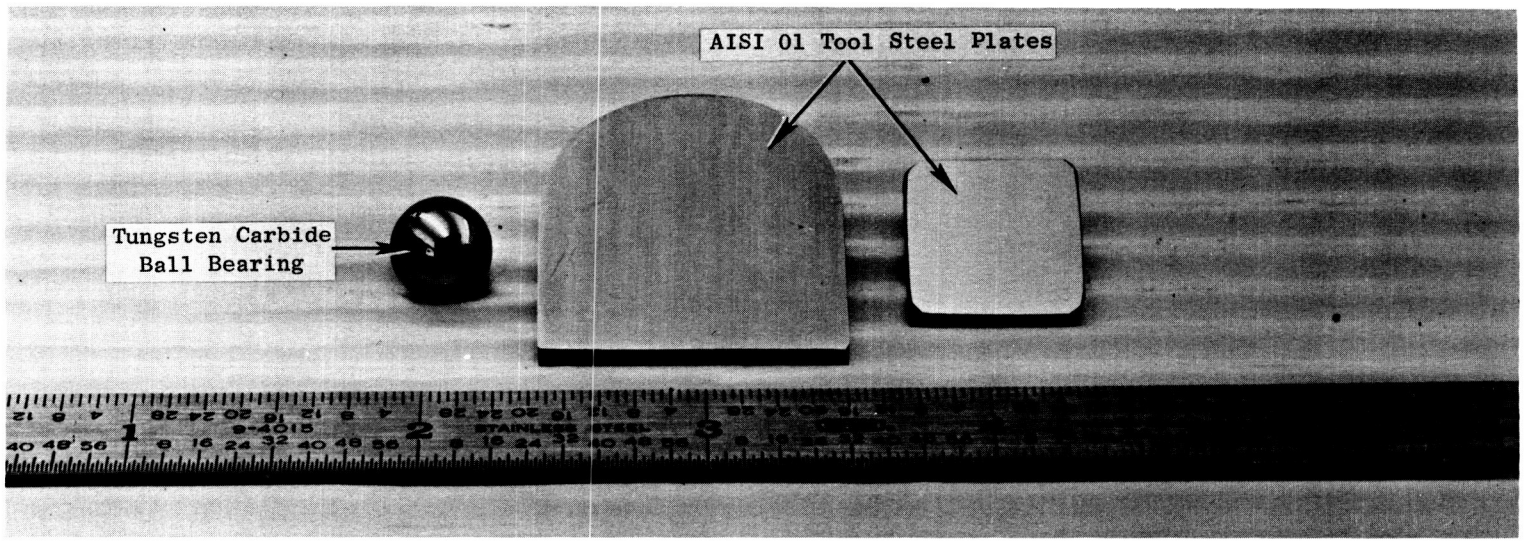

Figure 19. Force Transducer Assembly Components.

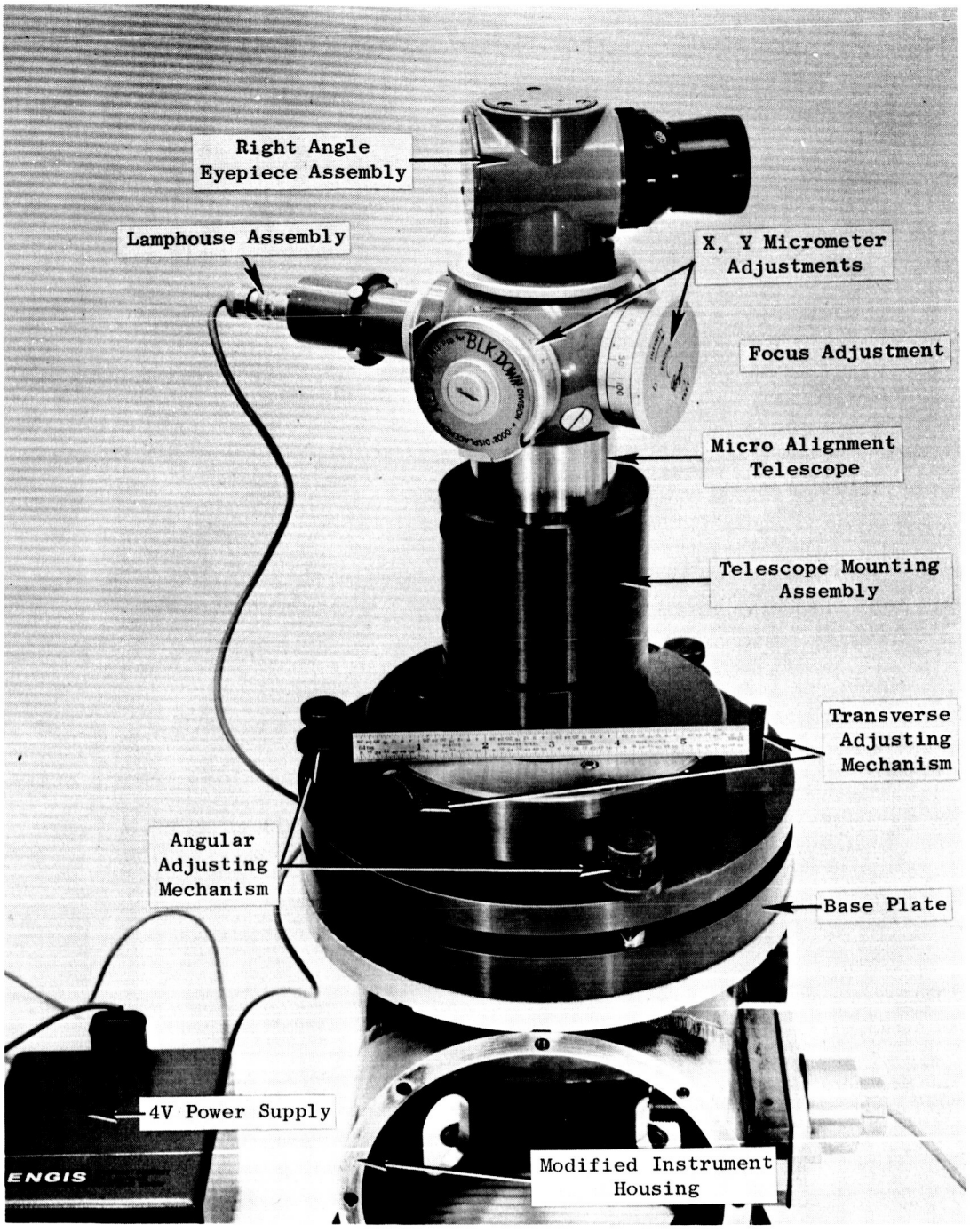

Figure 20. Micro Alignment Telescope and Mounting Assembly.

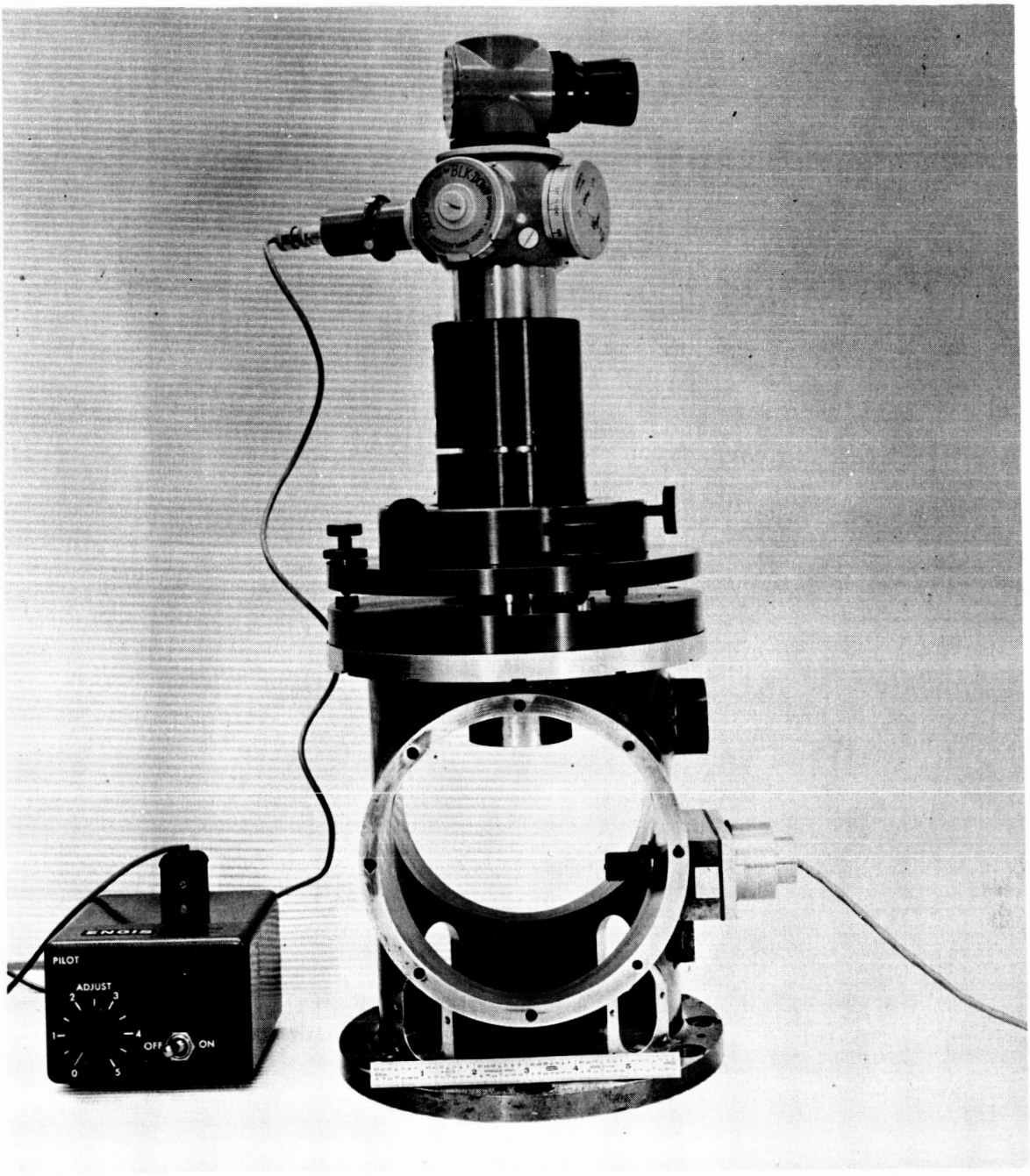

Figure 21. Micro Alignment Telescope and Mounting Assembly.

Part No.	Dia. A	Dia. B	Length
P1	1.2545 1.2544	1.2553 1.2552	3.260 3.240
P2	1.2525 1.2524	1.2533 1.2532	3.260 3.240

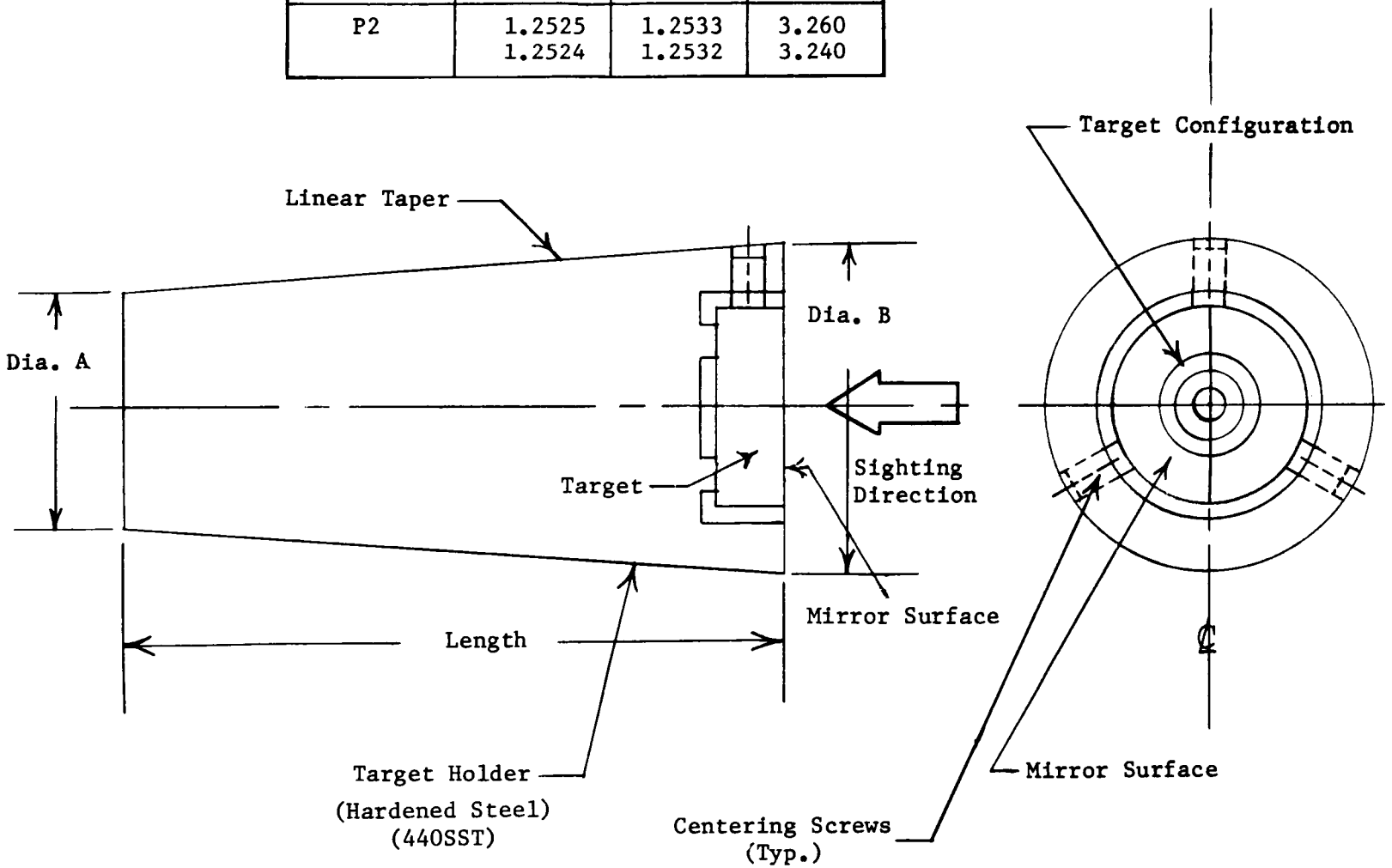

Figure 22. Reflecting Target Assembly.

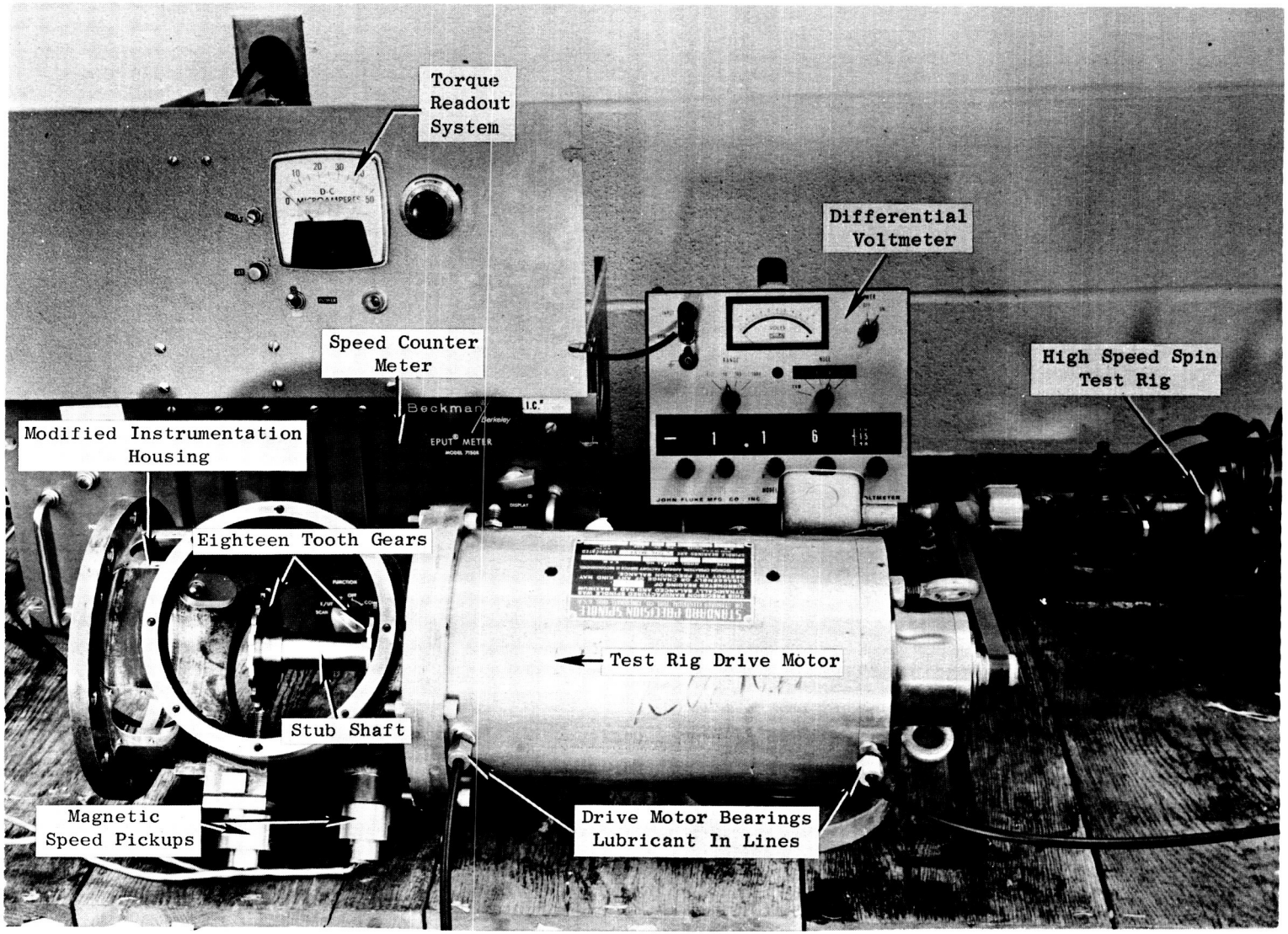

Figure 23. Torque Readout Calibration Rig.

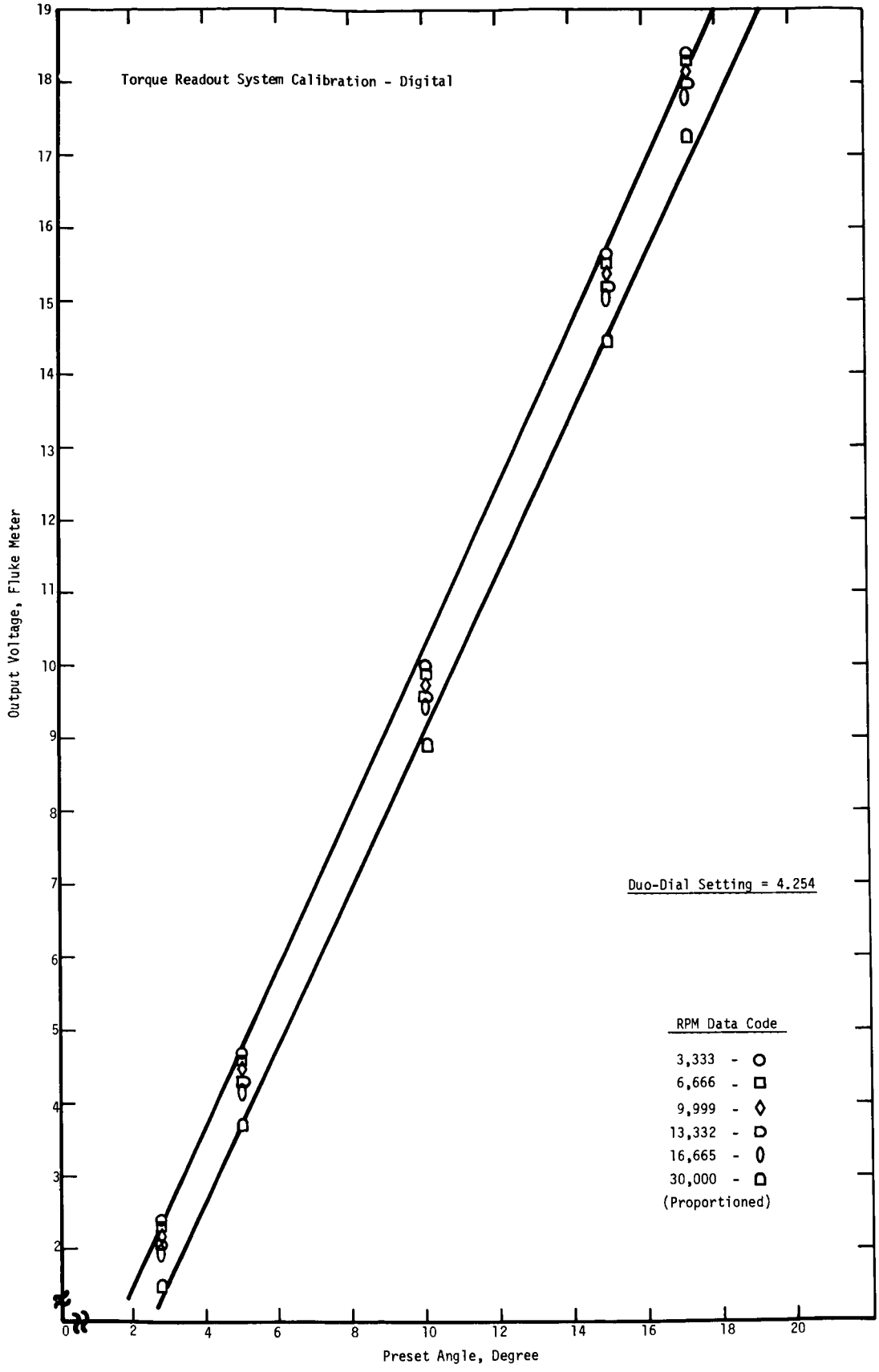

Figure 24. Output Voltage Verses Preset Phase Angle.

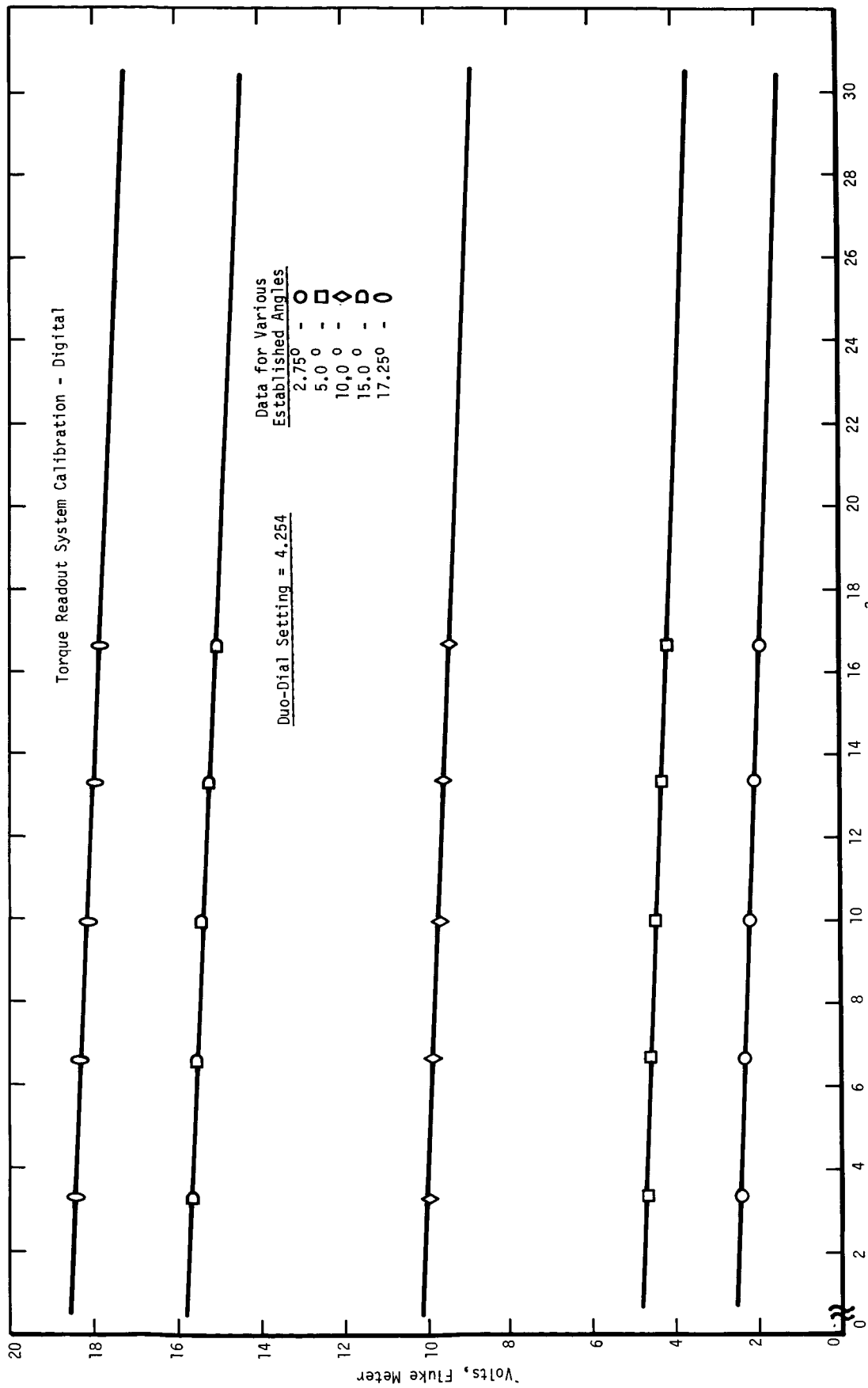

Figure 25. Speed Verses Volts.

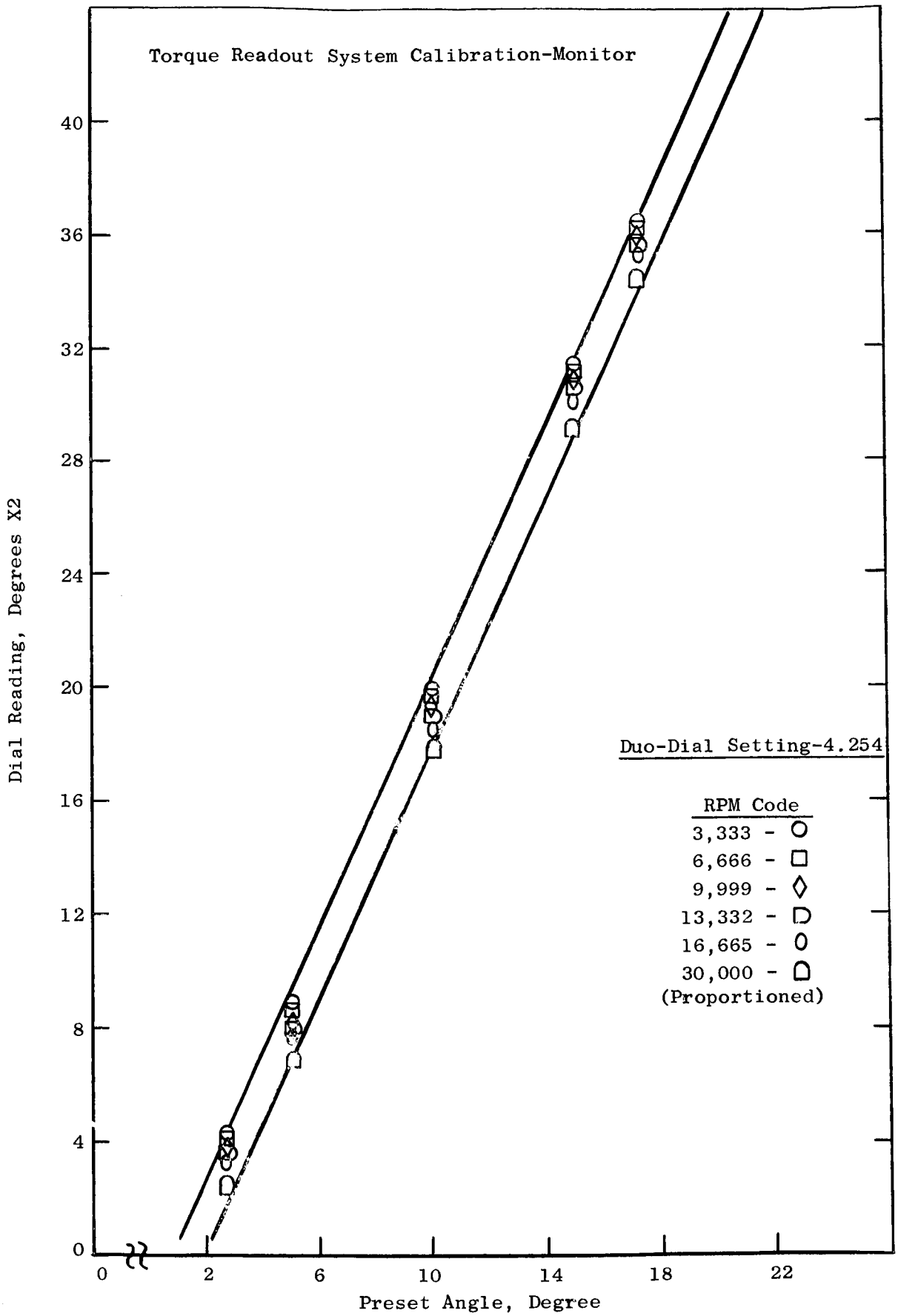

Figure 26. Degrees Verses Preset Angle.

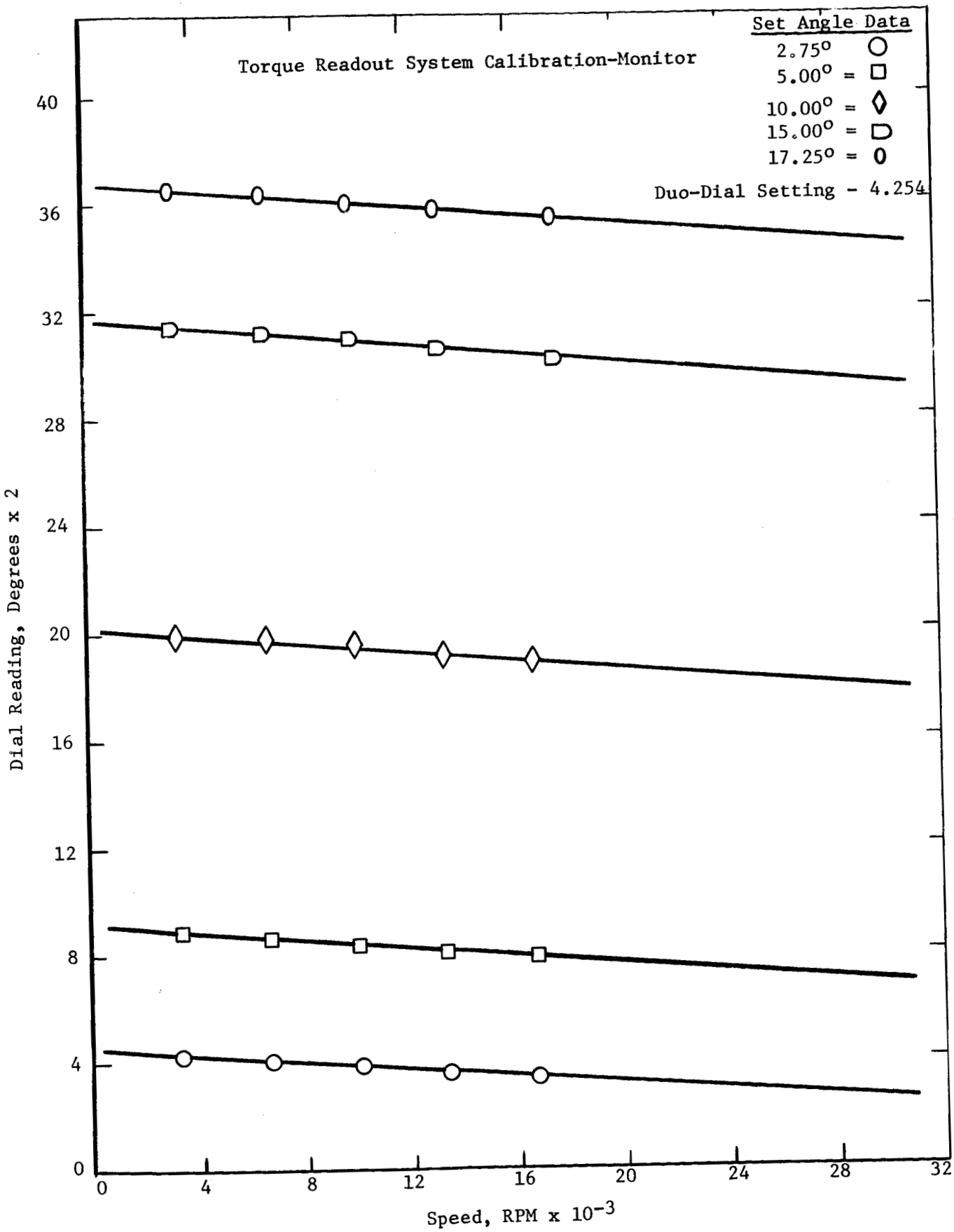

Figure 27. Speed Versus Degrees.

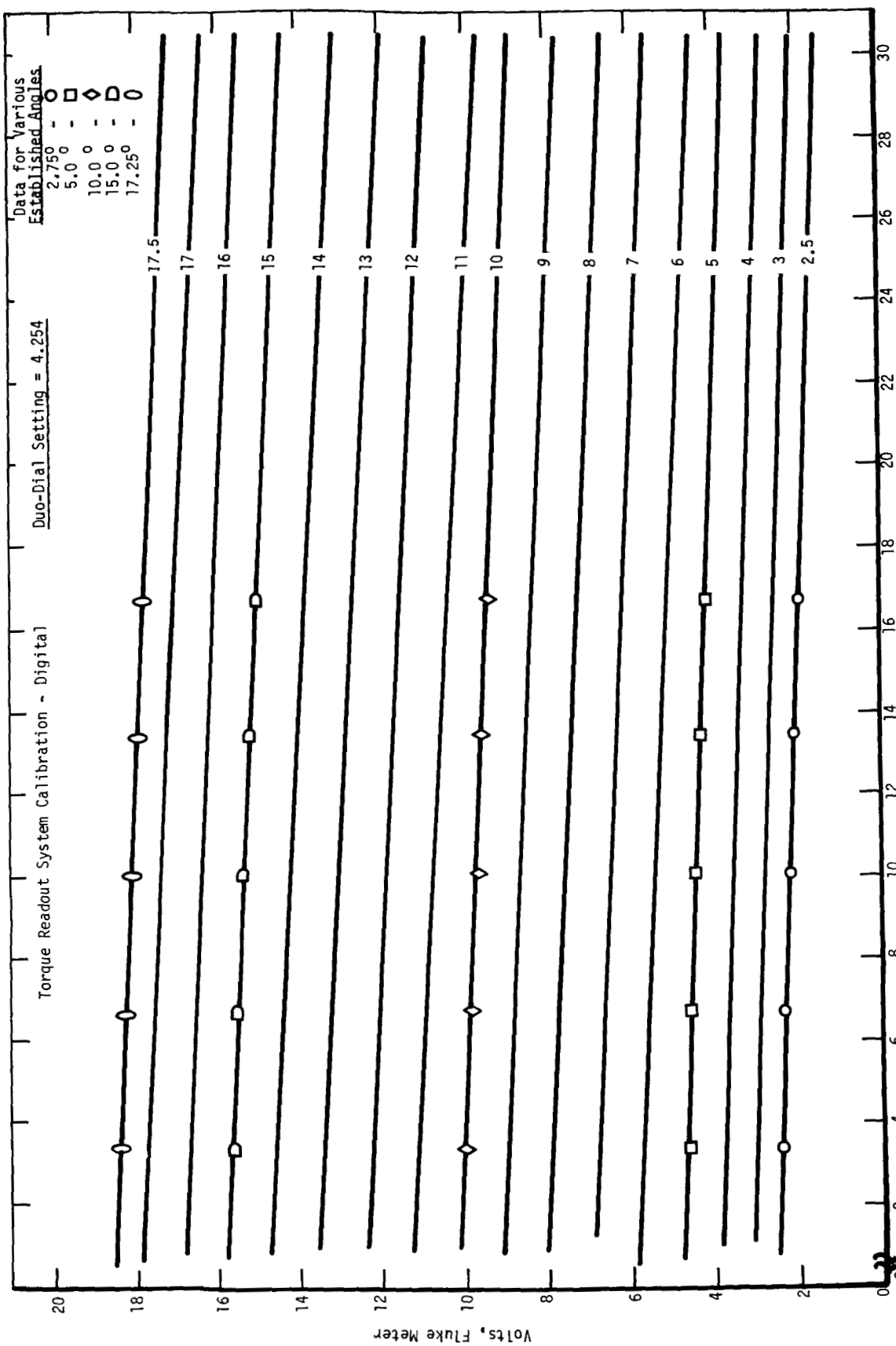

Figure 28. Speed Verses Volts.

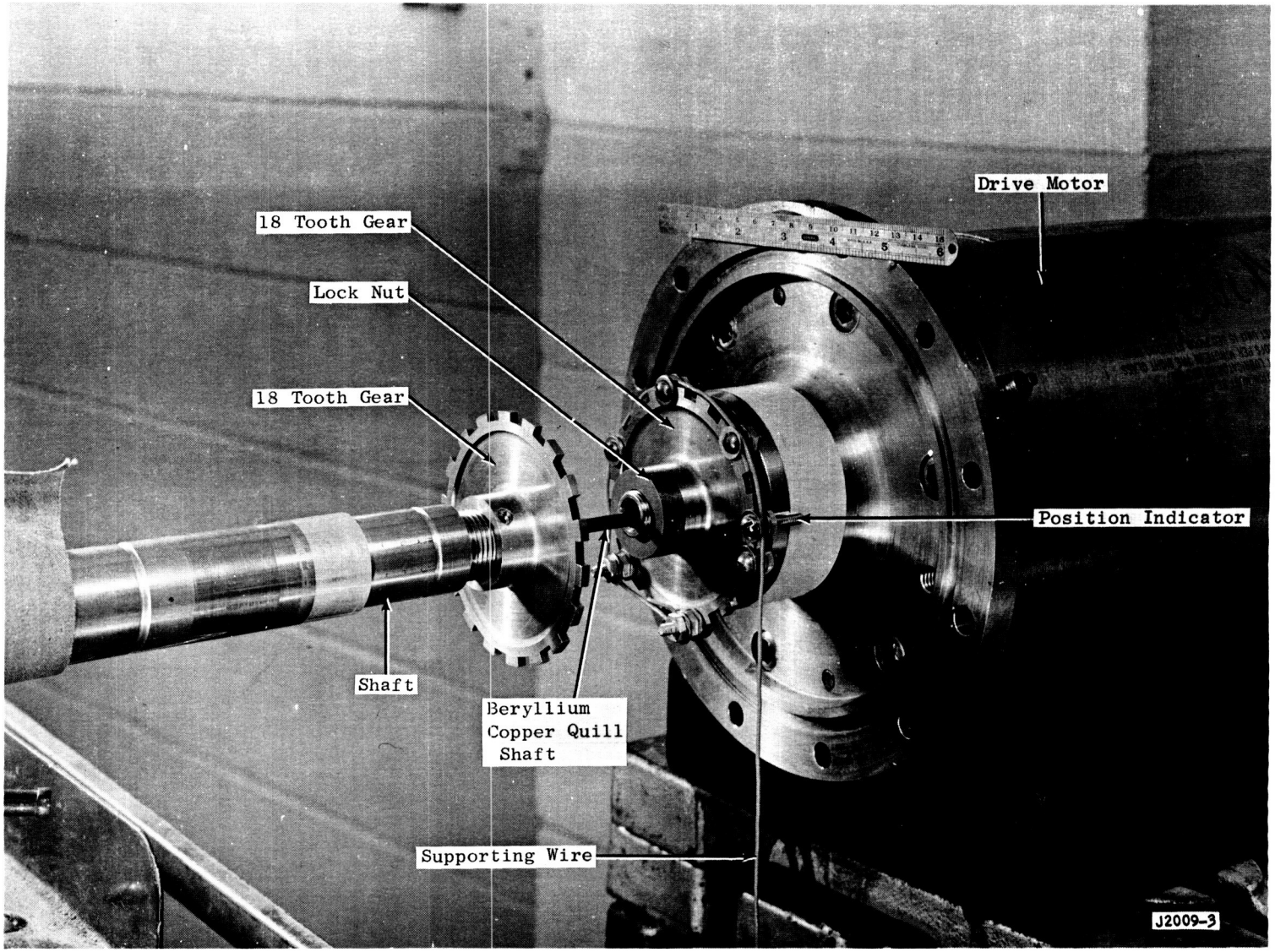

Figure 29. Torque Shaft Calibration System.

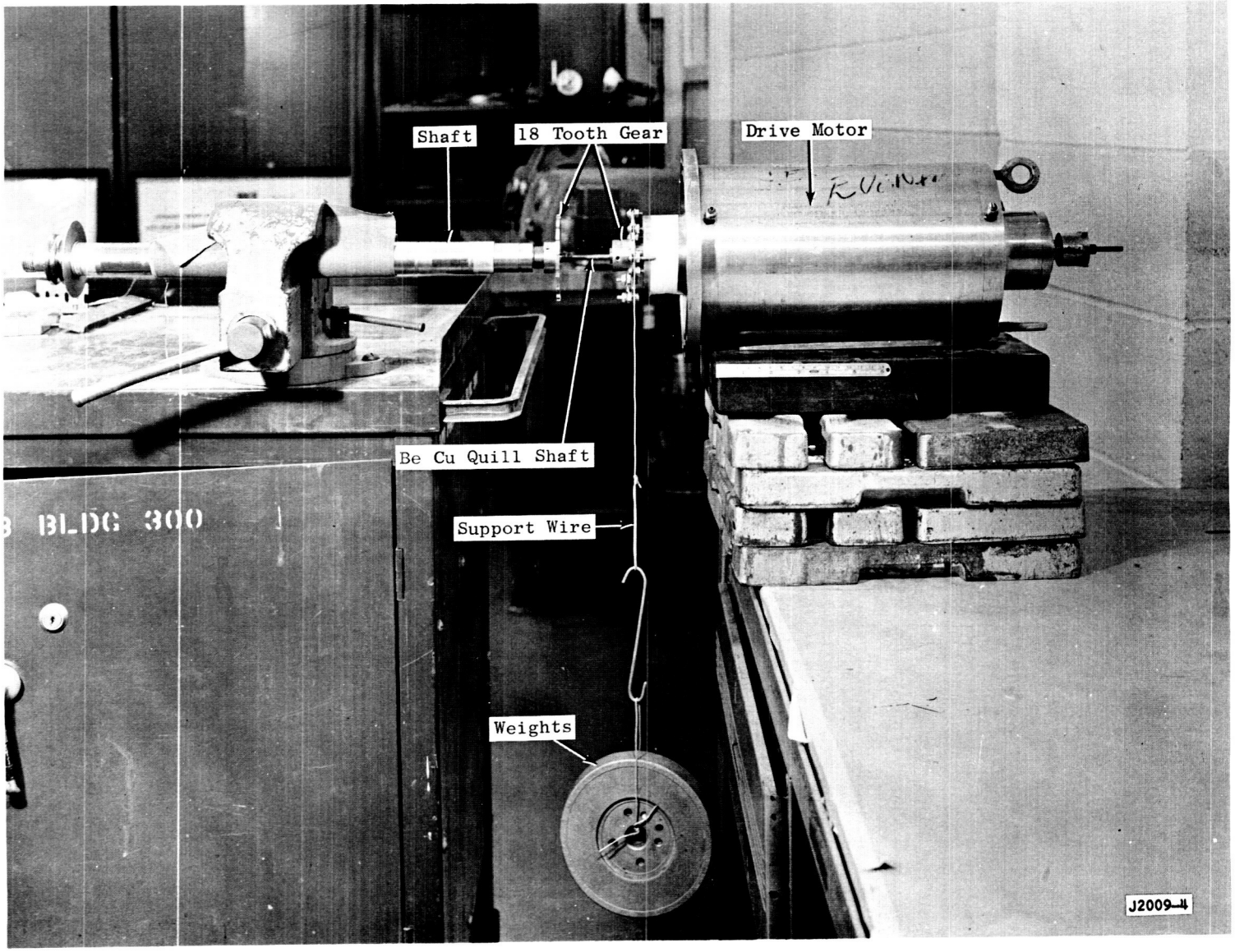

Figure 30. Torque Shaft Calibration System.

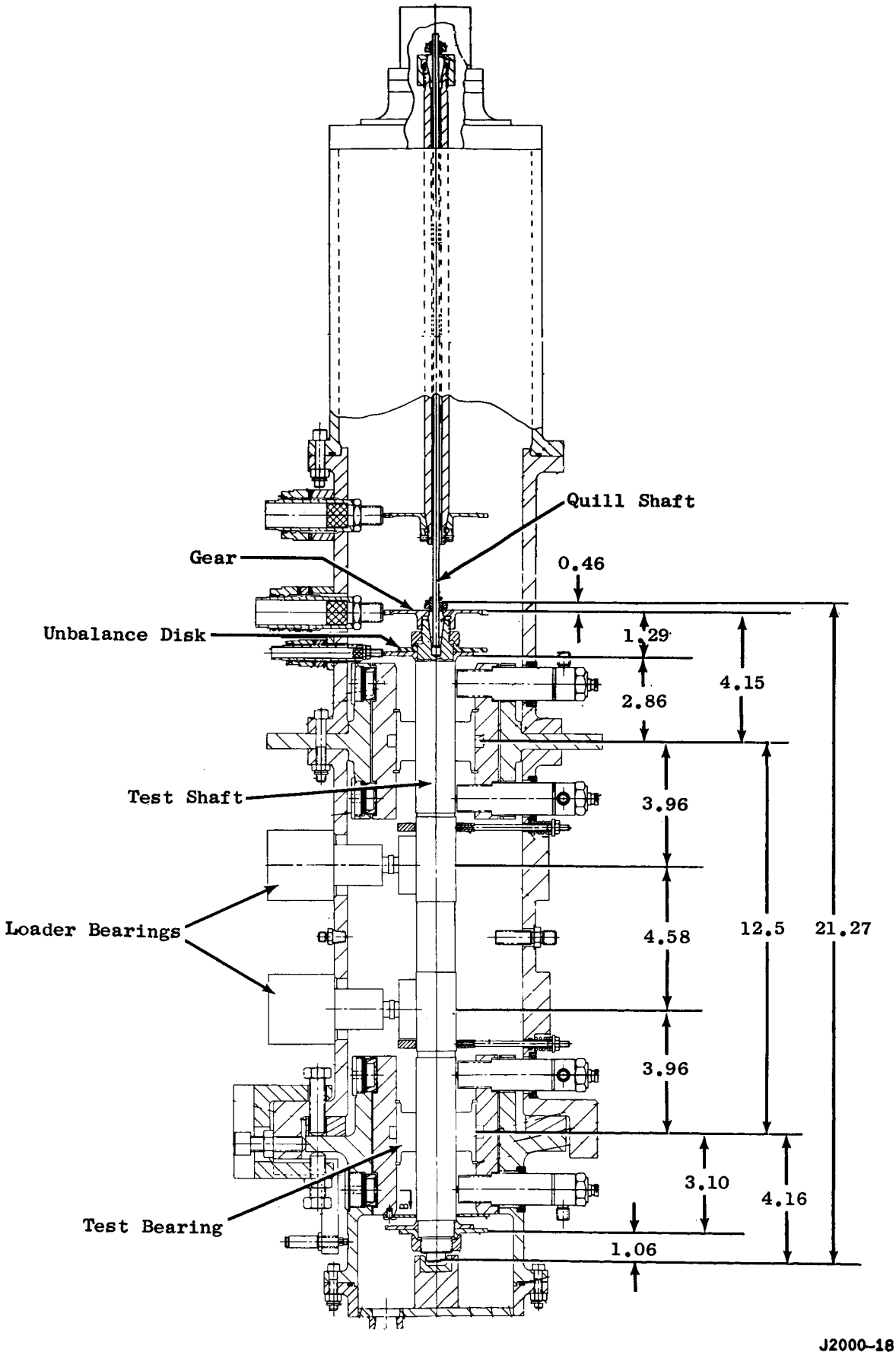

Figure 31. Hydrodynamic Journal Bearing Test Assembly.

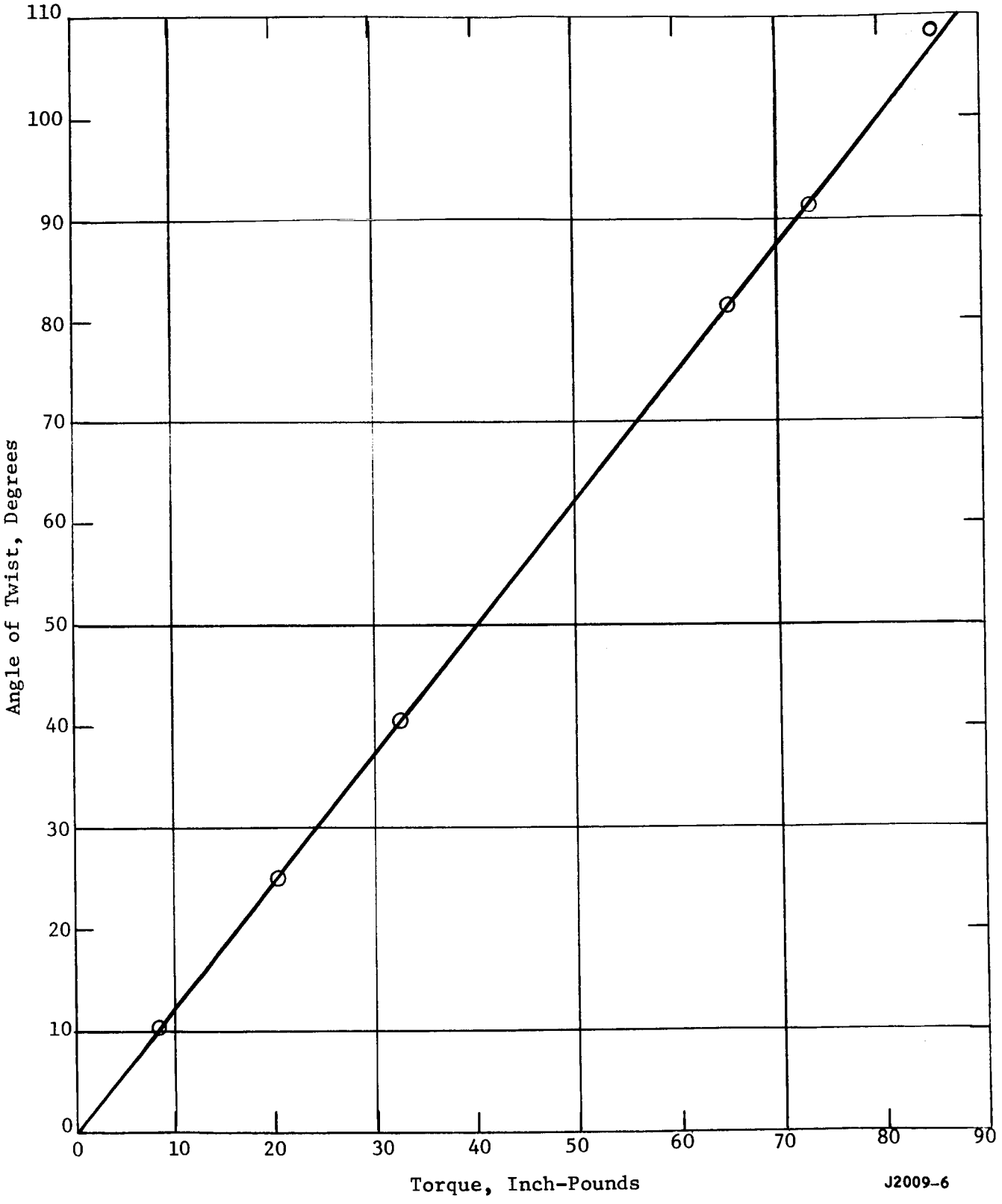

Figure 32. Torque Vs Angle of Twist Beryllium Copper Quill Shaft Number 0.188-1.

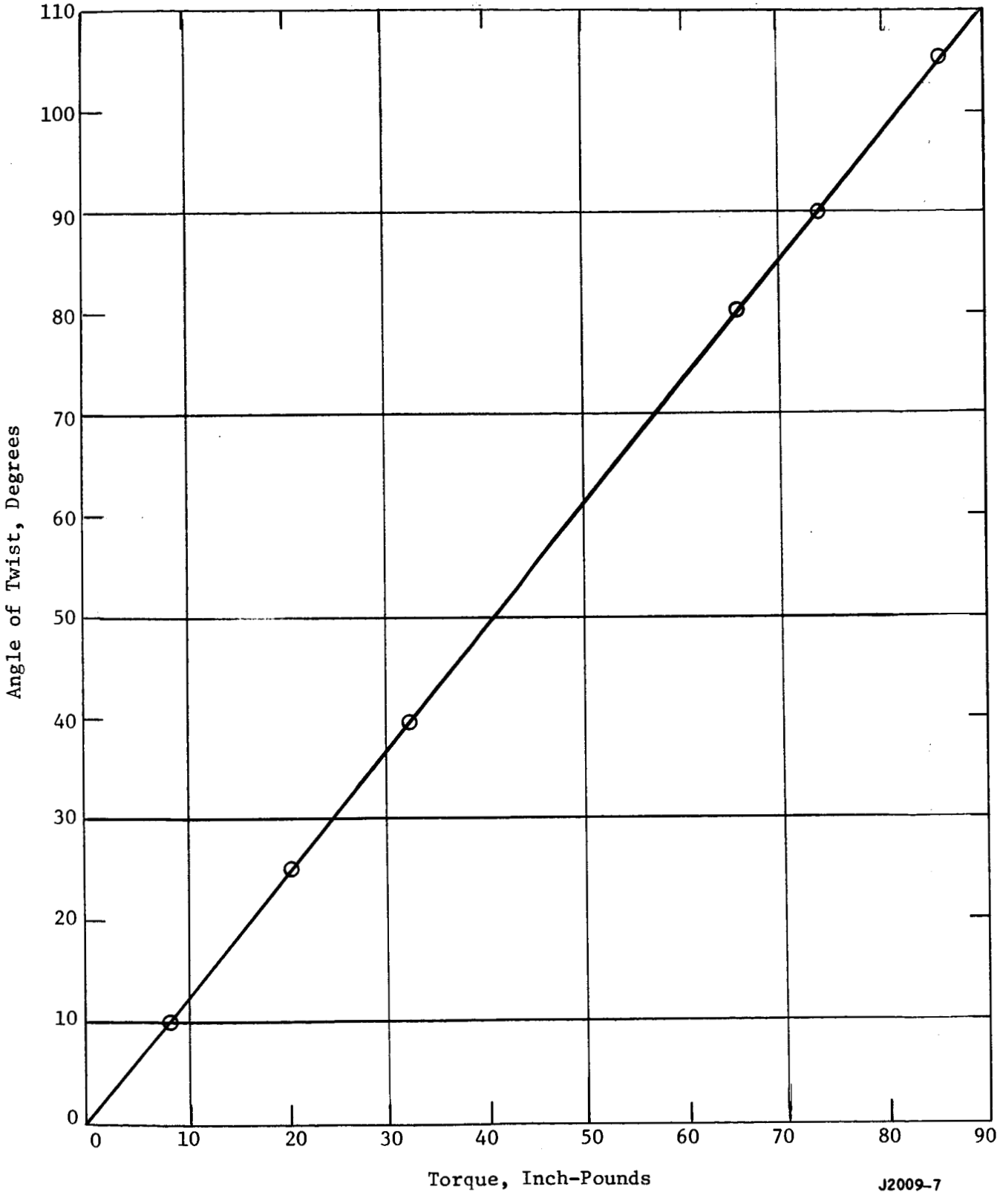

Figure 33. Torque Versus Angle of Twist Beryllium Copper Quill Shaft Number 0.188-2.

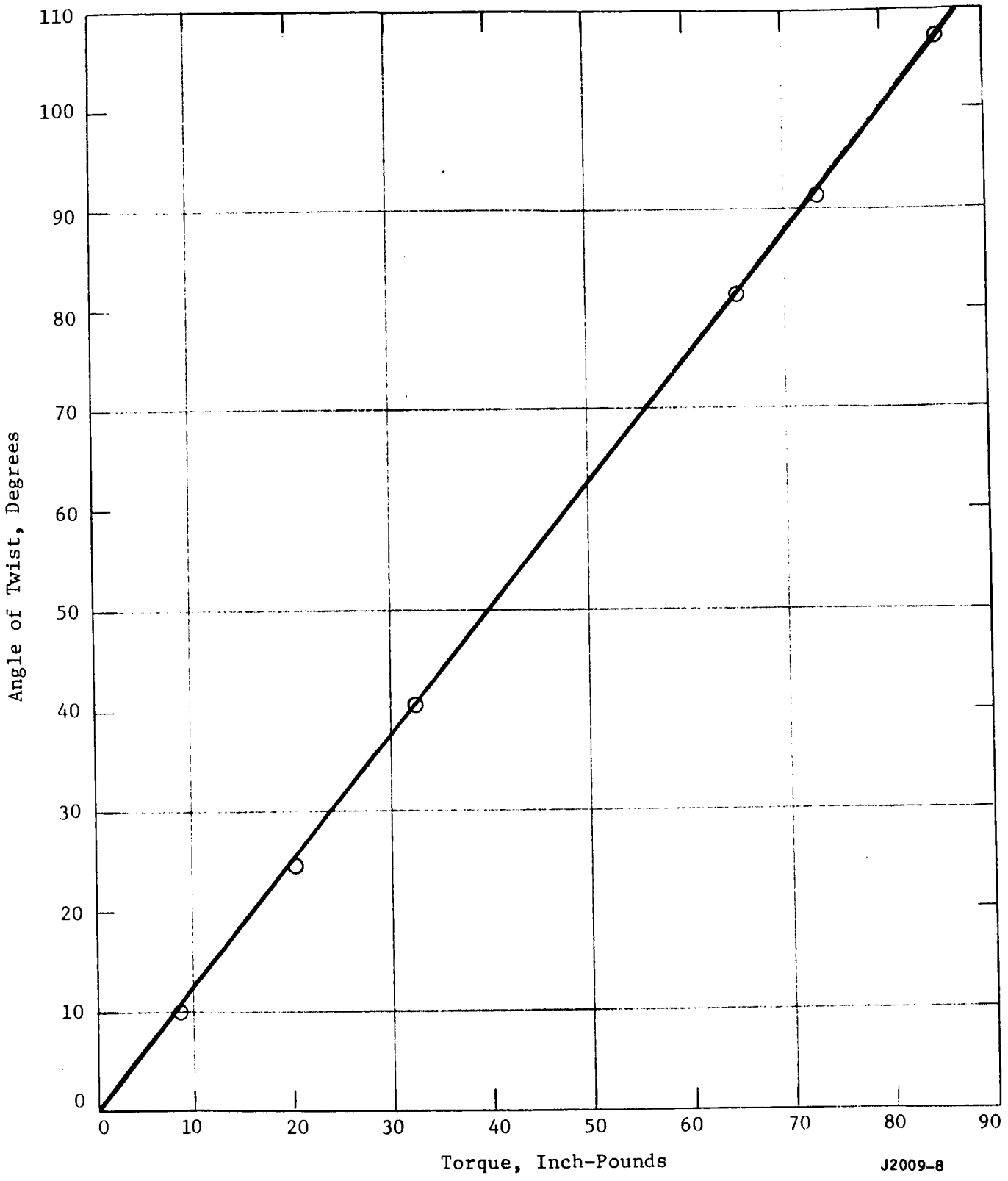

Figure 34. Torque Versus Angle of Twist Beryllium Copper Quill Shaft Number 0.188-3.

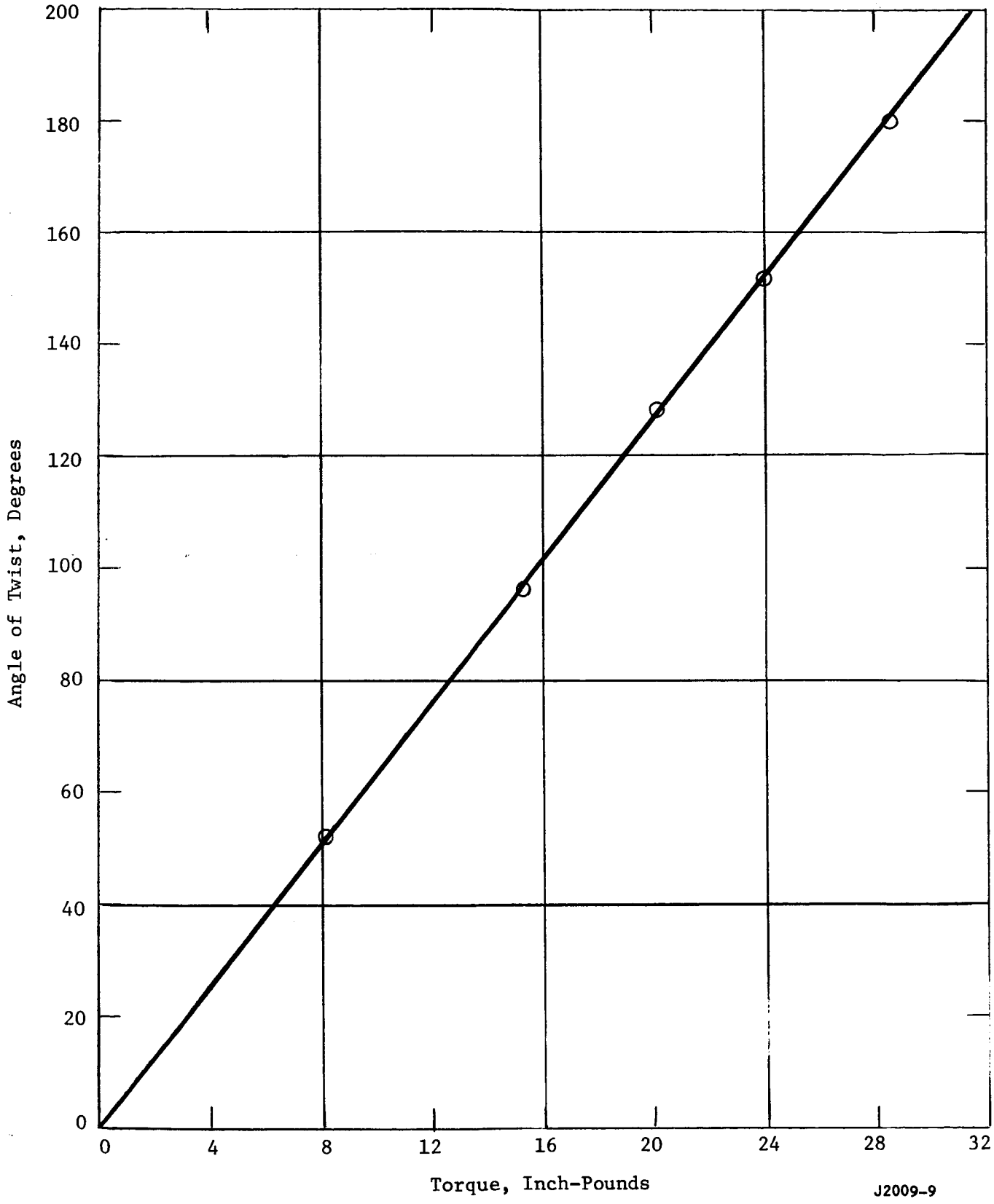

Figure 35. Torque Versus Angle of Twist Beryllium Copper Quill Shaft Number 0.125-3.

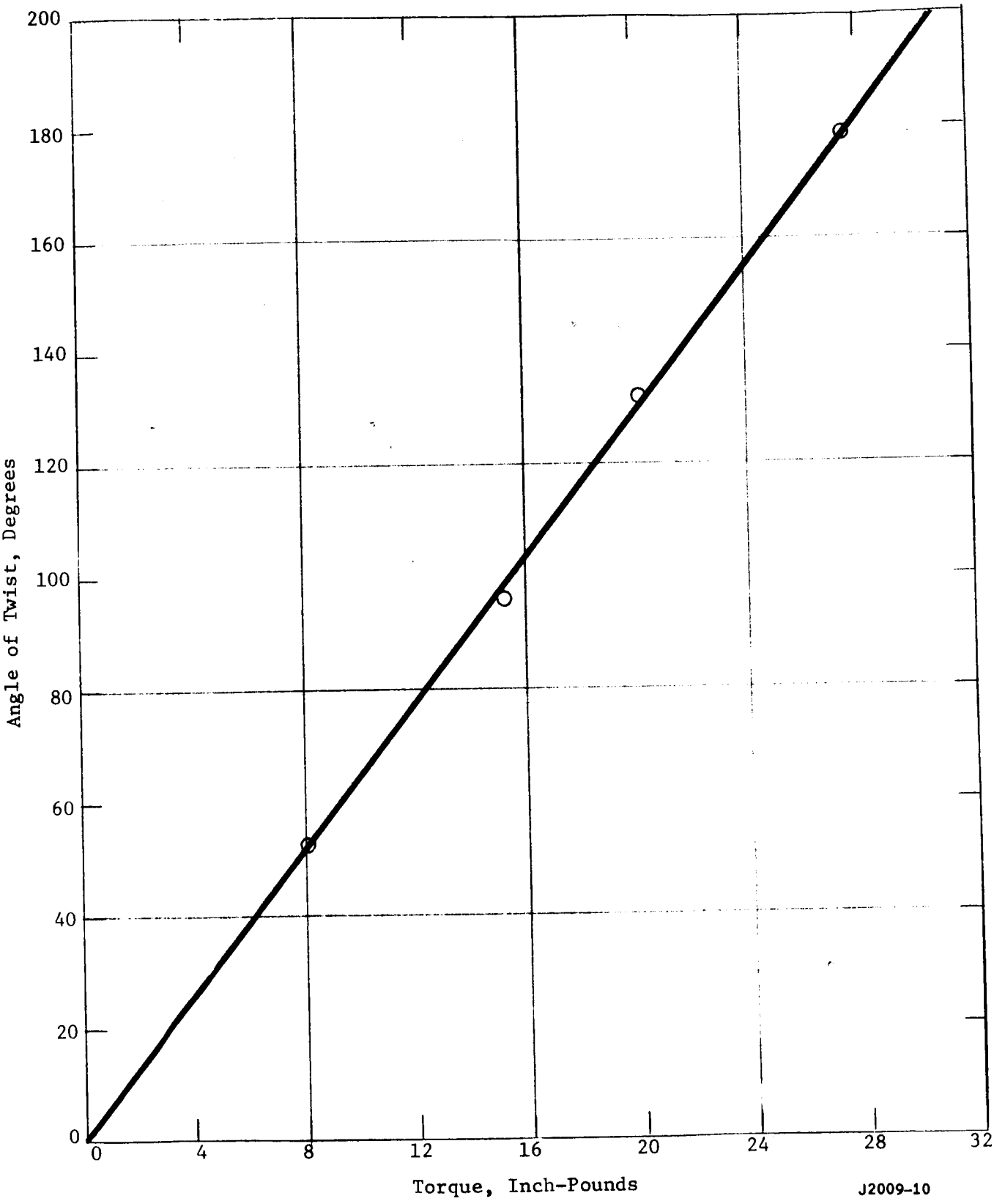

Figure 36. Torque Versus Angle of Twist Beryllium Copper Quill Shaft Number 0.125-4.

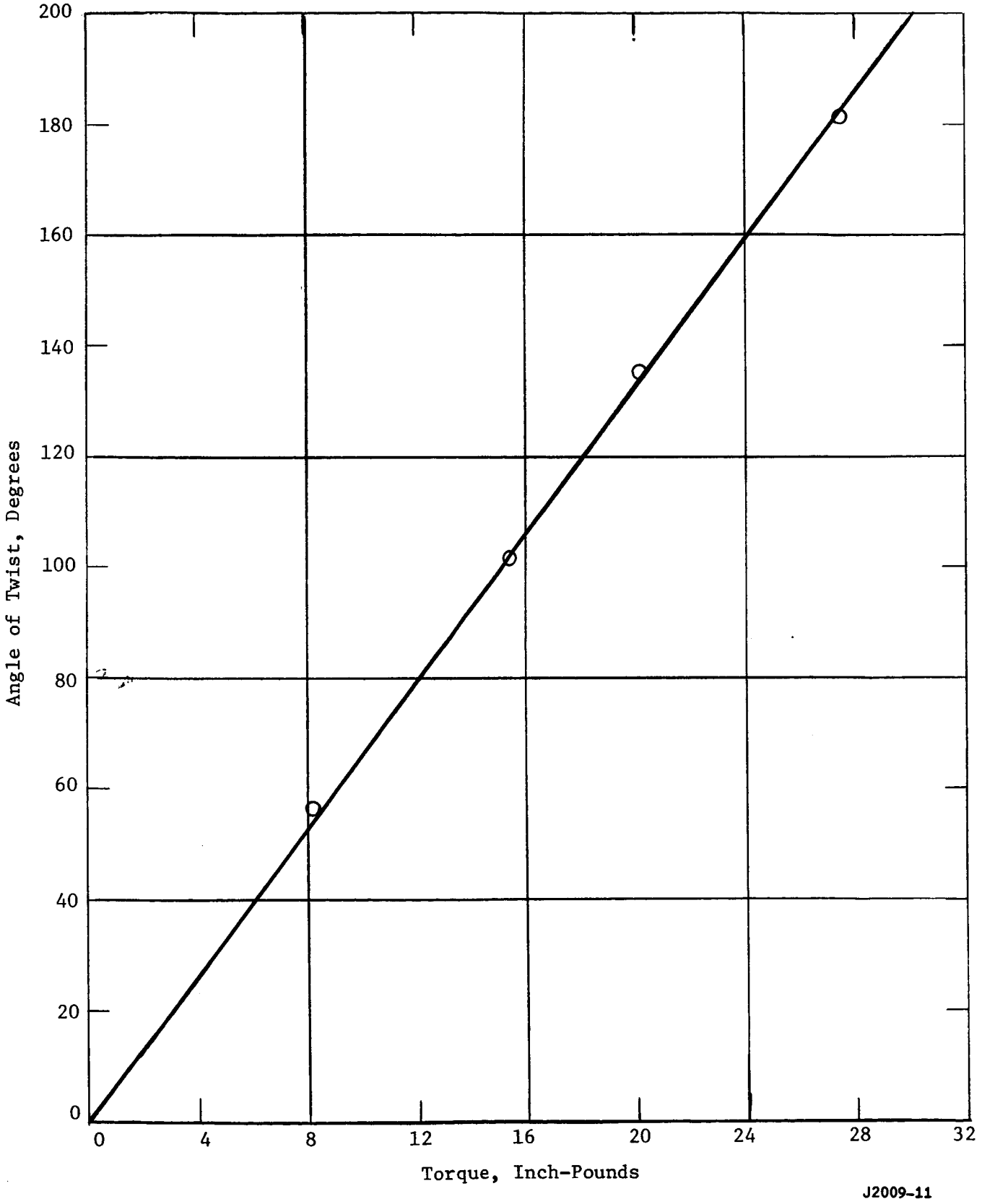

Figure 37. Torque Versus Angle of Twist Beryllium Copper Quill Shaft Number 0.125-5.

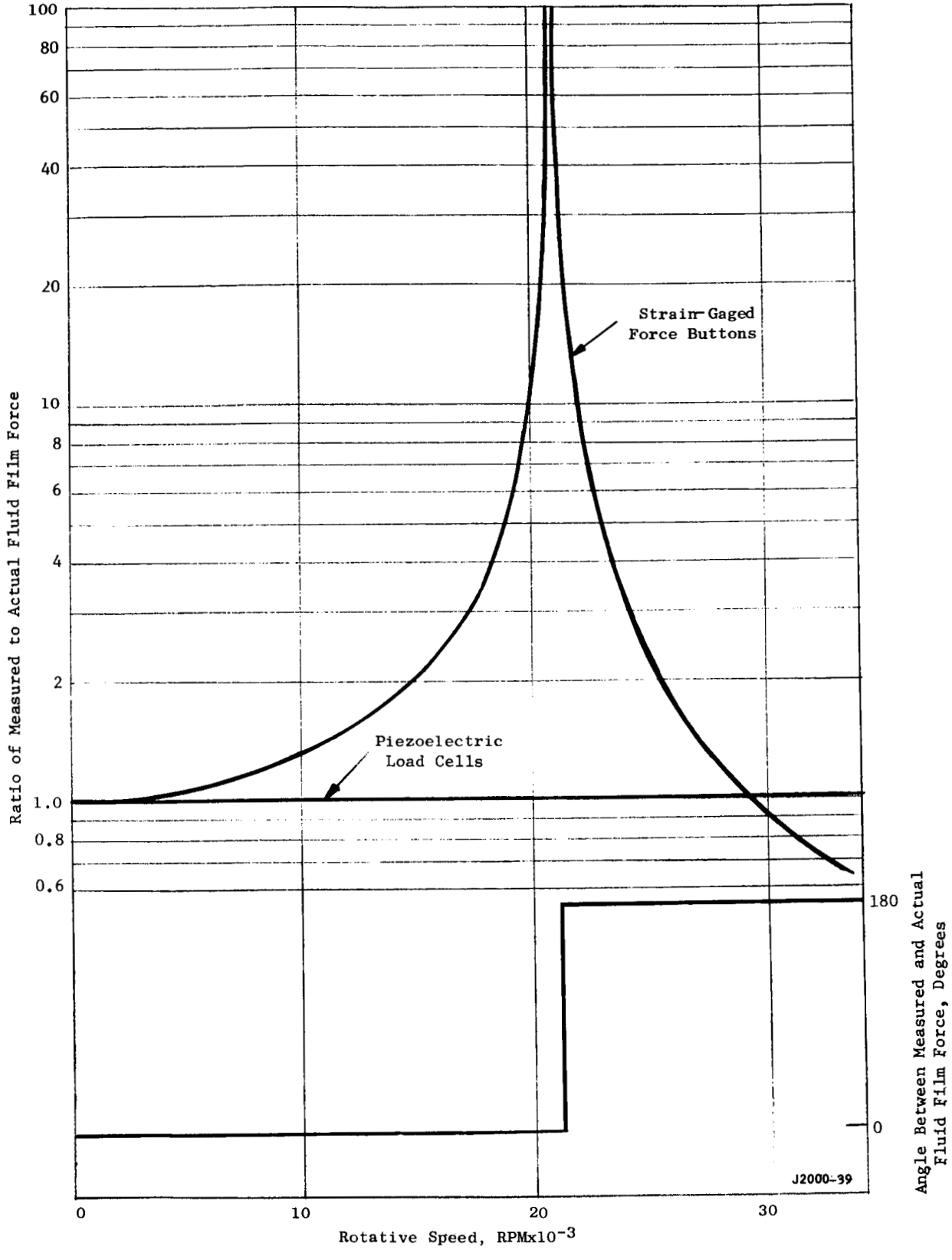

Figure 38. Effect of Force Sensor Selection on Force Measurement Errors.

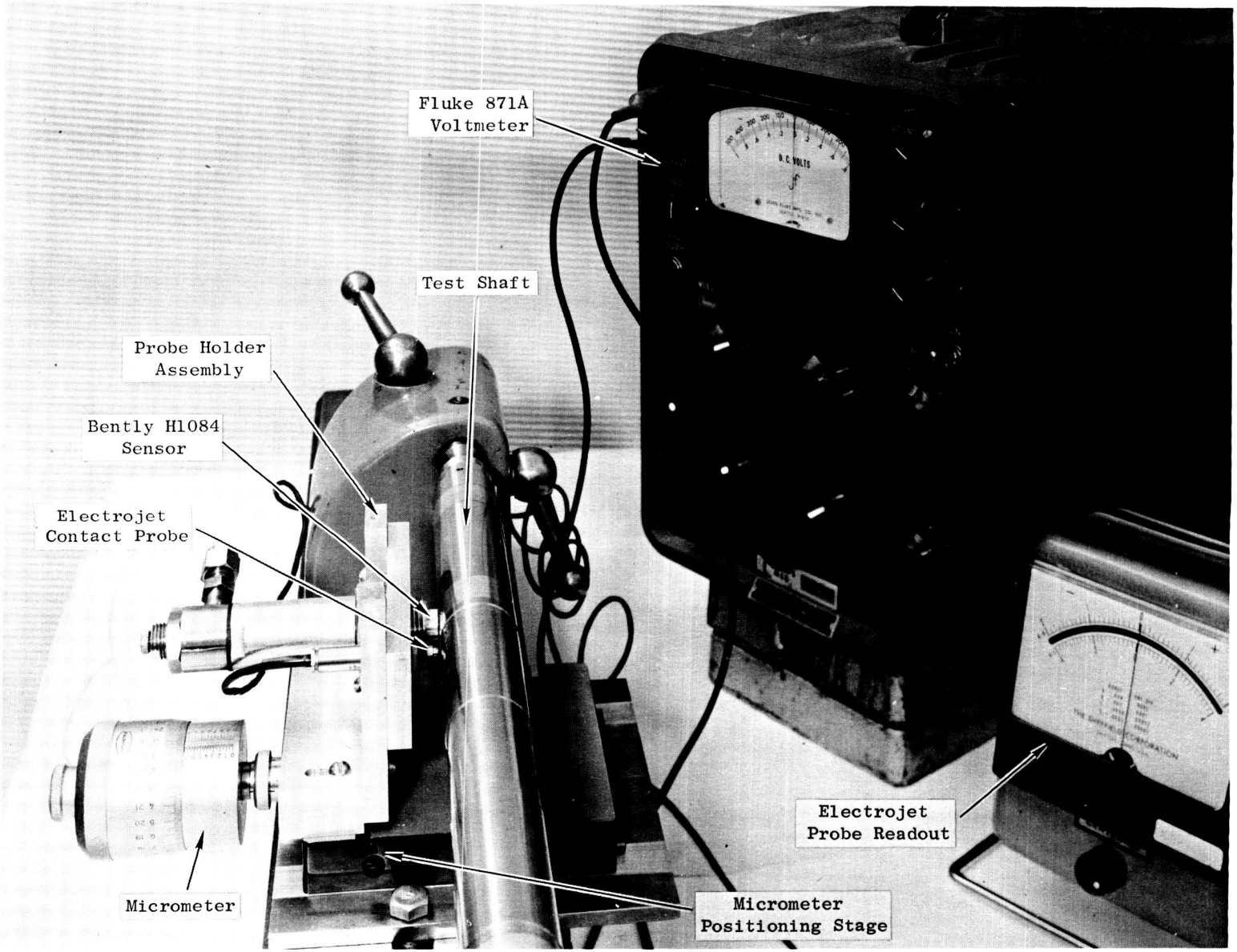

Figure 39. Apparatus for Static Calibration of Bently Probes.

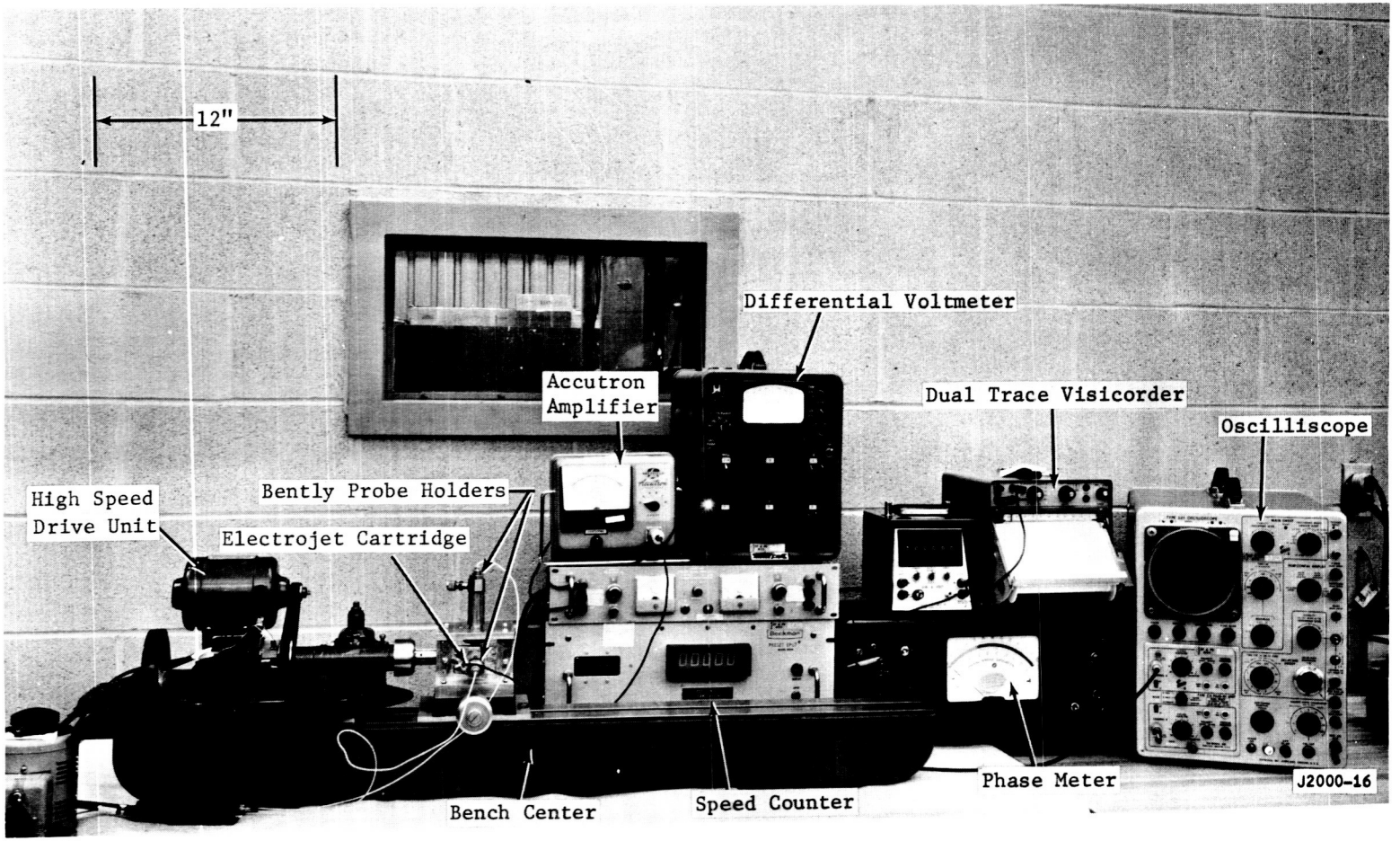

Figure 40. Electrojet Cartridge Calibration Setup.

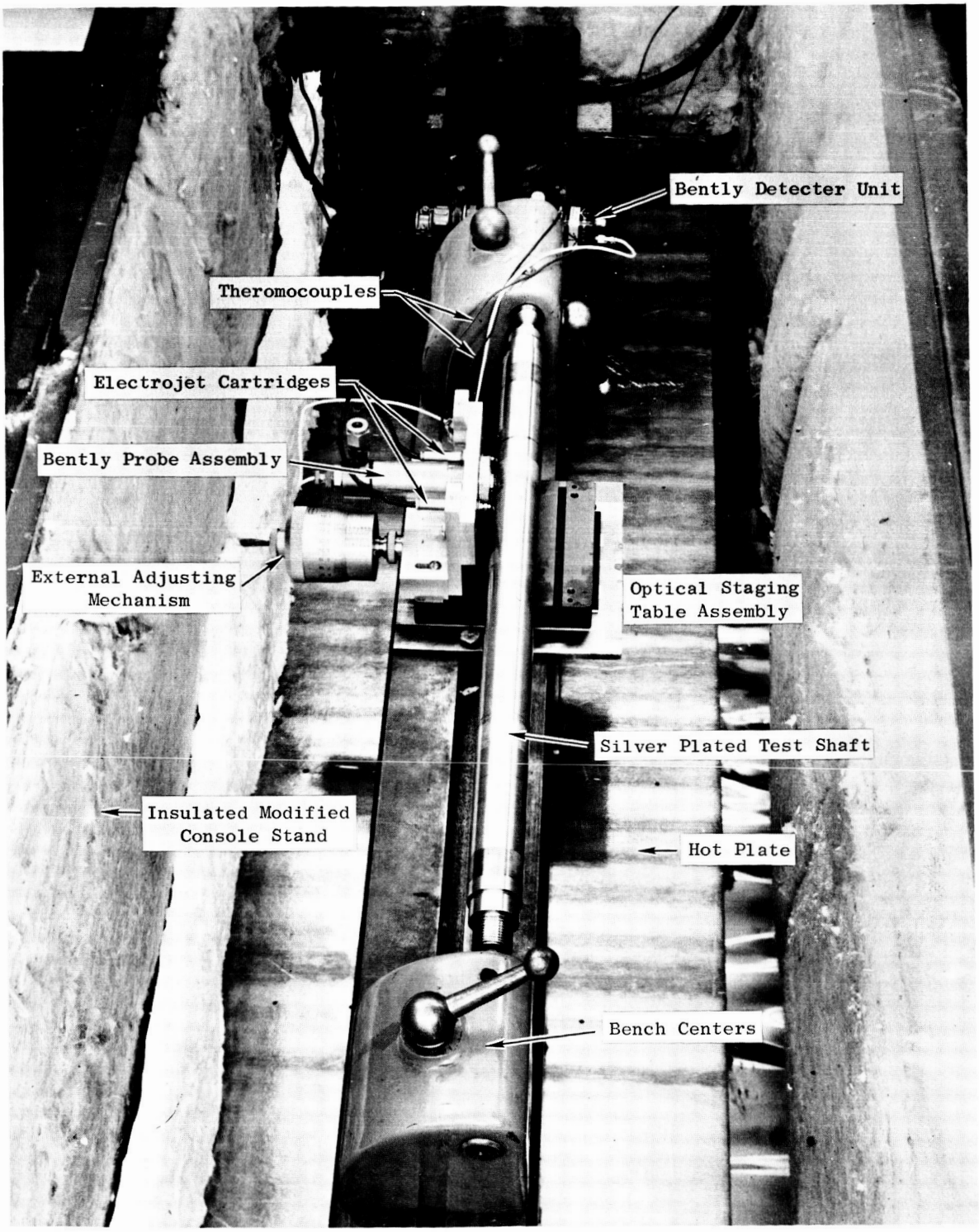

Figure 41. Bently Probe Elevated Temperature Calibration Test.

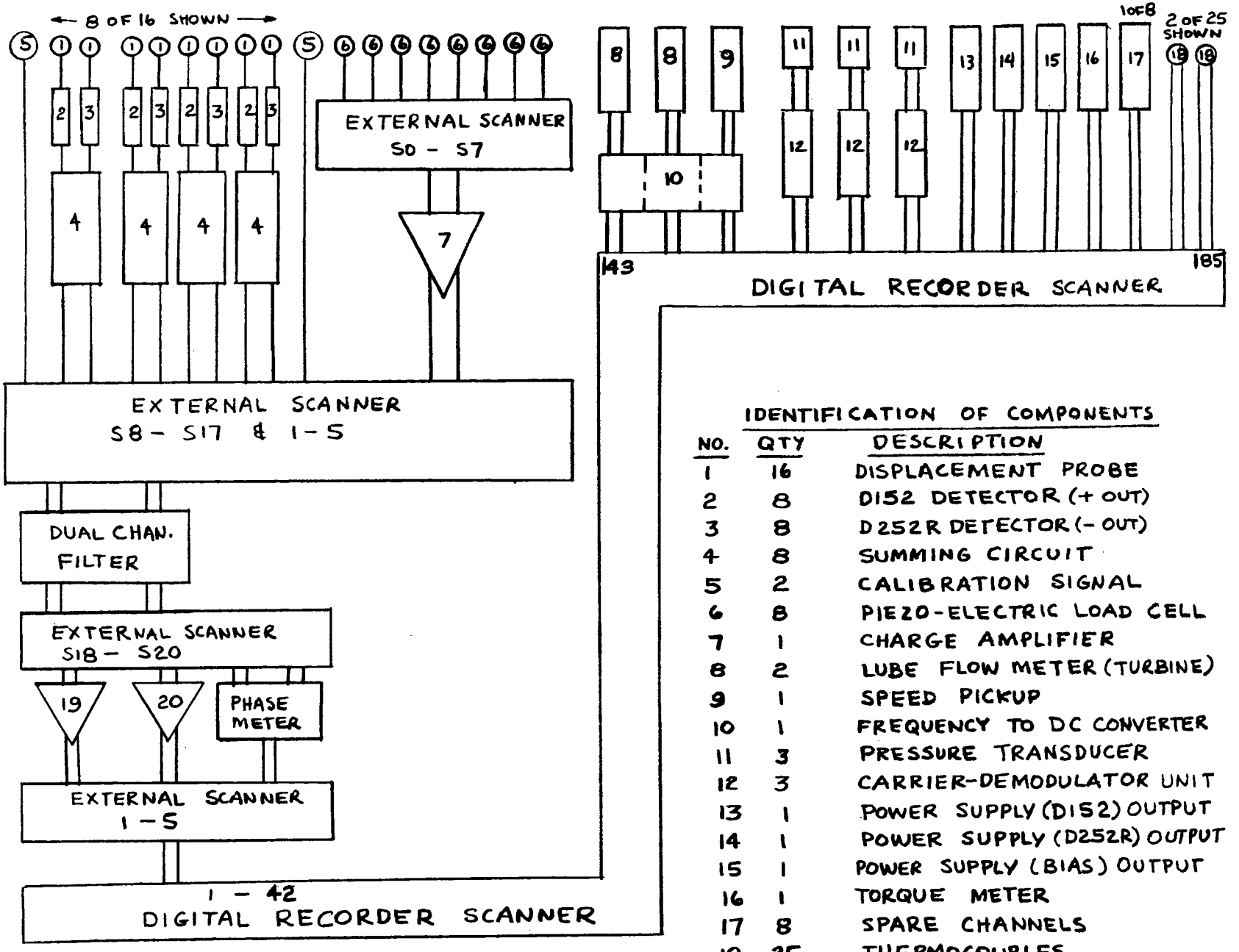

IDENTIFICATION OF COMPONENTS

NO.	QTY	DESCRIPTION
1	16	DISPLACEMENT PROBE
2	8	D152 DETECTOR (+ OUT)
3	8	D252R DETECTOR (- OUT)
4	8	SUMMING CIRCUIT
5	2	CALIBRATION SIGNAL
6	8	PIEZO-ELECTRIC LOAD CELL
7	1	CHARGE AMPLIFIER
8	2	LUBE FLOW METER (TURBINE)
9	1	SPEED PICKUP
10	1	FREQUENCY TO DC CONVERTER
11	3	PRESSURE TRANSDUCER
12	3	CARRIER-DEMODULATOR UNIT
13	1	POWER SUPPLY (D152) OUTPUT
14	1	POWER SUPPLY (D252R) OUTPUT
15	1	POWER SUPPLY (BIAS) OUTPUT
16	1	TORQUE METER
17	8	SPARE CHANNELS
18	25	THERMOCOUPLES
19	1	PEAK TO PEAK DETECTOR
20	1	AVERAGE LEVEL DETECTOR

J2008-4

Figure 42. System Scanning Network.

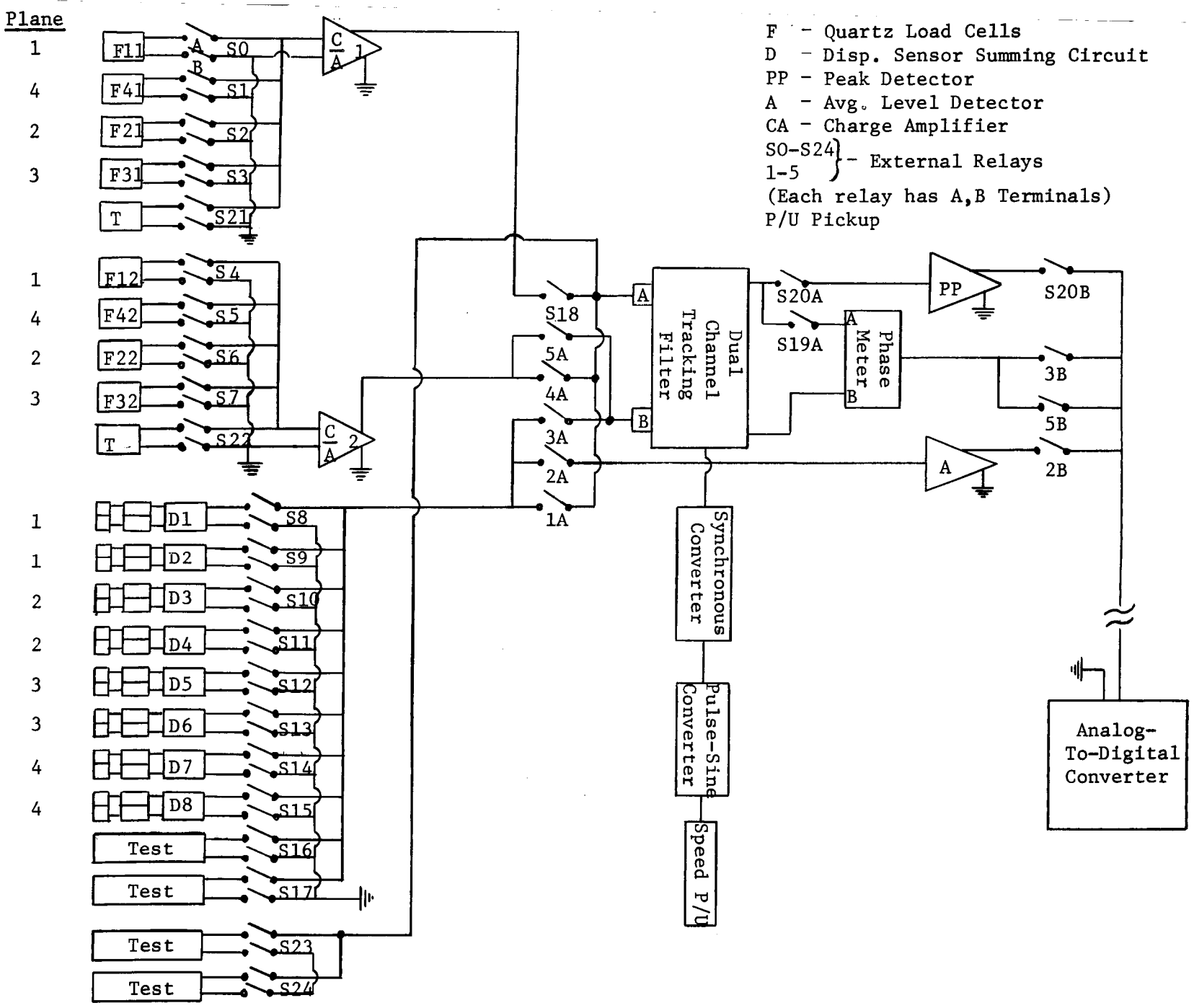

Figure 43. External Switching Network.

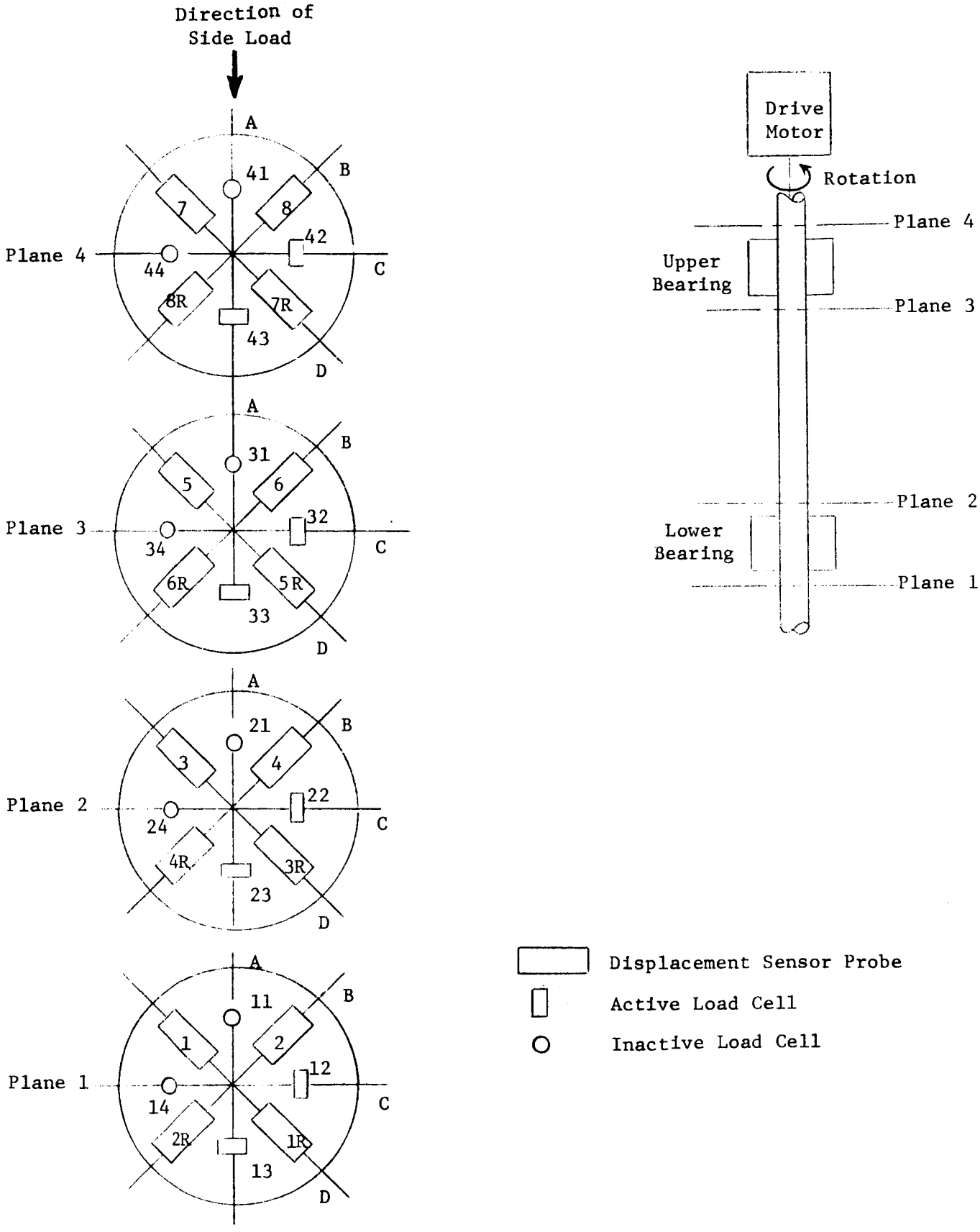

Figure 44. Hydrodynamic Journal Bearing Test Rig Force And Displacement Instrumentation. (Looking Downward)

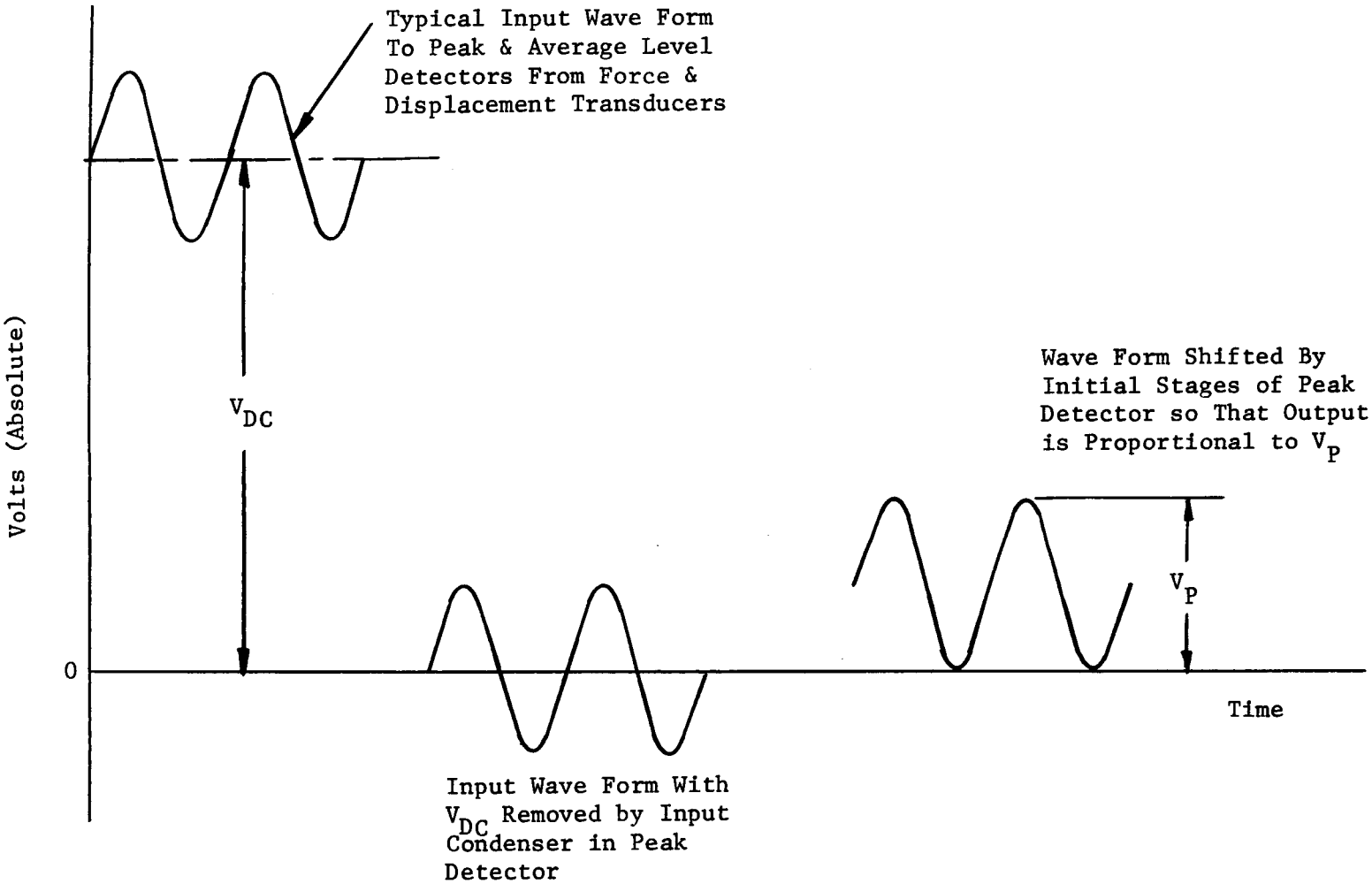

Figure 45. Typical Waveform Description Showing Desired Parameters.

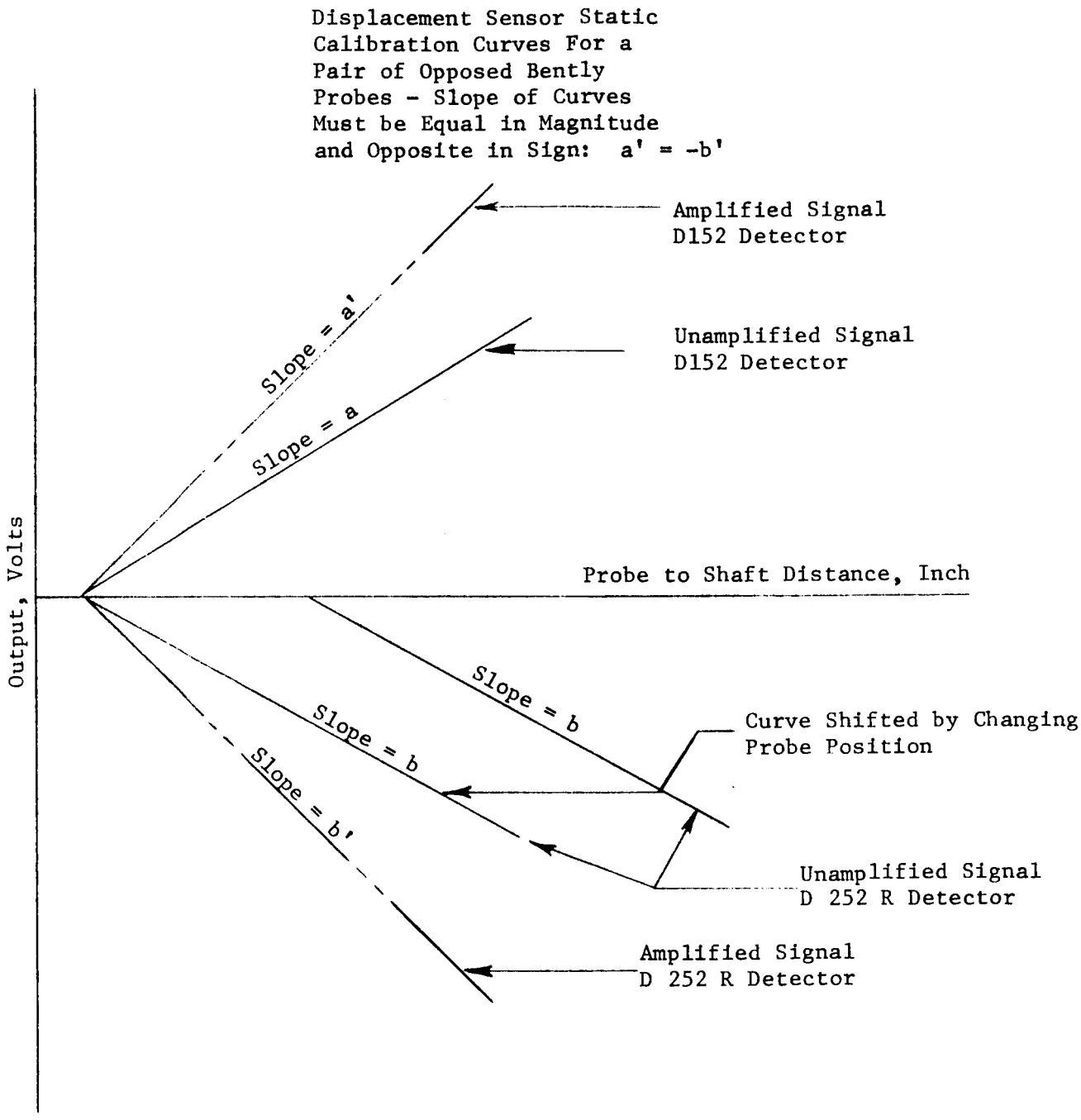

Figure 46. Adjustments Performed in Displacement Sensor Summing Circuits.

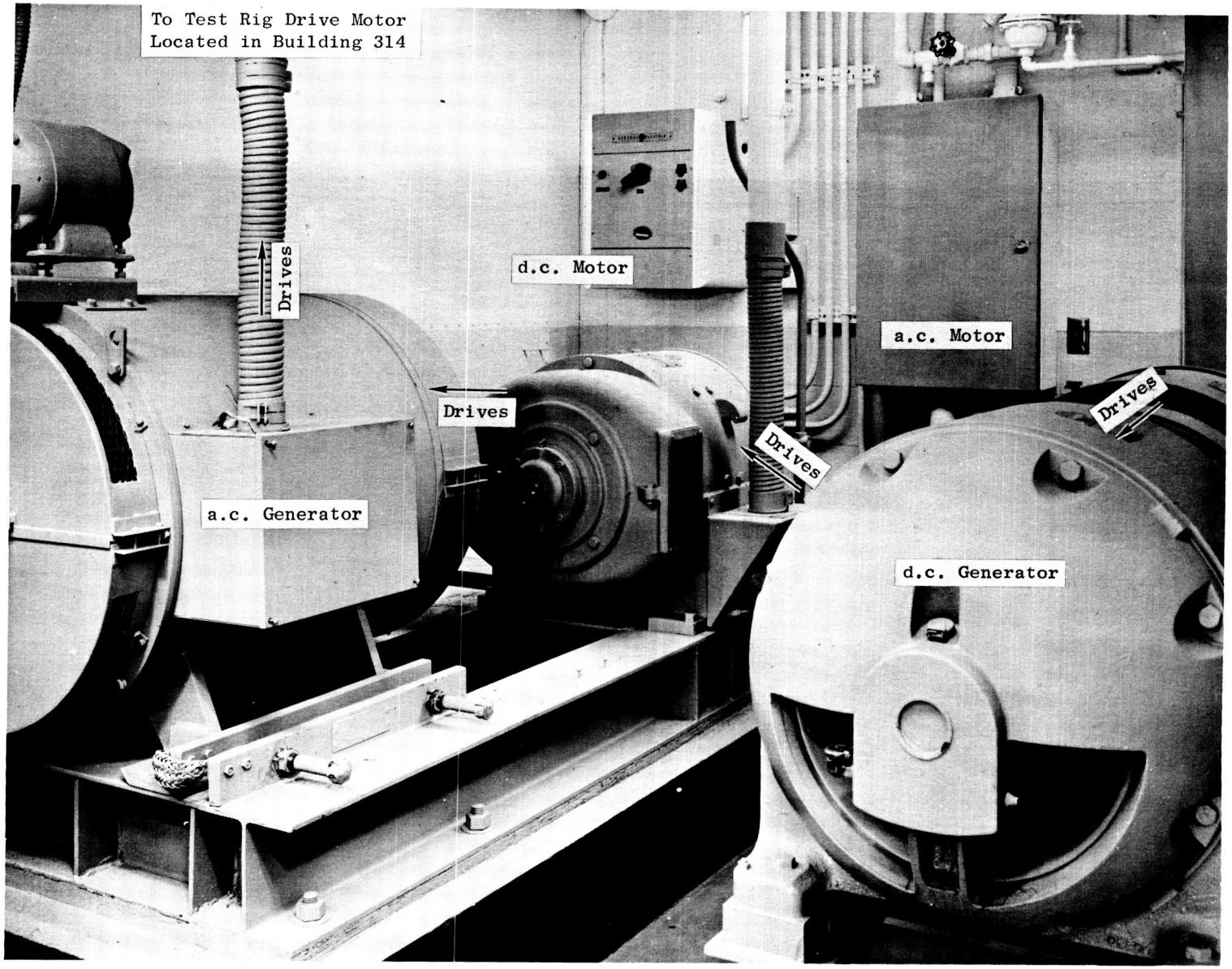

Figure 47. Motor Generator (M.G.) Set in Building 309.

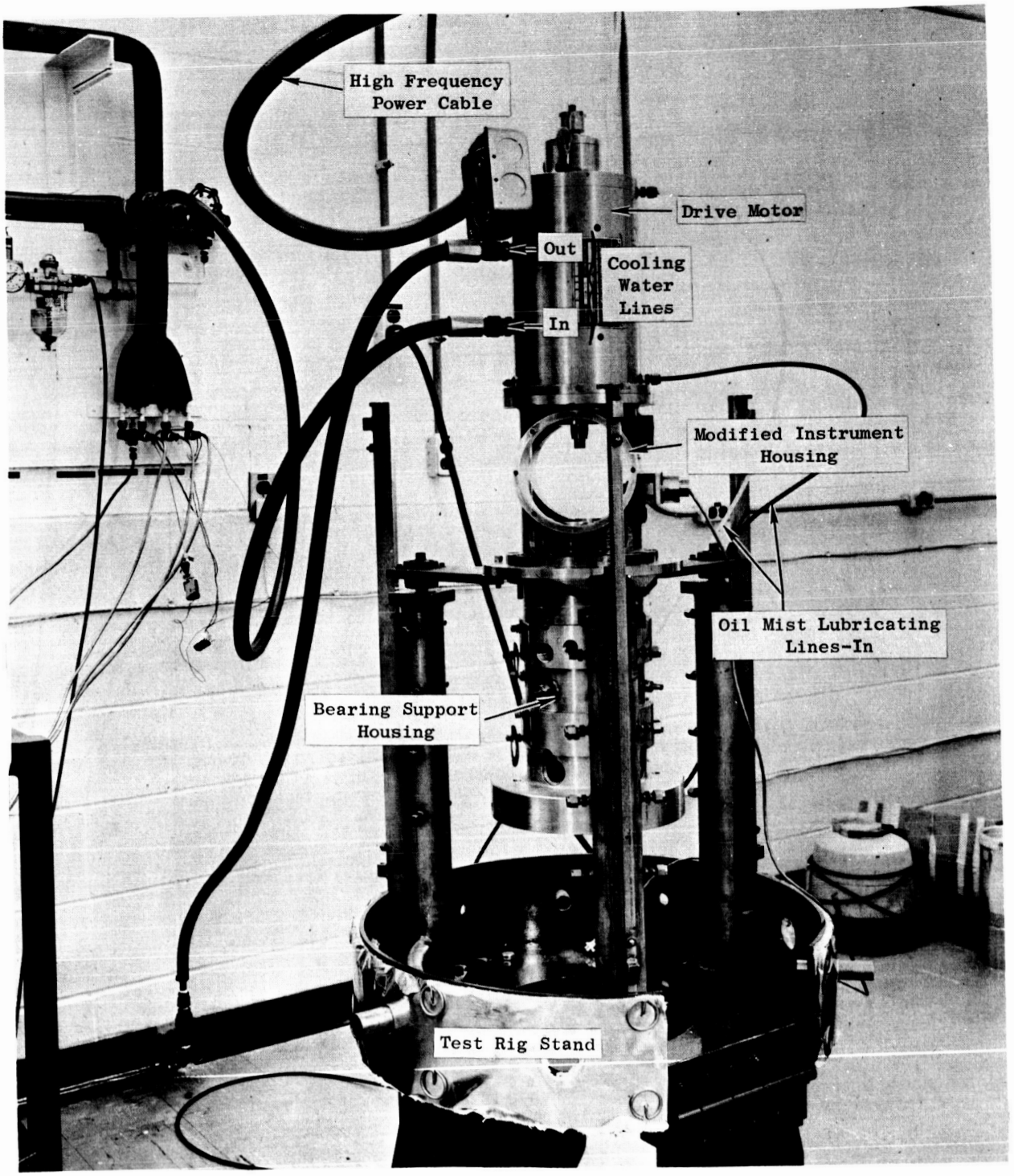

Figure 48. Drive Motor Checkout Test.

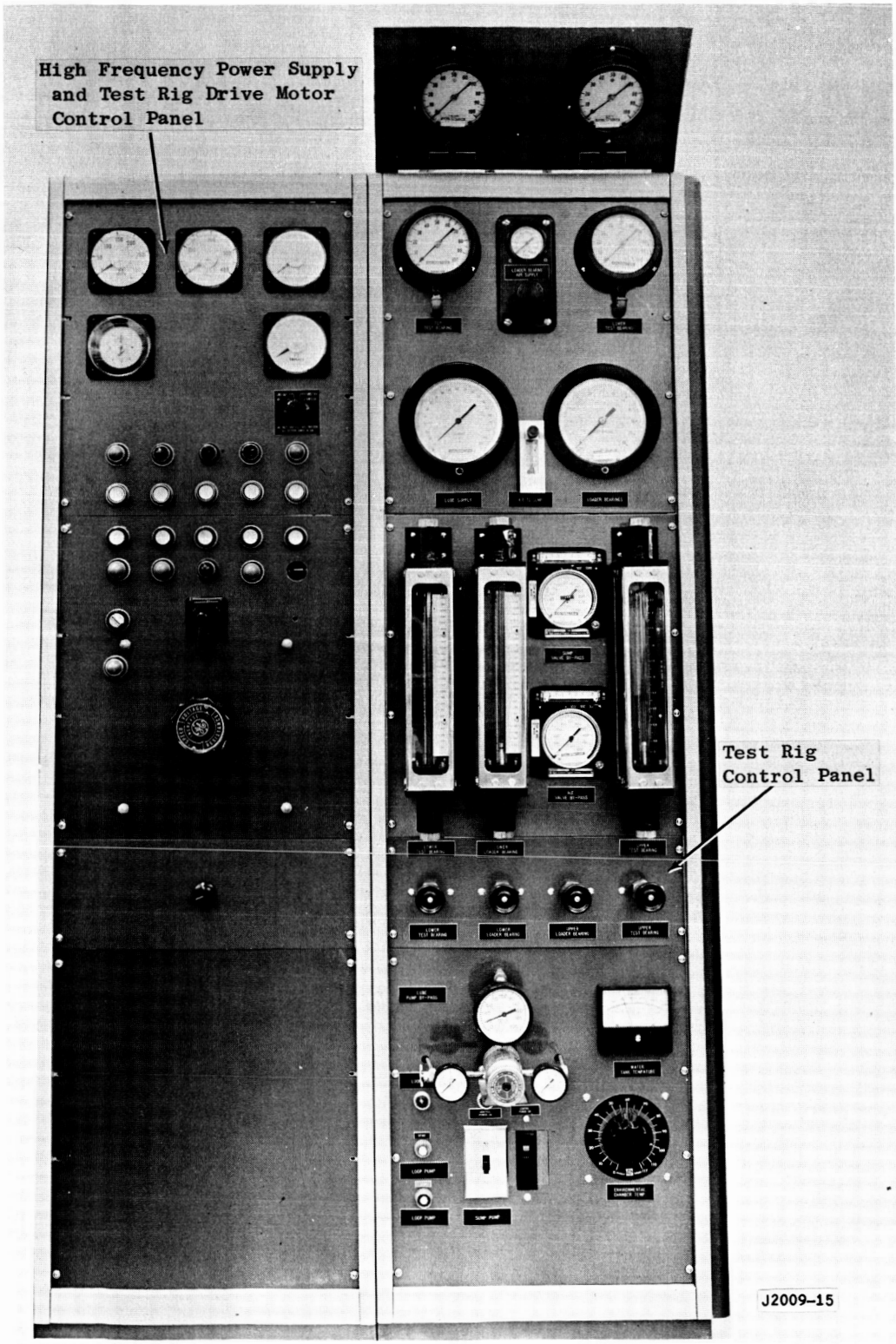

Figure 49. High Frequency Power and Test Rig Control Panel.

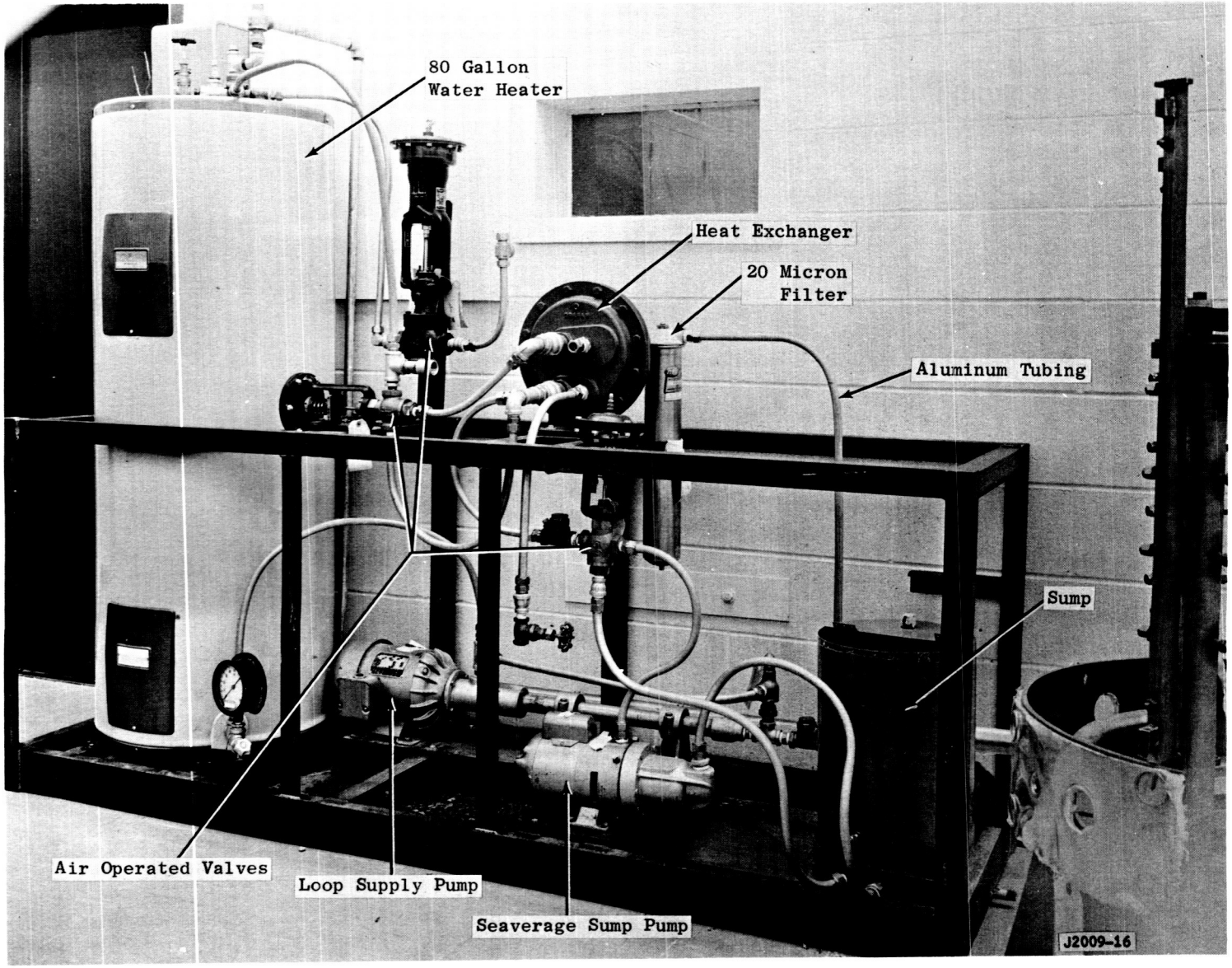

Figure 50. Distilled Water Lubricant Loop Package.

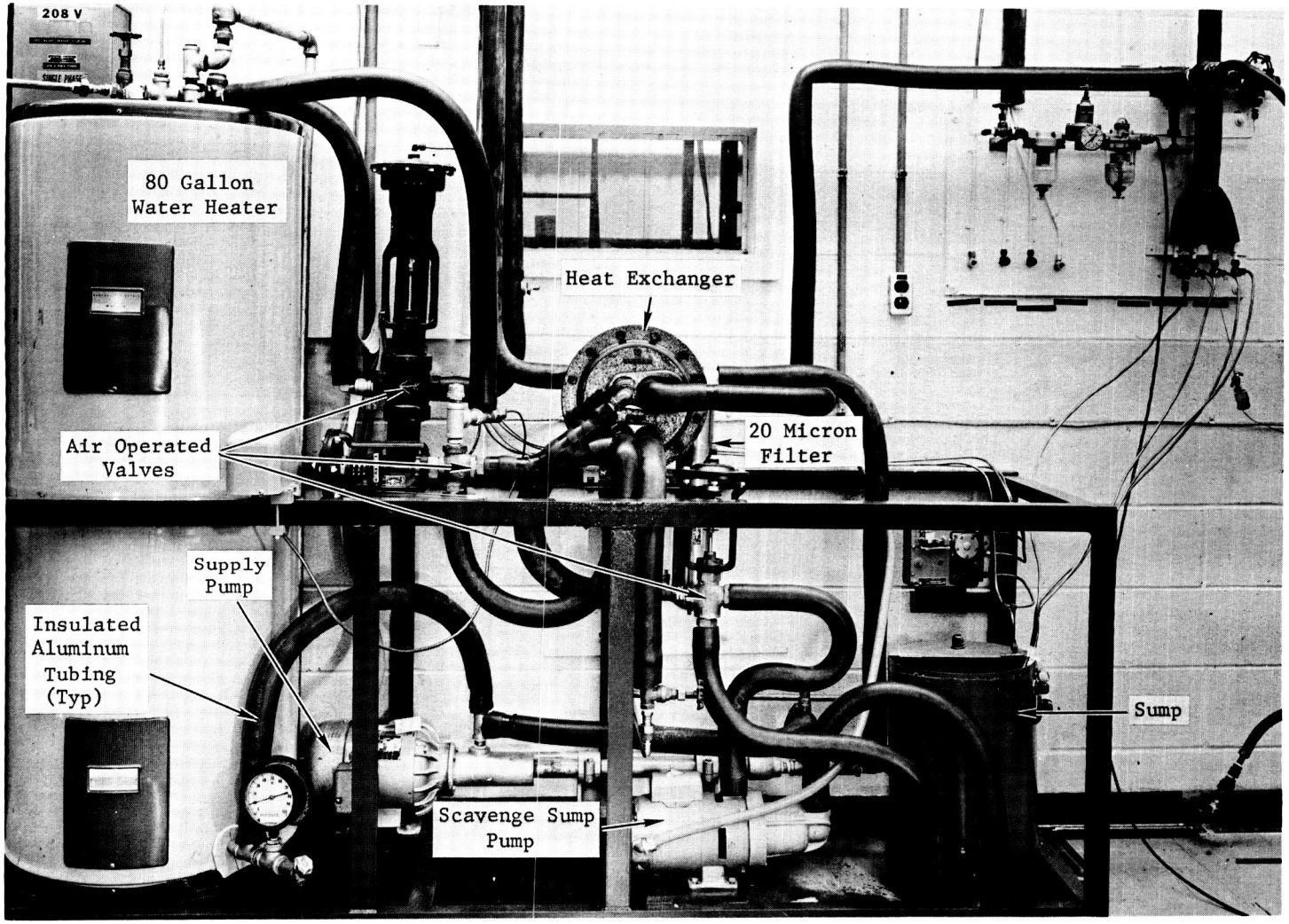

Figure 51. Distilled Water Lubricant Loop Package-Installed.

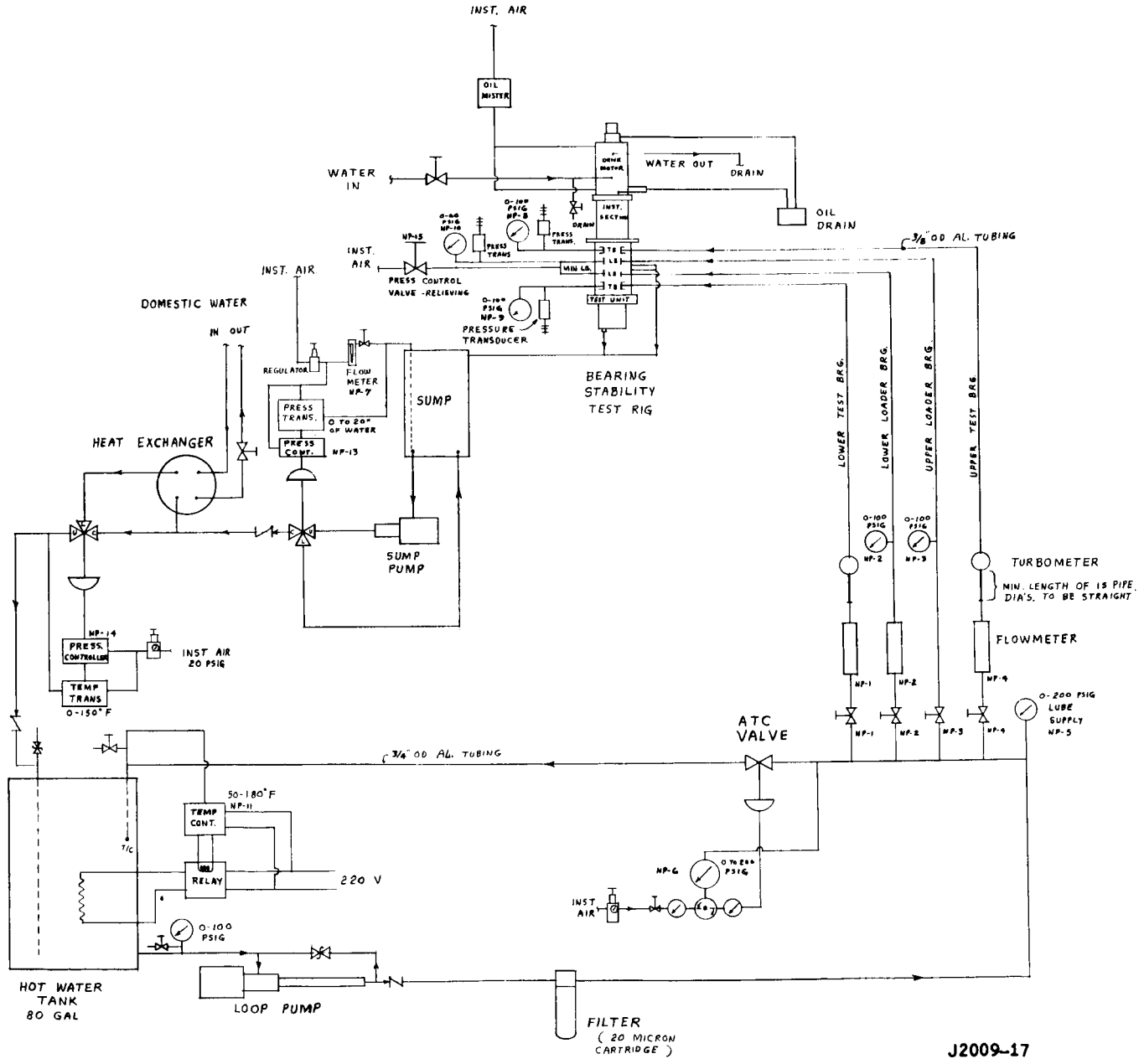

Figure 52. System Schematic Bearing Stability Facility.

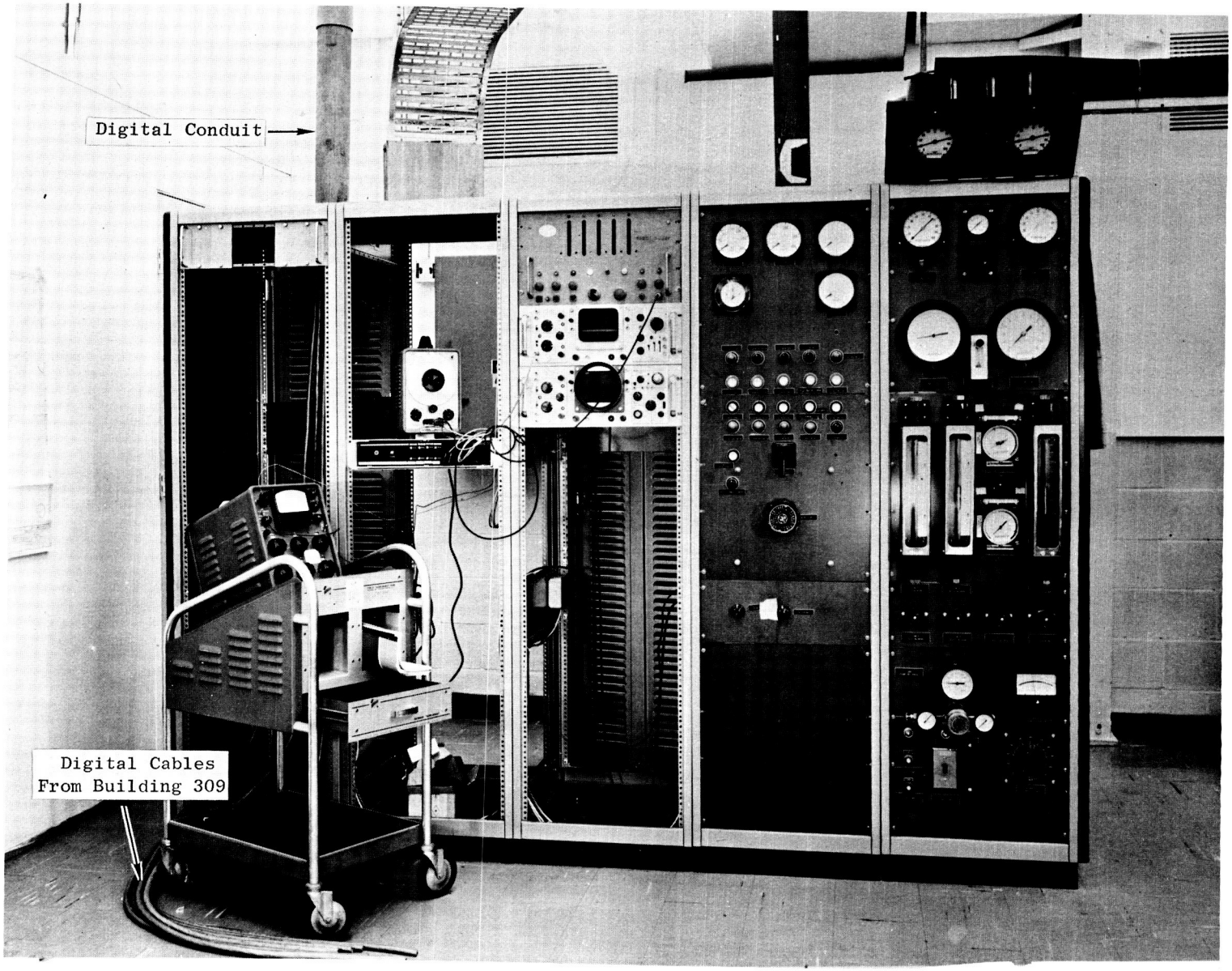

Figure 53. Test Rig Control Console-Partially Completed.

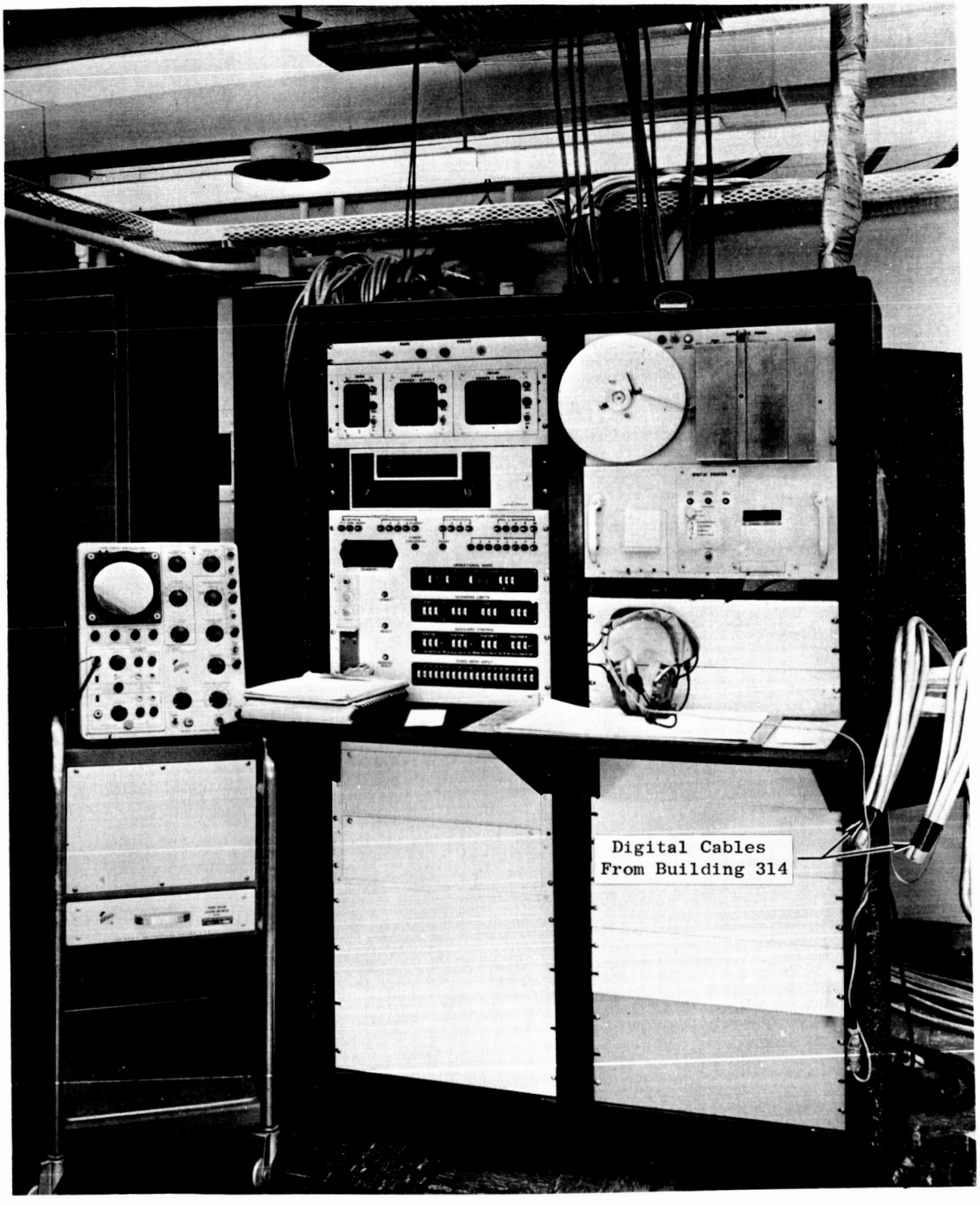

Figure 54. Digital Recording Station-Building 309.

DISTRIBUTION LIST FOR QUARTERLY REPORTS
CONTRACT NAS 3-6479

National Aeronautics & Space Administration
Washington, D. C. 20546
ATTN: S.V. Manson, Code RNP

National Aeronautics & Space Administration
Washington, D. C. 20546
ATTN: Dr. F. Schulman, Code RNP

NASA-Lewis Research Center
21000 Brookpark Road
Cleveland, Ohio 44135
ATTN: Dr. B. Lubarsky M.S. 500-201

NASA-Lewis Research Center
21000 Brookpark Road
Cleveland, Ohio 44135
ATTN: R.L. Cummings M.S. 500-201

NASA-Lewis Research Center
21000 Brookpark Road
Cleveland, Ohio 44135
ATTN: Ruth Weltmann M.S. 500-309

NASA-Lewis Research Center
21000 Brookpark Road
Cleveland, Ohio 44135
ATTN: J.J. Weber M.S. 3-19

NASA-Lewis Research Center
21000 Brookpark Road
Cleveland, Ohio 44135
ATTN: Joseph P. Joyce M.S. 500-201 (2)

NASA-Lewis Research Center
21000 Brookpark Road
Cleveland, Ohio 44135
ATTN: James Dunn M.S. 500-201

NASA-Lewis Research Center
21000 Brookpark Road
Cleveland, Ohio 44135
ATTN: Report Control Office M.S. 5-5

NASA-Lewis Research Center
21000 Brookpark Road
Cleveland, Ohio 44135
ATTN: William J. Anderson M.S. 6-1

NASA-Lewis Research Center
21000 Brookpark Road
Cleveland, Ohio 44135
ATTN: Henry Slone M.S. 500-201

NASA-Lewis Research Center
21000 Brookpark Road
Cleveland, Ohio 44135
ATTN: Warner Stewart M.S. 5-9

NASA-Lewis Research Center
21000 Brookpark Road
Cleveland, Ohio 44135
ATTN: Edmond Bisson M.S. 5-3

NASA-Lewis Research Center
21000 Brookpark Road
Cleveland, Ohio 44135
ATTN: Dorothy Morris M.S. 3-7

NASA-Lewis Research Center
21000 Brookpark Road
Cleveland, Ohio 44135
ATTN: J.E. Dilley M.S. 500-309

National Aeronautics & Space
Administration
Jet Propulsion Laboratory
California Institute of Technology
4800 Oak Grove Drive
Pasadena, California 91103
ATTN: John W. Stearns

National Aeronautics & Space
Administration
Scientific & Technical Information
Agency
P.O. Box 5700
Bethesda, Maryland 20014 (2 + Repro.)

National Aeronautics & Space
Administration
Western Operations Office
150 Pico Boulevard
Santa Monica, California 90406
ATTN: John Keeler

Aeronautical Systems Division
Wright Patterson Air Force Base
Dayton, Ohio 45433
ATTN: George Sherman - API

Aeronautical Systems Division
Wright Patterson Air Force Base
Dayton, Ohio 45433
ATTN: Charles Armbruster - ASRMFP-1

Aeronautical Systems Division
Wright Patterson Air Force Base
Dayton, Ohio 45433
ATTN: John Morris - ASRCNL-2

U.S. Atomic Energy Commission
Germantown, Maryland 20767
ATTN: Col. E.L. Douthett

U.S. Atomic Energy Commission
Germantown, Maryland 20767
ATTN: Herbert D. Rochen

U.S. Atomic Energy Commission
Germantown, Maryland 20767
ATTN: Dr. Nicholas Grossman
Chief, Engineering Department

Air University Library
Maxwell Air Force Base, Alabama
ATTN: Director

U.S. Atomic Energy Commission
Technical Information Service Extension
P.O. Box 62
Oak Ridge, Tennessee 37831

Mechanical Technology, Inc.
968 Albany-Shaker Road
Latham, New York
Attention: Dr. Beno Sternlicht

Office of Naval Research
Washington, D. C. 20546
ATTN: S. Doroff - Code 438

Armed Services Technical Information Agency
Arlington Hall Station
Arlington, Virginia 22212

Aerojet-General Corporation
Technical Library
Building 2015, Department 2410
P.O. Box 1947
Sacramento 9, California

Aerojet-General Corporation
Azusa, California 91703
ATTN: Robert Gordon
SNAP 8/Program Director

Aero-jet General Corporation
Azusa, California 91703
ATTN: John Marick

AiResearch Manufacturing Company
Sky Harbor Airport
402 South 35th Street
Phoenix, Arizona
ATTN: Librarian

AiResearch Manufacturing Company
Sky Harbor Airport
402 South 35th Street
Phoenix, Arizona
ATTN: Robert Gruntz

AiResearch Manufacturing Company
Sky Harbor Airport
402 South 35th Street
Phoenix, Arizona
ATTN: George Wheeler

Atomics International
Division of NAA
Canoga Park, California
ATTN: L.M. Flower

The Barden Corporation
Research Precision Division
Danbury, Connecticut
ATTN: Mrs. Bernice P.Lucas

M.S.A. Research Foundation
Callery, Pennsylvania
Attn: G.E. Kennedy

Contract NAS 3-6479

Battelle Memorial Institute
505 King Avenue
Columbus, Ohio 43201
ATTN: C.M. Allen

The Franklin Institute
Benjamin Franklin Parkway at 20th Street
Philadelphia, Pennsylvania 19103
ATTN: William Shuggarts

General Electric Company
Missile & Space Vehicle Department
3198 Chestnut Street
Philadelphia, Pennsylvania 19101
ATTN: Edward Ray

Mechanical Technology, Inc.
968 Albany-Shaker Road
Latham, New York
ATTN: Eli Arwas

Pratt & Whitney Aircraft Division
United Aircraft Corporation
East Hartford, Connecticut 06108
ATTN: Dr. William Lueckel
Eng. Bldg. 2-H

Pratt & Whitney Aircraft Division
United Aircraft Corporation
East Hartford, Connecticut 06108
ATTN: R.P. Shenchenko

Pratt & Whitney Aircraft Division
United Aircraft Corporation
East Hartford, Connecticut 06108
ATTN: Karl A. Domeisen
Exp. Eng. Eng. 1-F

Rocketdyne
Division of North American Aviation, Inc.
6633 Canoga Avenue
Canoga Park, California 91303
ATTN: Robert Spies

Sundstrand Aviation - Denver
A Division of Sundstrand Corporation
Denver, Colorado 80221
ATTN: P.H. Stahlhuth

Southwest Research Institute
8500 Culebra Road
San Antonio, Texas 78206
ATTN: Dr. R.A. Benton

UAC Library
United Aircraft Research Laboratories
Gate 5R, Silver Lane
East Hartford, Connecticut 06108

Westinghouse Electric Corporation
Research Laboratories
Pittsburgh, Pennsylvania 15236
ATTN: Mr. J. Boyd

Westinghouse Electric Corporation
Aerospace Division
Advanced Machine Systems Group
Lima, Ohio
ATTN: Allen King

The Franklin Institute
Benjamin Franklin Parkway at 20th St.
Philadelphia, Pennsylvania 19103
ATTN: Otto Decker

North American Aviation
Atomics International
P.O. Box 309
Canoga Park, California 91304
ATTN: Director, Liquid Metals
Information Center